Studies on the essential *YNL152w* open reading frame in *Saccharomyces cerevisiae*

Dissertation

Zur Erlangung des akademischen Grades eines

Doctor rerum naturalium

(Dr. rer. nat.)

eingereicht am Fachbereich Biologie/Chemie der Universität Osnabrück

von

Ivan Francisco Ciklic

aus Cordoba, Argentinien

Osnabrück, May 2007

Promotionskomission:

Erstgutachter: Prof Dr. Jürgen Heinisch   Zweitgutachter: Prof. Dr. Karlheinz Altendorf

Prof. Dr. Joachim Ernst   Dr. Hans Peter Schmitz

"Dedicated to the everlasting memory of my dear Grandfather Cristobal who inculcated me the love for knowledge and the beauty of nature".

Table of contents

1. Introduction

1.1 The yeast *Saccharomyces cerevisiae* as a model organism

Since ancient times the yeast *Saccharomyces cerevisiae* has been used for the production of food. The most known applications are the production of bread, beer and wine. For instance, there are reports of winemaking going back some 7400 years (Perez-Ortin *et al.*, 2002). Today its diverse metabolism is exploited for the production of pharmaceuticals, flavorings, enzymes, and various other fine chemicals. Because of its importance to mankind, detailed studies have been carried out on its physiology. Consequently, *S. cerevisiae* is not only a very important industrial food microorganism, but has become a leading eukaryotic model. It was the first eukaryote whose genome was completely sequenced (Goffeau *et al.*, 1996) and studies on its functional genomics are far ahead of other fungi and eukaryotes in general. Thus, important breakthroughs have been triggered by *S. cerevisiae*: The first transcriptome microarray, a comprehensive analysis of protein-protein interactions (Uetz *et al.*, 2000), the first proteome chip (Zhu *et al.*, 2001) and the completion of the whole gene knock-out project (Giaever *et al.*, 2002). Taken together, these studies lead to a broad understanding of many different essential processes, like e.g. cell division and signal transduction. Some characteristic features of *S. cerevisiae* are summarized in **Table 1.1**.

1.2 Cytokinesis in *Saccharomyces cerevisiae*

Cytokinesis is the final stage of the cell cycle. In this process, the cellular constituents of the mother cell are partitioned into two daughter cells, permitting the increase in cell number. Any malfunction of the cell division could be lethal for both the mother and the daughter cell. Therefore it is a tightly temporally-spatially regulated process. The basic mechanisms of cytokinesis has been conserved from bacteria to fungi, plants and animals (Nanninga, 2001). To allow for cytokinesis, actin like proteins or a functional cytoskeleton composed of actin and/or tubulin polymers is absolutely essential for all

Table 1.1

Features making the yeast *S. cerevisiae* a eukaryotic model organism (modified from Heinisch, 2005).

Yeast as a model eukaryote

Unicellular eukaryote with all typical features (e.g., organelles, cell cycle regulation, aging, apoptosis)

Microorganism with short generation time (1.5 h), high cell densities ($>10^8$ cells/ml) and high surface/volume ratio

Well-known physiology (enzyme = "in yeast")

Extensive industrial use because of long history in alcohol production and in bakeries

Mendelian genetics (sexual life cycle; tetrad analysis)

Variety of established vector-and transformation systems

High efficiency of homologous recombination (genetic engineering)

Complete genome sequence available since 1996

Collections of deletion mutants for all open reading frames

Affordable DNA chips for transcriptome analyses

Complete set of GFP fusions

Large scale protein interaction maps

>20 years used for heterologous gene expression

---

these organisms. Even bacterial cells contain ancestral tubulin and actin, encoded by FtsZ and FtsA, respectively (Errington *et al.*, 2003; Guertin *et al.*, 2002). With the exception of plants, all cells utilize a contractile ring to generate a constriction at the division site. Beyond these mechanistic similarities, macromolecular complexes are hardly conserved through the kingdoms. However, cell division in yeast and animal cells is highly conserved (Walther and Wendland, 2003). Therefore organisms such as *S. cerevisiae* and *S. pombe* have become very valuable models for the study of these events. A major difference between yeast and animal cell division is that yeast cells build up a septum of cell wall material after the formation of the contractile actomyosin ring. This is a consequence of the structural organization of yeast cells, in which the

presence of a cell wall allows them to grow in a variety of osmotic conditions. Hence this barrier must be kept during cytokinesis.

In the following sections the principal events that occur during cytokinesis of *S. cerevisiae* will be described and its coordination with the nuclear cycle will be discussed (**Fig. 1.1**). Moreover species-specific features of *S. cerevisiae* will be highlighted.
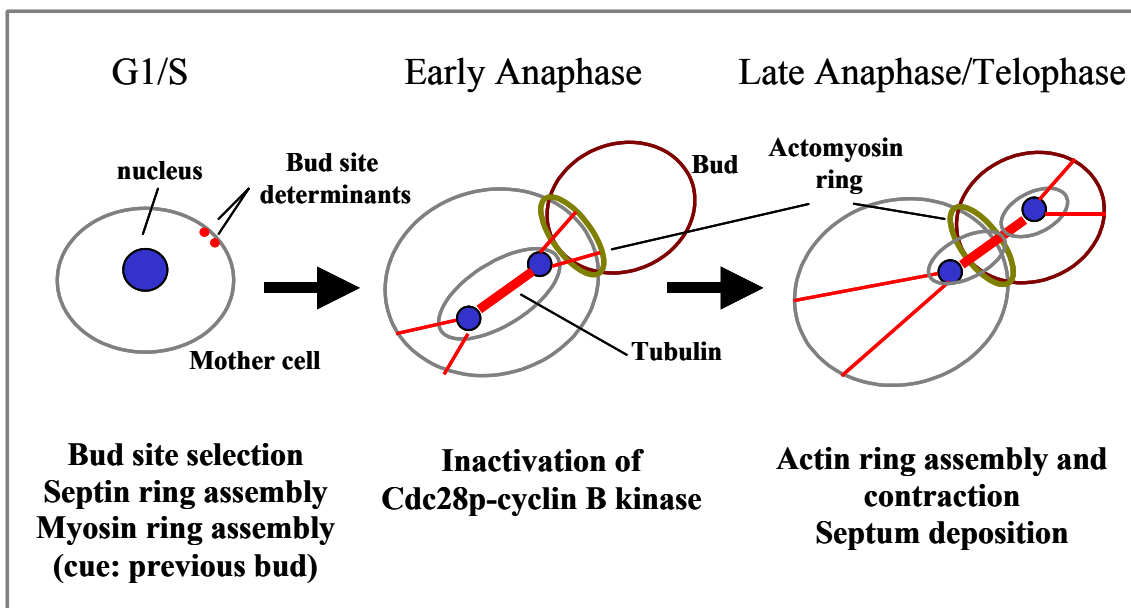
Fig. 1.1 Key steps during cell cycle progression to ensure cytokinesis in *S. cerevisiae* (modified from Balasubramanian *et al*, 2004). Bud site selection occurs early in the cell cycle during G1/S. Mitotic exit occurs in early anaphase and involves a signaling casacade leading to inactivation of the cyclin-Cdc28p-complex. During transition from anaphase to telophose, the actomyosin ring is assembled and its contraction takes place simultaneously with septum deposition.

1.2.1 Division site selection

In contrast to animal cells in which the division plane is determined during onset of the mitotic anaphase, in *S cerevisiae* cells the division plane is defined much earlier in the cell cycle, i.e. at late G1, and is chosen depending on the prior division site. Thus, *S. cerevisiae* cells bud with two different patterns depending on their ploidy. In haploid *MAT***a** or **α** cells, the new bud emerges adjacent to the preceding bud site (axial),

whereas in diploid *MAT*a/α cells the new bud occurs alternating between the poles (bipolar) (Casamayor and Snyder, 2002; Chant, 1999). At least four landmark proteins are thought to be responsible for the axial budding pattern, Bud3p, Bud4p, Axl1p and Axl2p (Casamayor and Snyder, 2002; Chant, 1999; Lord *et al.*, 2002). Deletion of any of the encoding genes in haploid cells converts the axial bud-site selection to a bipolar pattern. In contrast, deletion of *BUD3* in diploid cells has no obvious phenotype. Rather, the bipolar pattern depends on the activity of two other landmark proteins, Bud8p and Bud9p. Upon deletion of both *BUD8* alleles, diploid cells use the proximal pole (the one that was connected to the mother cell) for budding. This is consistent with the reported localization of Bud8p at the distal pole (Harkins *et al.*, 2001; Taheri *et al.*, 2000). Conversely, diploid *bud9/bud9* yeast cells bud at the distal pole (Zahner *et al.*, 1996). All these proteins are produced in the previous cell cycle and mark the cortical site(s). These landmarks are then recognized by the general bud-site selection machinery composed of a GTPase module that includes the Ras-related small GTPase Rsr1p/Bud1p (Bender and Pringle, 1989; Chant and Pringle, 1991), its guanine nucleotide-exchange factor (GEF) Bud5p (Chant and Pringle, 1991) and its GTPase-activating protein (GAP) Bud2p (Park *et al.*, 1993; Park *et al.*, 1999). Later on, the Rsr1p GTPase module interacts with the polarity-establishment machinery: The Cdc42p GTPase module (Johnson, 1999), which includes the Rho-type GTPase Cdc42p, its GEF Cdc24p and its GAPs (Caviston *et al.*, 2003; Gladfelter *et al.*, 2002; Smith *et al.*, 2002). Finally, Cdc42p works through its effectors to organize the actin cytoskeleton to control polarized growth (Pruyne and Bretscher, 2000). In parallel, it also regulates septin ring assembly to control cytokinesis (discussed below). The septin ring also plays a role in positioning the axial- and bipolar-specific landmarks for bud-site selection in the next cycle (Casamayor and Snyder, 2002; Chant, 1999; Harkins *et al.*, 2001). Thus, the landmark proteins and the septin ring appear to position each other in a cyclic fashion (Chant, 1999). The significance of the specific budding pattern is not clear and deletion of any of the known bud-site selection genes, including *RSR1*, does not cause a significant cytokinesis defect. Hence bud-site selection is not a part of the cytokinetic machinery. However, the Cdc42p GTPase module downstream from the bud-site selection machinery is essential for cell polarization and, as a consequence, for cytokinesis (Balasubramanian *et al.*, 2004).

"In general the mechanisms for cleavage site determination are highly species-specific. Animal cells and fission yeast cells use other structures to define the division

plane (spindle apparatus or nucleus, respectively) and do so at other phases of the cell cycle (anaphase, late G2). Nevertheless, some molecular analogies can be drawn. For example, the local activation of GTPase modules plays a critical role both in budding yeast and animal cells. However, the GTPases involved are usually not orthologous" (Balasubramanian *et al.*, 2004).

1.2.2 Assembly of the actomyosin contractile ring

Actomyosin-based contractile rings have been shown to play an important role in cytokinesis in many organisms. In *S. cerevisiae* it is not essential and there exist two functionally overlapping pathways. The first one involves the formation of an actomyosin contractile ring mediated by the type II Myo1p and the formin Bni1p (Vallen *et al.*, 2000). The second pathway controls cell separation and septum formation and involves a number of proteins including Hof1p and the formin Bnr1p. The existence of two redundant pathways is a unique advantage for *S. cerevisiae* because the effects of gene deletion on actomyosin contraction can be monitored (Vallen *et al.*, 2000).

"At least three types of proteins are associated with the actomyosin ring during cytokinesis: i) Proteins committed to actomyosin ring function only. ii) Proteins required for both actomyosin ring function and septum formation. iii) Proteins that are thought to coordinate these two processes. Regarding the first point, most, if not all of the actomyosin ring-associated proteins are evolutionary conserved" (Balasubramanian *et al.*, 2004). The arrival of these proteins at the bud neck is sequential within the cell cycle, starting from late G1 to the beginning of cytokinesis and/or cell separation. Their chronological order of assembly at the bud neck is as follows: In late G1 phase, the septins (described bellow) followed by the myosin II heavy chain Myo1p, its regulatory light chain Mlc2p, and the formin Bnr1p. In S phase, the myosin II essential light chain Mlc1p. During G2/M phase, Hof1p, Iqg1 and the formin Bni1p. Finally, in late anaphase the actin ring and Cyk3p. "Thus, a functional actomyosin ring forms only in late anaphase even though some of the components arrive at the division site much earlier" (Balasubramanian *et al.*, 2004).

The septin ring is composed of septin family proteins encoded by *CDC3*, *CDC10*, *CDC11* and *CDC12* (Gladfelter *et al.*, 2001; Sanders and Field, 1994), there are also two other septin proteins found exclusively during sporulation Spr3p and Spr28p. With the exception of *CDC11*, the deletion of any of the components of the septin ring is

lethal for the cell, resulting in a complete block in cytokinesis. Both the type II myosin Myo1p and a septum forming enzyme Chs2p fail to localize to the bud neck in septin mutants, suggesting that the septins may function as a scaffold that is required for the anchoring or maintenance of the actomyosin ring and the septum-forming apparatus (Bi *et al.*, 1998; Lippincott and Li, 1998; Roh *et al.*, 2002b). The septin ring may also serve several other functions: (1) As a rigid backbone that stabilizes the bud neck (Faty *et al.*, 2002), (2) As a barrier to maintain exocytosis and other factors directed to the daughter cell (Barral *et al.*, 2000; Takizawa *et al.*, 2000). (3) Septins may play a role in the positioning of the spindle in the mother/daughter cell axis (Kusch *et al.*, 2002).

Besides myosin II-type proteins, three other factors are required for the formation of the actomyosin ring, IQGAP and two formins. The type II heavy chain Myo1p is required for actin ring formation (Bi *et al.*, 1998), but its regulatory light chain Mlc2p is not. *IQG1* is an essential gene and is required for ring formation as well as for cytokinesis. *IQG1* encodes a multidomain protein consisting of an N-terminal Calponin-homology domain, central IQ repeats, and a C-terminal GTPase-activating protein domain (Shannon and Li, 1999). The localization of Iqg1p to the bud neck apparently depends on its interaction with Mlc1p which localizes prior to Iqg1p. The formins Bni1p and Bnr1p are required for actin ring formation, presumably because of their ability to nucleate actin filaments, which is regulated by Rho1p (Tolliday *et al.*, 2002). Although the actomyosin ring is clearly important for cytokinesis, its formation is not strictly essential in budding yeast. Elimination of the actomyosin ring by deleting the only type II myosin, Myo1p, does not cause lethality nor does it prevent cytokinesis. Rather, Myo1p-deficient cells exhibit abnormal septum formation, inefficient cytokinesis and cell separation (Bi *et al.*, 1998). The existence of an alternative pathway for cytokinesis independent of actomyosin ring formation is further supported by the fact that increased dosage of either Cyk3p or Hof1p, can bypass the requirement of Iqg1p in cell viability and cytokinesis without restoring the actin ring (Korinek *et al.*, 2000). It seems that cells lucking a functional actomyosin ring, divide by formation of a secondary septum (Schmidt *et al.*, 2002).

1.2.3 Membrane deposition and septum formation

There is a specific feature that distinguishes fungal from animal cells in cell division: The formation of a chitin rich septum. This is of particular interest to scientists

studying human fungal pathogens, because of the development of antifungal drug therapies with the septum formation as a target (Walther and Wendland, 2003). Moreover, membrane remodeling is also required for cell division, with the need for membrane deposition at the division site of yeast cells during cytokinesis. The molecular mechanisms responsible for the targeting to this site are not yet clear (Balasubramanian *et al.*, 2004). It has been suggested that exocytosis plays a crucial role in this process (VerPlank and Li, 2005). Accordingly, numerous components associated with exocytosis relocate from the bud cortex to the bud neck in late anaphase, just before cytokinesis. These include the type V myosin Myo2p and its associated light chain Mlc1p, with function in vesicle transport, the multi-subunit exocyst complex, and its regulator, the Rab GTPase Sec4p as well as regulators of the actin cytoskeleton, such as Cdc42p and Rho1p. Because Cdc42p and Rho1p regulate actin assembly and secretion (Adamo *et al.*, 2001; Guo *et al.*, 2001; Zhang *et al.*, 2001), these GTPases may coordinately regulate the actomyosin ring and targeted membrane deposition during cytokinesis. In fact, the major role of this targeted membrane deposition in budding yeast is to deliver the integral membrane proteins that mediate septum formation (Balasubramanian *et al.*, 2004). Chs2p, the catalytic subunit of chitin synthase II, localizes to the bud neck in late anaphase (Chuang and Schekman, 1996; Roh *et al.*, 2002a). Deletion of *CHS2* is not lethal but causes a strong defect in cytokinesis. Actomyosin rings can form in such mutants but fail to contract efficiently (Bi, 2001; Schmidt *et al.*, 2002). Chs3p, the catalytic subunit of chitin synthase III, responsible for the synthesis of approximately 90% of cellular chitin (Orlean, 1997), localizes to the emerging bud early in the cell cycle, and relocates to the bud neck in late anaphase (Chuang and Schekman, 1996). Simultaneous deletion of both *CHS2* and *CHS3* is lethal and the double mutant cells display a defect in cytokinesis (Shaw *et al.*, 1991). This suggests that Chs3p also plays a role in septum formation. The localization of Chs2p and Chs3p to the bud neck depends on the septins (DeMarini *et al.*, 1997; Roh *et al.*, 2002a).

Mlc1p and Iqg1p must also play a role in septum formation, which presumably requires targeted secretion. Mlc1p interacts with Myo2p, but this interaction appears dispensable for cytokinesis (Stevens and Davis, 1998). Iqg1p also co-immunoprecipitates with Sec3p, a component of the exocyst (Osman *et al.*, 2002), but the significance of this interaction in cytokinesis remains unclear. But despite all this circumstantial evidence, it is not known how the secretory apparatus is targeted to the

bud neck, nor how the actomyosin ring is coupled to targeted membrane deposition (Balasubramanian *et al.*, 2004). Finally, there is evidence for interplay between the deposition of septum material and the actomyosin ring. Contraction of the actomyosin ring guides membrane deposition so that the septum forms efficiently at the right position. Conversely, septum deposition modulates the contractility of the actomyosin ring (Bi, 2001). Hof1p and Cyk3p may be in part responsible for this linkage between ring constriction and septum formation, however, the molecular mechanisms that mediates this coordination are still obscure (Balasubramanian *et al.*, 2004).

1.2.4 Coordination of cytokinesis with the nuclear cycle

It is very important for cell viability that cytokinesis occurs only after proper chromosome segregation. Therefore, it is not surprising that cytokinesis is tightly regulated in a cell-cycle dependent manner. In *S. cerevisiae* cytokinesis starts in late anaphase or early telophase and thus must be coordinated with the nuclear cycle. Recent evidence suggests that this coordination is performed, at least in part, by the mitotic exit network (MEN). "MEN" is a signaling cascade starting with the GTPase Tem1p with the protein phosphatase Cdc14p as a final target (**Fig. 1.2**). During anaphase, the kinase Cdc5p activates the MEN in three different ways: i) It activates Tem1p by inhibition of its GAP Bfa1p through phosphorylation (Hu *et al.*, 2001; Simanis, 2003). ii) It increases the activity of the Ser/Thr kinase Dbf2p (Lee *et al.*, 2001). iii) It releases Cdc14p from the nucleolus, after phosphorlylation of Net1p, the core subunit of the RENT complex (Regulator of Nucleolar silencing and Telophase) (Yoshida and Toh-e, 2002). After Cdc14p has been released, it dephosphorylates the transcription factor Swi5p to raise the level of Sic1p, an inhibitor of the Cdc28p-cyclin B kinases. Another function of Cdc14p is the dephosphorylation of Cdh1p. In this state, the latter interacts with the anaphase promoting complex (APC) to drive cyclin degradation (Gray *et al.*, 2003; Simanis, 2003; Visintin *et al.*, 1998). The coordinated action of both the cyclin-dependent kinase inhibitor Sic1p and APC/Cdh1p reduce the level of Cdc28p-cyclin B, consequently leading to mitotic exist.
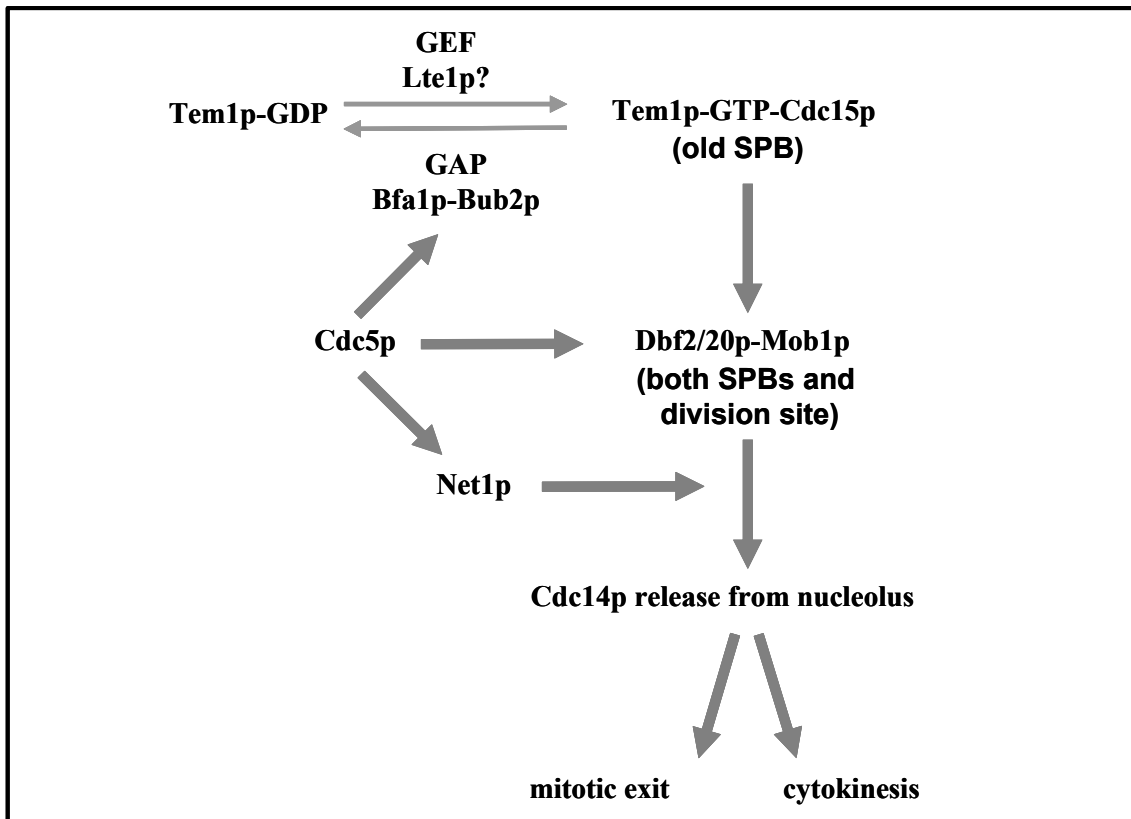
Fig. 1.2 Schematic representation of the MEN (Mitotic Exit Network) pathway in S.cerevisiae. Terms in parenthesis indicate the intracellular localization of the proteins.

There is evidence that support a role of the MEN in cytokinesis, which is independent of its role in mitotic exit. In the lapse between S/G2 phase to the end of anaphase, all known MEN components are associated with spindle pole bodies (SPB). At that time, some of them translocate to the bud neck, consistent with a role of MEN in cytokinesis (Simanis, 2003). Moreover, overexpression of the kinase inhibitor Sic1p (Hwa Lim *et al.*, 2003) or deletion of the Cdc14p-sequestering protein Net1p (Lippincott *et al.*, 2001), can rescue mitotic exit in Tem1p, Cdc15p, Dbf2p and Dbf20p mutants of the MEN pathway. However all these mutants are still defective in cytokinesis, suggesting that MEN indeed plays a role in cytokinesis independent of mitotic exit and independent of Cdc14p release from the nucleolus.

What are the targets of MEN in cytokinesis? All MEN mutants can form an actomyosin ring (Hwa Lim *et al.*, 2003; Lippincott *et al.*, 2001; Vallen *et al.*, 2000), but these rings are not able to contract, or do so inadequately (Hwa Lim *et al.*, 2003; Lippincott *et al.*, 2001). There are two possible explanations for this: Either the contraction of the actomyosin ring itself is not fully functional in MEN mutants and

thus its contraction is inhibited. Or MEN mutants are defective in septum formation, which is known to affect the contraction, but not the assembly of the ring (Bi, 2001; Schmidt *et al.*, 2002). In agreement with the latter assumption, MEN mutants are defective in chitin deposition, which is required for septum formation at the bud neck (Hwa Lim *et al.*, 2003). One good candidate as a target of the MEN in septum formation is Hof1p, which is phosphorylated in a MEN-dependent manner and is thought to coordinate actomyosin ring function with septum formation (Vallen *et al.*, 2000). Furthermore, it has been recently reported, that SCF[Grr1] (Skp1-cullin-F-box protein complex)-mediated degradation of Hof1p at the end of mitosis, is necessary for efficient actomyosin ring contraction and proper cell separation during cytokinesis. Hence, this may represent a novel mechanism to couple exit from mitosis with initiation of cytokinesis (Blondel *et al.*, 2005).

1.2.5 Role of the Hof1 protein in cytokinesis and septum formation

Because of its relevance for this work, the function of Hof1p in cytokinesis and septum formation will be further analyzed in this subchapter.

The protein Hof1p (Homolog Of Fifteen; named because its homology with *S. pombe* Cdc15) is encoded by the *S. cerevisiae YMRO32w* open reading frame (Kamei *et al.*, 1998) and it is a member of the "*pombe* Cdc15 homology"(PCH), protein family (Lippincott and Li, 2000). The founding member of the PCH family is the *Schizosaccharomyces pombe* Cdc15 protein, which is known from mutation studies to be involved in cytokinesis in the fission yeast (Balasubramanian *et al.*, 1998; Fankhauser *et al.*, 1995). In addition to yeasts, homologues of Cdc15 have been identified in other organism, for instance the mouse PSTPIP and PSTPIP2 (Spencer *et al.*, 1997; Wu *et al.*, 1998), and the human Cip4 (Aspenstrom, 1997). Many of them appear to have a function in cytokinesis, although Cip4 is involved in GTPase signaling rather than cytokinesis (Aspenstrom, 1997). As it is usually the case in other PCH-family members, the structure of Hof1p (**Fig. 1.3**) contains an N-terminal FER-CIP4 Homology (FCH) domain, immediately followed by a region with coiled-coil forming potential. At the C-terminal region a Src homology domain (SH3) is located, which in general binds to proline rich motifs. Finally, a proline/glutamic-acid/serine/threonine (PEST) rich region involved in protein turnover, is present between the coiled-coil region and the SH3 domain (Kamei *et al.*, 1998; Lippincott and Li, 2000).

Fig. 1.3 Domain structure of Hof1p a member of the PCH protein family, showing all the representative features (see text for details).

Hof1p was first described as a binding partner of the formin Bnr1p and was related to cytokinesis because of the deletion mutant phenotype. This shows a temperature-sensitivity, with arrested cells presenting large and elongated buds (Kamei *et al.*, 1998). The protein was also described by another group (Lippincott and Li, 1998), who named it Cyk2p because of its implication in contractile ring activity like Cyk1p/Iqg1p. In these and two subsequent works (Lippincott and Li, 2000; Vallen *et al.*, 2000), the dynamics and localization of Hof1p was exhaustively studied. Hof1p localizes to the bud neck, and initially it was believed to reside there throughout the complete cell cycle (Kamei *et al.*, 1998; Lippincott and Li, 1998). Later on it was shown that Hof1p only localizes to the bud neck between G2/M transition and cytokinesis. In addition, the cell cycle specific Hof1p localization pattern at the bud neck was shown to correlate with the phosphorylation state of Hof1p (Vallen *et al.*, 2000). In a typical time-lapse analysis using a functional Hof1p-GFP construct for localization studies in a fluorescent microscope, the initial signal usually appears as double rings, asymmetric in their intensities, with the stronger signal at the side of the mother cell. In most cases, the double rings briefly became equal in intensity and then fuse into a single ring. After a clear septum is formed, the diameter of the ring reaches its minimal size. At this time, the single ring splits into faint and fuzzy double rings, which remain approximately the same size until cell separation. The Hof1p-GFP signal disappears when cell separation is completed (Vallen *et al.*, 2000). Such behavior is consistent with a role for Hof1p in cytokinesis, but it is in sharp contrast to that of the actomyosin ring contraction, which

contracts to a single dot before septum formation is finished (Bi *et al.*, 1998; Lippincott and Li, 2000). This difference in the contraction pattern suggests that Hof1p is not part of the actomyosin contractile system (Vallen *et al.*, 2000).

Although these data indicate a function of Hof1p in cytokinesis, its specific role in this process is still controversial. Initially, a dual function in regulating actomyosin ring dynamics and septin distribution was proposed (Lippincott and Li, 1998). On the other hand, the current model suggests that Hof1p is involved in septum formation and participates in one of the two redundant cytokinetic pathways (Vallen *et al.*, 2000). This notion is based on different lines of evidence. In the first place, chitin deposition in *hof1* null cells is delocalized at the non-permissive temperature (Kamei *et al.*, 1998; Lippincott and Li, 1998; Vallen *et al.*, 2000). Secondly, the only known proteins that localize to the bud neck, in a similar manner as Hof1p, are those that are either components of chitin synthase III (CSIII), such as Chs3p and Chs4p (Chuang and Schekman, 1996; DeMarini *et al.*, 1997), or proteins involved in recruiting CSIII to the bud neck, such as Bni4p (DeMarini *et al.*, 1997). Finally, if the *hof1* deletion caused only a defect in cell separation, digestion of the cell wall would be sufficient to disrupt the formed cell chains, which is not the case (Vallen *et al.*, 2000). In addition to these data, three other pieces of novel evidence were considered by the authors, to conclude a role of Hof1p in septum formation. First they analyzed the localization of Hof1p in the cell cycle, which resulted to be cell cycle regulated, as already mentioned above. Second, they found that *myo1* deletion and *hof1* deletions were synthetically lethal, suggesting that they have parallel roles in cytokinesis. This would be inconsistent with the hypothesis that Hof1p regulates actomyosin contraction. Third and finally, they visualized Myo1p-GFP and septum formation simultaneously in different mutants, which allowed them to analyze the roles of different genes in regulating actomyosin contraction and septum formation. As a result of these analyses the proteins Hof1p, Bni1p, Bnr1p and Myo1p, were dissected into two independent cytokinetic pathways: One, dependent on actomyosin contraction and mediated by Myo1p and Bni1p; and the other one, dependent on septum formation and mediated by Hof1p and Bnr1p (Vallen *et al.*, 2000).

Continuing with the role of Hof1p during cytokinesis, recently the interaction of the Hof1p SH3 domain with Vrp1p, the yeast ortholog of the human Wiskott Aldrich syndrome protein (WASP)-interacting protein, has been characterized. Vrp1p is involved in actin assembly and it is also required for cytokinesis as well as for proper

localization of Hof1p at the bud neck. A novel Hof1 trap domain (HOT) in Vrp1p, composed of three proline-rich motifs, is responsible for this interaction. Apparently the function of this interaction is to prevent a putative negative effect of the Hof1p SH3 domain on cytokinesis (Ren *et al.*, 2005). Recently, it has also been reported that the Hof1p PEST motif interacts with the SCF^{Grr1} complex at the end of mitosis, leading to its degradation by the activity of the 26S proteasome (Blondel *et al.*, 2005). On one hand, this degradation is necessary to allow efficient contraction of the actomyosin ring and cell separation during cytokinesis. On the other hand, the degradation depends on the phosphorylation state of Hof1p, which seems to be altered by the activity of the MEN pathway.

1.3 Cytoskeleton organization and vesicle trafficking in *S. cerevisiae*

In all eukaryotic cells the cytoskeleton plays a central role in the regulation of such critical processes as cell morphogenesis, endocytosis, cell polarity and cytokinesis (Moseley and Goode, 2006). "The cytoskeleton comprises microtubules, intermediate filaments and actin. A distinctive future of microtubules and actin filaments is their rapid dynamics. Their ability to grow and shrink is an important factor for the generation of forces and to allow the rapid reorganization of the cytoskeleton in response to intra- as well as extracellular signals. Although microtubules are involved in the mobilization of large structures within the cytoplasm, cortical events such as polarized cell growth and cell cleavage at cytokinesis generally depend on actin. Actin acts through the formation of localized and specialized structures, rather than through a global control of its dynamic properties. Thus, actin is able to respond to various local signals to fulfill diverse functions" (Norden *et al.*, 2004). These events are driven by the coordinated activities of a set of actin-associated proteins, and numerous upstream signaling molecules (Moseley and Goode 2006). In the first study that described actin organization in *S. cerevisiae* (Adams and Pringle, 1984) two major actin structures present throughout the cell cycle were found, cortical actin patches and actin cables. Actin patches are believed to be associated with plasma membrane invaginations (Mulholland *et al.*, 1994) and contain numerous proteins involved in endocytosis (Schott *et al.*, 2002). Therefore, actin patches would mediate the internalization of plasma membrane domains and extracellular material. On the other hand, actin cables

play a crucial role in intracellular movement of cargo within the cell. In polarized cells, the formins Bni1 and Bnr1 are localized to the bud cortex, participating in both actin cable nucleation and overall polarization of actin cables (Evangelista *et al.*, 1997; Sagot *et al.*, 2002). This in turn would direct the proper transport of vesicles and organelles towards the growing bud.

1.3.1 Exocytosis: The exocyst complex

The activity of polarized actin cables alone is not enough to direct the transport of vesicles to the right position in the plasma membrane. In eukaryotic cells, the docking of exocytic vesicles with the plasma membrane has been shown to involve a protein complex known as the "exocyst". The exocyst complex comprises eight proteins: Sec3p, Sec5p, Sec6p, Sec8p, Sec10p, Sec15p, Exo70p and Exo84p. It was originally described in *S. cerevisiae*, where the exocyst has been shown to be essential for exocytosis. The encoding genes for the six "Sec" proteins, so called because of their inhibited secretion mutant phenotype, were discovered more than two decades ago in two classic genetic screens (Novick and Schekman, 1979; Novick *et al.*, 1980). Later on, these proteins were shown to physically interact with each other, and the exocyst complex containing the six Sec proteins and two additional subunits Exo70p and Exo84p was purified (TerBush *et al.*, 1996). Mammalian homologues have been identified of all eight yeast exocyst proteins (Hsu *et al.*, 1996). "The exocyst proteins localize to regions of active cell surface expansion: The bud tip at the beginning of the cell cycle and the mother-daughter cell connection during cytokinesis. Thus, the exocyst is thought to be involved in directing vesicles to their precise sites of fusion. Although it is clear that the exocyst plays a central role in exocytosis little is known about how it is controlled (Lipschutz and Mostov, 2002)". Nevertheless, it has been shown that many small GTPases regulate the exocyst, including members of the Rho, Rab and RaI (only in mammals) protein families. The first GTPase found to interact with the exocyst was the yeast Sec4p, which is the founding member of the animal Rab family (Guo *et al.*, 1999). Sec4p is essential for post-Golgi events in yeast secretion and genetic analysis suggested that Sec4p acts upstream of the exocyst. The exocyst subunit Sec15p associates specifically with secretory vesicles and interacts with Sec4p-GTP, which is anchored to the surface of the vesicular membrane. Apparently this interaction triggers further interaction between Sec15p and other subunits of the exocyst, eventually leading

to docking and fusion of secretory vesicles with specific domains of the plasma membrane. Another class of GTPases found to interact with the exocyst belongs to the Rho family. Thus, several *rho1* mutants were identified in a screen searching for mutations that affected localization of GFP tagged exocyst proteins (Guo *et al.*, 2001). The effect of Rho1p on the exocyst was found not to be dependent on a reorganization of the actin cytoskeleton, a characteristic function of Rho GTPases. Rather, Rho1p-GTP interacts directly with the Sec3p exocyst subunit, which has been proposed as a landmark that defines polarized domains of the plasma membrane (Finger *et al.*, 1998). "Another Rho family protein, Cdc42p, also interacts with Sec3p, and this interaction is required for the initial targeting of Sec3p to the emerging bud. Both Rho1p and Cdc42p interact with the amino terminus of Sec3p and have been found to compete for Sec3p binding *in vitro*. Therefore, it is possible that *in vivo* Cdc42p and Rho1p interact with Sec3p at different stages of the cell cycle" (Lipschutz and Mostov, 2002). In contrast to Rho1p and Cdc42p, Rho3 was found to associate with a different exocyst subunit, Exo70p (Adamo *et al.*, 1999; Robinson *et al.*, 1999). The effects of mutation in the Rho3p effector domain suggest roles for this protein in regulation of the actin organization, transport of exocytic vesicles to the bud, and docking of vesicles with the plasma membrane (Robinson *et al.*, 1999). On the other hand, vesicle docking was also proposed to be mediated by Exo70p (Adamo *et al.*, 1999).

In summary, the exocyst in conjunction with the actin cytoskeleton plays a central role in several aspects of exocytosis and vesicle traffic, apparently being directed by interactions between specific exocyst subunits and different small GTP-binding proteins.

1.3.2 Endocytosis: Internalization of membrane vesicles

Endocytosis is the membrane trafficking process by which plasma membrane components and extracellular material are internalized into cytoplasmic vesicles and delivered to early and late endosomes, eventually either recycling back to the plasma membrane or arriving at the lysosome/vacuole. Through genetic studies in yeast and biochemical studies in mammalian cells, it has become apparent that multiple cellular processes are linked to endocytosis, including actin cytoskeletal dynamics, ubiquitylation, lipid modification, and signal transduction (Shaw *et al.*, 2001).

The initial events during internalization of membrane vesicles require the coupling of the endocytic process with actin dynamics (Ayscough, 2005). The first evidence for a link between cytoskeleton and cytokinesis in *S. cerevisiae*, came from genetic screens for endocytic mutants (Benedetti *et al.*, 1994; Kubler and Riezman, 1993; Raths *et al.*, 1993). Such screens identified proteins like Sla2p which directly bind to actin, Vrp1p the yeast homologue of the actin regulator verprolin and End7p, which was actin itself (Munn *et al.*, 1995). One characteristic of the endocytic process in yeast is the high degree of functional redundancy revealed by the genetic studies. Thus, the presence of distinct endocytic pathways has been frequently suggested. The presence of a single pathway may compensate, at least in part, for the absence of the other, while disruption of two pathways causes very marked defects in endocytosis (Dewar *et al.*, 2002; Goode and Rodal, 2001).

Actin patches have been found to be associated with membrane invagination sites (Mulholland *et al.*, 1994; Rodal *et al.*, 2005). The colocalization of other actin-binding proteins a this site led to the suggestion that actin may play a role in formation or function of these membrane structures. Indeed, recent data has provided clear evidence for the existence of sequential formation of complex during generation of endocytic vesicles (Kaksonen *et al.*, 2003). Actin-binding proteins and presumably actin itself, are only recruited at the later stages of the process, and following their incorporation, two types of movements are detected, an initial slow movement followed by a fast one. "The timing of the events was found to be extremely reproducible, suggesting both temporal and spatial regulation of complex formation. Each endocytic event, including scission and inward movement is proposed to occur within a time span of 45-60 s. Las17p, the yeast homologue of WASP, is the earliest marker so far tested. It is practically static during its lifetime within the patch. After about 10 s the following proteins enter the patch, the endocytic adaptor Sla1p (a putative Ynl152wp binding partner, see section **1.4.3**), Sla2p and Pan1p, which is an activator of the Arp2/3 complex. These proteins are initially nonmotile (about 10-15 s) but then show some slow movement (about 5 s). This movement occurs shortly after recruitment of actin and actin-binding proteins. Sla1p and Pan1p are then disassembled from the complex, and this is followed by rapid movement of the endocytic vesicle into the cell. This last stage is most variable in time and is thought to represent the time for the vesicle to travel to, and to dock with an endosome" (Ayscough, 2005). The exact role of actin remodeling during endocytosis remains poorly understood. Nevertheless, some proteins likely to function in the actin

remodeling have been identified, though the arrangements that they facilitate are not known. "The Arp2/3 complex belongs to some of the proteins likely to be important. The non-motile, slow and fast movement stages of vesicle formation were each associated with the recruitment of a distinct activator for Arp2/3. In turn, these activators are able to drive polymerization of actin, probably in response to different signals" (Ayscough, 2005). Two other proteins that may play a role in regulating actin structures in these early steps in endocytosis are Myo5p and Sla2p. The endocytic defect and accumulation of invaginations in the *myo5* mutant would be consistent with inefficient scission (Jonsdottir and Li, 2004). On the other hand, a *sla2* deletion results in a significant reduction of fluid-phase endocytosis, and formation of enlarged structures at the membrane that may represent partial arrest of the endocytic process, possibly because the appropriate actin structures can not be formed (Gourlay *et al.*, 2003; Raths *et al.*, 1993). As described for the assembly, it is likely that disassembly of cortical patches occurs in sequential regulated steps. One family of proteins to play a key role in this process are the Ark/Prk protein kinases (Smythe and Ayscough, 2003). The double deletion has a dramatic effect on the organization of actin cytoskeleton, with no detectable uptake of fluid-phase markers such as Lucifer Yellow (Cope *et al.*, 1999; Zeng and Cai, 1999). In such mutants actin-binding proteins and endocytic marker proteins are localized in a single clump in the cell. The data indicate the importance of Ark1p and Prk1p for the turnover of actin-endocytic complexes. In addition, they suggested that proteins remaining within the complex are responsible for the inappropriate polymerization or stabilization of actin. Consistent with this role, in an *ark1/prk1* double deletion, Sla1p is found within the large endocytic-actin clumps (Ayscough *et al.*, 1999). Presumably, if Sla1p remains associated with the invaginating patches, the appropriate remodeling of actin is hampered. Restoration of wild-type Prk1p, but not kinase-dead Prk1p, allows recovery of Sla1p and actin localization as well as resumption of endocytosis. Sla1p and Pan1p are in fact pivotal in this process of cortical patch disassembly. Both proteins have been shown to be substrates of the Ark1p and Prk1p kinases, and for Sla1p it seems that switching on Prk1p activity causes it to disassemble from the complex (Zeng *et al.*, 2001). Thus, phosphorylation of key components of the initial actin-endocytic complex lead to their disassembly from the forming vesicle, allowing its subsequent fast movement away from the plasma membrane. Further progression of the primary endocytic vesicles involves the transfer of the transported components to an early endosome where some proteins are sorted for

recycling back to the plasma membrane. Others continue through the endosomal pathway to the late endosome/pre-lysosome and then to the lysosome where degradation takes place. Early endosomes are peripheral organelles that are heterogeneous in appearance, whereas late endosomes are pre-lysosomal organelles with more spherical morphology, defined by the time it takes for endocytosed macromolecules to be delivered to them (Hicke *et al.*, 1997; Piper and Luzio, 2001; Zeng *et al.*, 2001). "There has been considerable dispute about whether the transport between early and late endosomes is best explained by vesicular transport or by the maturation of early endosomes. While both models provide for an intermediate between both compartments, the difference lies in whether the intermediate is a specific transport vesicle budded from the early endosome or is what remains after removal of components from early endosomes" (Piper and Luzio, 2001). Late endosomes are capable of homotypic fusion reactions with themselves (Antonin *et al.*, 2000) and heterotypic fusions with lysosomes (Luzio *et al.*, 2000). The former may play an important role in morphological remodeling and the latter in creating a hybrid organelle that has been proposed to represent the "cell stomach". Sorting of proteins also takes place within late endosomes and may be dependent of the properties of their trans-membrane domains, or as a result of ubiquitilation. Finally, yeast class E Vps proteins and their mammalian orthologs are the best candidates to make up the machinery that controls the overall inward budding process, which starts in early endosomes (Piper and Luzio, 2001).

1.4 Yeast cell signaling and *YNL152w*

In the following sections, the yeast cell integrity pathway will be shortly described, as well as a previously made genetic screen (Schmitz, 2001), designed to identify putative negative regulators of the pathway. This is necessary to understand the context in which the gene *YNL152w* was identified as a starting point of the work presented here.

1.4.1 The yeast Pkc1p-mediated cell integrity pathway

Cell integrity in the yeast *S. cerevisiae* is ensured by a rigid cell wall composed of glucans, mannoproteins and chitin (Klis *et al.*, 2002). Cell wall remodeling is required under certain physiological conditions (e.g. budding and cell growth or mating) or after disturbances caused by external stresses (e.g. heat or the presence of drugs interfering with cell wall polymers or with the plasma membrane). The latter include Calcofluor white, Congo red and SDS. It is generally assumed that both the physiological conditions and the occurrence of lesions at the cell surface are monitored by a specific signaling pathway in yeast, mediated by the sole protein kinase C present in this simple eukaryotes ("cell integrity pathway"; "Pkc1p pathway"; reviewd in Heinisch *et al.*, 1999; and Levin 2005). Sensors spanning the plasma membrane (such as Slg1p and Mid2p) convey the signal to a small intracellular GTPase, Rho1p (it is important to recall that Rho1p is also involved in actin assembly and secretion, as already mentioned). Via its GEF Rom2p (and presumably Rom1p to a minor extent) Rho1p is converted to its GTP-bound state and activates the protein kinase C (Pkc1p). This in turn activates a typical MAP kinase (<u>M</u>itogen <u>A</u>ctivated <u>P</u>rotein kinase) cascade, ultimately leading to the phosphorylation of the transcription factors Rlm1p and SBF whose targets are genes involved in cell wall biosynthesis and cell cycle control, respectively (Levin, 2005).

Several questions in this model still remain to be answered: 1) The molecular nature of the signal and the exact mode of action of the sensors has not yet been determined. 2) Although the components resulting in an activation of the signaling pathway have been described, those leading to a down-regulation upon removal of the stress basically remain elusive. 3) Since septum formation and cytokinesis requires a massive remodeling of cell wall components and architecture (e.g. the bulk of chitin present in the yeast cell wall is recruited to the site of budding), a cross-talk between septum formation and the Pkc1p-pathway should exist.

1.4.2 Identification of the *YNL152w* ORF during a genetic screen

In preliminary experiments a genetic screen was designed to isolate mutants with a defect in the down-regulation of the Pkc1p-signaling pathway (Schmitz, 2001). This screen was based on a construct encoding a fusion protein of the transcription factor
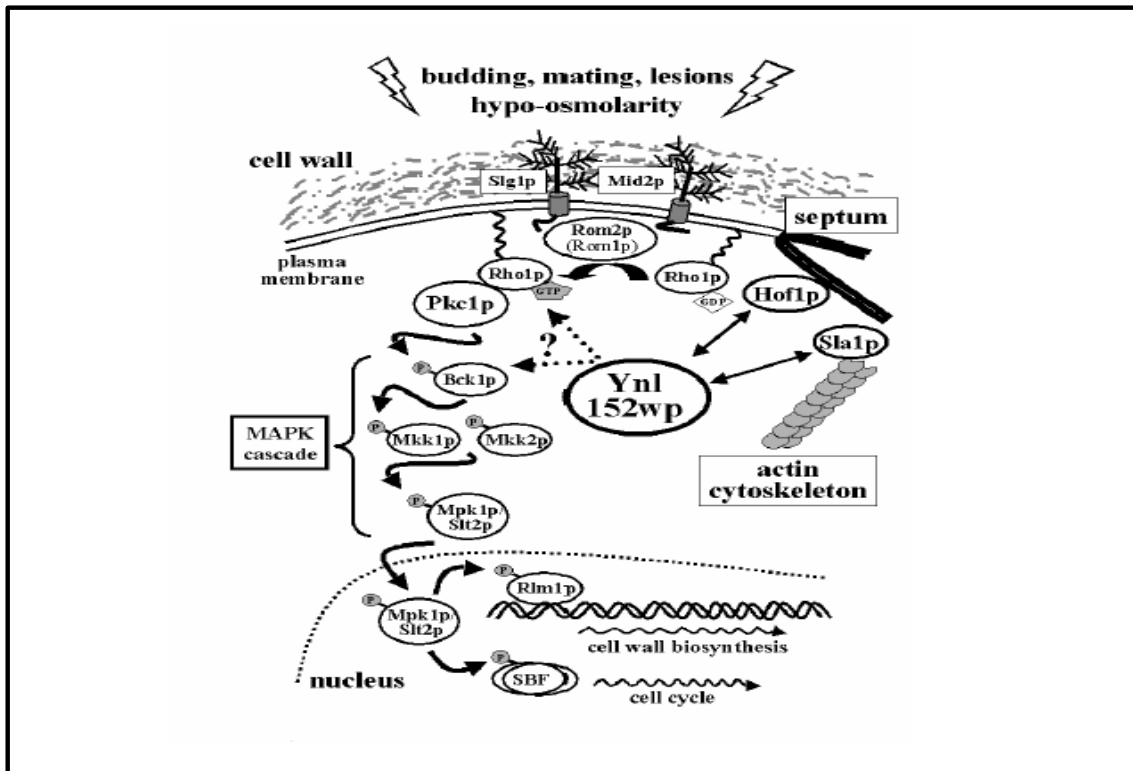
Fig. 1.4 Representation of the Pkc1p-mediated cell integrity pathway in *S. cerevisiae*. The picture also shows Ynl152wp whose encoding gene was isolated during a genetic screen searching for putative negative regulators (Schmitz, 2001). Genome-wide two-hybrid analyses indicated an interaction with Hof1p and Sla1p, which are involved in septum formation and actin dynamics, respectively (modified from Heinisch 2005).

Rlm1p with the bacterial *lexA*-DNA-binding domain, which confers transcriptional activation to a reporter gene (*lacZ*) only after phosphorylation by the MAP kinase of the pathway (Mpk1p; **Fig. 1.4**). Transposon-insertion mutants with enhanced expression of the reporter gene under standard growth conditions were isolated and characterized. One of them contained the transposon insertion at the 3'-end of the gene *YNL152w*, which

has not been investigated yet. The insertion leads to a loss of the C-terminal 8 amino acids of the encoded protein, which are substituted by a sequence of unrelated amino acids introduced by the transposon insertion. As expected from the design of the screen, the mutant strain (named Tn24) is still viable. In contrast, a complete deletion of the gene has been reported to be lethal under standard growth conditions (http://www.yeastgenome.org/).

1.4.3 Characteristics of the *YNL152w* ORF and its predicted protein

Virtually all the information available for the *YNL152w* gene and its predicted protein comes from genome-wide studies and is accessible at the yeast genome database (http://www.yeastgenome.org/). *YNL152w* codes for a putative protein of 409 amino acids and is required for cell viability (Giaever *et al.*, 2002). Thus, the encoded protein must play an essential role. The domain structure of Ynl152wp shows a putative phospholipid-binding domain (C2) close to the N terminus (**Fig. 1.5**).
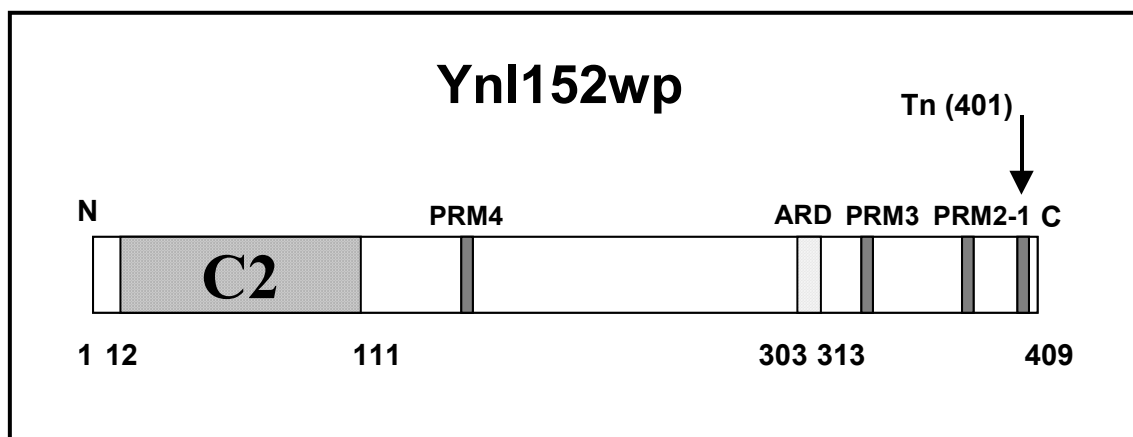
Fig. 1.5 Domain structure of the protein Ynl152wp showing a C2 phospholipid like binding domain close to the N terminus, and an aspartate-rich domain (ARD) between amino acids 303-313. During a BLAST homology search, also 4 proline rich motifs (PRM) were identified. The arrow is pointing the insertion site of the transposon in the mutant strain Tn24, isolated during a genetic screen (Schmitz, 2001).

Based on the homology, a phospholipid-binding activity was proposed (Hazbun *et al.*, 2003), however, no biochemical evidence has been provided so far. Between amino acids 303-313, an aspartate rich domain (ARD) with unknown functional relevance has been identified.

In genome-wide two-hybrid studies, two proteins have been shown to interact with Ynl152wp. One is Sla1p (Tong *et al.*, 2002), which is involved in endocytosis and actin dynamics, the other one is Hof1p which participates in cytokinesis and septum formation (described in **1.2.5**). The latter has been identified in two independent screens (Ito *et al.*, 2001; Tong *et al.*, 2002). Interestingly both proteins bear one (Hof1p) or more (Sla1p) SH3 domains and seem to be functionally related. Together, this would suggest an affinity of Ynl152wp for SH3 domains and also provide a hint for its function. Indeed, four proline-rich motifs (PRM), which in principle can bind to SH3 domains (Tong *et al.*, 2002) were identified in a Ynl152wp BLAST homology search (**Fig. 1.5**). Considering the protein localization, a C-terminal *YNL152w*-GFP fusion was found more or less homogenously distributed in the cytoplasm (Huh *et al.*, 2003). Although the protein localization is usually a clue for its function, in this case, it is not very informative.

1.5 Aims of the thesis

YNL152w is necessary for cell viability under standard growth conditions (Giaever *et al.*, 2002). It was also identified in a genetic screen designed to isolate mutants with an enhanced activity of the Pkc1p pathway (Schmitz, 2001), hence it is potentially involved in its down-regulation. On the other hand, two independent genome-wide two-hybrid studies, found the protein Hof1p as a putative binding partner of Ynl152wp (Ito *et al.*, 2001; Tong *et al.*, 2002). Hof1p is involved in the cytokinesis process and in septum formation (Vallen *et al.*, 2000). Finally, since Pkc1p is activated by structural changes or stresses applied to the cell wall (Heinisch *et al.*, 1999), there should be a connection between septum deposition during cytokinesis and the activation of the pathway. Therefore, this thesis aimed to:

1) Further characterize the essential *YNL152w* ORF.

2) Examine the potential connection between the Pkc1p pathway and the *YNL152w* gene.

3) Investigate a possible role of *YNL152w* in cytokinesis in correlation with the protein Hof1p, involved in this process.

2. Materials and Methods

2.1 Materials

2.1.1 Chemicals, materials and enzymes

2.1.1.1 Chemicals

Acetic acid (Riedel-de Haen, Seelze), Adenine (Serva, Heidelberg), Agar (Invitrogen, Paisley), Ultrapure- agarose (Invitrogen, Paisley), Ampicillin-sodium salt (Serva, Heidelberg), L-Alanine (Fluka, Buchs), L-Arginine (Serva, Heidelberg), Bromphenolblue (Serva, Heidelberg), BSA [bovine serine albumin] (Serva, Heidelberg), Caffeine (Serva, Heidelberg) Calcium chloride (Riedel-de Haen, Seelze), Hydrochloric acid (Riedel-de Haen, Seelze), DAPI staining (Invitrogen Molecular Probes, Leiden), dNTP-mix (Roche, Mannheim), Dimethylformamide (Merck, Darmstadt), Ethanol (Riedel-de Haen, Seelze), Ethidium Bromide (Appli Chem, Darmstadt), Hering sperm DNA (Roche, Mannheim), 5-Fluoroorotic acid (Fermentas, St. Leon-Rot), Formaldehide (Sigma, Steinheim), G418-sulfate (CALBIOCHEM-NOVABIOCHEM (UK) LTD, Beeston, Nottingham), Galactose (Serva, Heidelberg), Glucose (Serva, Heidelberg), Glycerol (Appli Chem, Darmstadt), Glycin (Riedel-de Haen, Seelze), L-Histidine (Serva, Heidelberg), IPTG (Roth), (L-Isoleucine (Serva, Heidelberg), Isopropanol (Fluka, Buchs), Kanamycin (Serva, Heidelberg), Lambda-DNA (Fermentas, St. Leon-Rot), L-leucine (Serva, Heidelberg), Lithium acetate (Roth, Karlsruhe), L-Lysine (Serva, Heidelberg), Magnesium chloride (Merck, Darmstadt), Magnesium Sulfate (Riedel-de Haen, Seelze), Manganese chloride (Fluka, Buchs), L-Methionine (Serva, Heidelberg), ONPG [o-Nitrophenyl-β-D-Galactopyranoside] (Serva, Heidelberg), Peptone (BACTO^{TM}), DL-Phenylalanine (Serva, Heidelberg), Polyethylenglycol 4000 (Roth, Karlsruhe), Potassium acetate (Riedel-de Haen, Seelze), Potassium chloride (Merck, Darmstadt), Raffinose (Serva, Heidelberg), Rubidium chloride (Fluka, Buchs), Sodium acetate (Merck, Darmstadt), Sodium Carbonate (Riedel-de Haen, Seelze), Sodium chloride (Riedel-de Haen), Sodium citrate (Serva, Heidelberg), Sodium hydroxide (Riedel-de Haen, Seelze), Sodium perchlorate (Riedel-de Haen, Seelze), Sodium phosphate (Riedel-de Haen, Seelze), D-Sorbitol (Serva, Heidelberg), Sytox Green (Invitrogen Molecular Probes, Leiden), L-Threonine (Serva, Heidelberg), Tris (Riedel-de Haen), Tryptone (BACTO^{TM}), L-Tryptophan (Sigma, Steinheim), L-Tyrosine (Serva, Heidelberg), Uracil (Serva, Heidelberg), L-Valine (Serva, Heidelberg), YNB w/o amino acids (Difco^{TM}), X-Gal (Appli Chem, Darmstadt), Yeast extract (BACTO^{TM}).

2.1.1.2 Materials

Expand "TM High Fidelity PCR System" (Roche, Mannheim), Glass beads (Roth, Karlsruhe), "High Pure Plasmid Isolation Kit" (Roche, Mannheim), "High Pure PCR Product Purification Kit" (Roche, Mannheim). Non-fluorescent microspheres for FACS

calibration (Invitrogen, Leiden).

2.1.1.3 Enzymes

The restriction enzymes used in this work were from Roche (Mannheim) or from MBI Fermentas (St. Leon-Rot). Besides, the following enzymes were used: Alkaline phosphatase (Roche, Mannheim), T4 DNA-ligase (Roche, Mannheim), Zymolyase (Seikagaku Kogyo Co., Tokio) and β-glucuronidase/arylsulfatase (Roche, Mannheim).

2.1.2 Strains and media

2.1.2.1 *Saccharomyces cerevisiae* strains

Strain	Genotype	Source
MCH-7B	*MATα ura 3-52 leu2-3,112 his3-11,15 Δtrp1::loxP MAL SUC GAL*	Jacoby *et al.*, 1999
MCH-22D	*MATa/MATα ura 3-52/ura 3-52 leu2-3, 112/leu2-3,112 his3-11,15/ his3-11,15 Δtrp1::loxP/ Δtrp1::loxP MAL/MAL SUC/ SUC GAL/GAL* (correspondent diploid strain from MCH-7B)	J. Heinisch
HD56-5A	*MATα ura 3-52 leu2-3,112 his3-11,15*	Arvanitidis and Heinisch, 1994
DHD5	*MATa/MATα ura 3-52/ura 3-52 leu2-3, 112/leu2-3, 112 his3-11, 15/ his3-11, 15* (correspondent diploid strain from HD56-5A)	J. Heinisch
GAL1-YNL152w	*MATa or α ura 3-52 leu2-3, 112 his3-11, 15 YNL152w::GAL1/10p-YNL152w (KanMX)*	R. Rodicio and this work *
MCH-22D-Δynl152w	*MATa/MATα ura 3-52/ura 3-52 leu2-3, 112/leu2-3, 112 his3-11, 15/ his3-11, 15 Δtrp1::loxP/ Δtrp1::loxP MAL/MAL SUC/ SUC GAL/GAL YNL152w/Δynl152w:: KanMX*	A. Straede

* = The construct was made by R. Rodicio and the tetrad analysis in this work.

Strain	Genotype	Source
TN24	*MATα ynl152w::mTN3 ura3-52 leu2-3, 112 his3-11,15 ∆trp1::loxP MAL SUC GAL*	H.P. Schmitz, 2001

In the following C-terminal *ynl152w*-deletion series (derived from heterozygous DHD5) only the haploid strains are shown. Homozygous diploid strains were constructed by crossing.

Strain	Genotype	Source
YNL3	*MAT**a** or α ura 3-52 leu2-3, 112 his3-11, 15 ynl152w:: ynl152w∆3 (KlLEU2)*	R. Rodicio
YNL8	*MAT**a** or α ura 3-52 leu2-3, 112 his3-11, 15 ynl152w:: ynl152w∆8 (KanMX)*	R. Rodicio
YNL17	*MAT**a** or α ura 3-52 leu2-3, 112 his3-11, 15 ynl152w:: ynl152w∆17 (KlLEU2)*	R. Rodicio
YNL30	*MAT**a** or α ura 3-52 leu2-3, 112 his3-11, 15 ynl152w:: ynl152w∆30 (KlLEU2)*	R. Rodicio
YNL42	*MAT**a** or α ura 3-52 leu2-3, 112 his3-11, 15 ynl152w:: ynl152w∆42 (KlLEU2)*	R. Rodicio
YNL90	*MAT**a** or α ura 3-52 leu2-3, 112 his3-11, 15 ynl152w:: ynl152w∆90 (KlLEU2)*	R. Rodicio
YNL150	*MAT**a** or α ura 3-52 leu2-3, 112 his3-11, 15 ynl152w:: ynl152w∆150 (KlLEU2)*	R. Rodicio
YNL250	*MAT**a** or α ura 3-52 leu2-3, 112 his3-11, 15 ynl152w:: ynl152w∆250 (KlLEU2)*	R. Rodicio
YNL270	*MAT**a** or α ura 3-52 leu2-3, 112 his3-11, 15 ynl152w:: ynl152w∆270 (KlLEU2)*	R. Rodicio
TN24-RLM1	*MAT**a**/α YNL152w/ynl152w::mTN3 RLM1 /rlm1::lexA-RLM1-lacZ (KlLEU2)ura3-52/ ura3-52 leu2-3,112/ leu2-3,112 his3-11/ his3-11,15 TRP1/∆trp1::loxP MAL SUC GAL* (segregants from this strain were used)	R.Rodicio and this work

Strain	Genotype	Source
YNL42-RLM1	*MAT**a**/α YNL152w/ynl152w::ynl152wΔ42 (KlLEU2) /rlm1::lexA-RLM1-lacZ (KlLEU2) ura3-52/ ura3-52 leu2-3,112/ leu2-3,112 his3-11/his3-11,15 TRP1/Δtrp1::loxP MAL SUC GAL (segregants from this strain were used)*	R.Rodicio and this work *
YNL150-RLM1	*MAT**a**/α YNL152w/ynl152w::ynl152wΔ150 (KlLEU2) /rlm1::lexA-RLM1-lacZ (KlLEU2) ura3-52/ ura3-52 leu2-3,112/ leu2-3,112 his3-11/his3-11,15 TRP1/Δtrp1::loxP MAL SUC GAL (segregants from this strain were used)*	R.Rodicio and this work *
YNLΔASP	*MAT**a** or α ura 3-52 leu2-3, 112 his3-11, 15 HOF1::HOF1-GFP (KanMX) ynl152w:: ynl152wΔAsp(KlLEU2)*	R. Rodicio
HOF1-GFP	*MAT**a**/α ura 3-52 leu2-3, 112 his3-11, 15 HOF1::HOF1-GFP (KanMX)*	Invitrogen
YNL42-HOF1GFP	*MAT**a** or α ura 3-52 leu2-3, 112 his3-11, 15 HOF1::HOF1-GFP (KanMX) ynl152w:: ynl152wΔ42 (KlLEU2)*	This work *
YNL90-HOF1GFP	*MAT**a** or α ura 3-52 leu2-3, 112 his3-11, 15 HOF1::HOF1-GFP (KanMX) ynl152w:: ynl152wΔ90 (KlLEU2)*	This work *
YNL150-HOF1GFP	*MAT**a** or α ura 3-52 leu2-3, 112 his3-11, 15 HOF1::HOF1-GFP (KanMX) ynl152w:: ynl152wΔ150 (KlLEU2)*	This work *
YNLASP-HOF1GFP	*MAT**a** or α ura 3-52 leu2-3, 112 his3-11, 15 HOF1::HOF1-GFP (KanMX) ynl152w:: ynl152wΔAsp(KlLEU2)*	This work *
GAL1-GFPYNL	*MAT**a** or α ura 3-52 leu2-3, 112 his3-11, 15 ynl152w::GAL1/10-GFP-YNL152w (KanMX)*	This work *
LD3R-7B	*MAT**a** leu1 SUC3 mal0*	S. Hohmann

* = These strains were obtained by crossing and tetrad analysis.

Strain	Genotype	Source
SMC-19A	*MATα leu1 MAL2-8^c*	F. Zimmermann

2.1.2.2 Yeast media

Rich medium (YEP): 1 % yeast extract, 2 % peptone

Carbon source:

YEPD: 2 % glucose

YEPGal: 2 % galactose

YEPRaf: 2 % raffinose

YEP-glycerol-ETOH: 2 % glycerol-1 % ethanol

Synthetic medium: 0.67 % Yeast Nitrogen Base w/o amino acids (YNB)

Amino acids as described by Zimmermann (1975)

Carbon source: 2 % glucose, 2 % galactose or 2 % raffinose

pH = 6.3

Sporulation medium: 1 % potassium acetate, pH = 6.0

The plates were made with the addition of 1.5 % agar. Cultivation was at 30 °C unless otherwise stated. Caffeine was added after autoclaving the medium as a preheated (60 °C) solution to reach the desired final concentration in the plate. 5-FOA plates were made with synthetic medium without uracil. After autoclaving, the media is cooled down at about 55 °C and the 5-FOA powder is added at a final concentration of 1mg/ml.

2.1.2.3 Storage of the yeast strains

Yeast strains were stored in agar plates at 4 °C and approximately every two months replaced by fresh plates. The strain collection was also preserved in glycerol cultures. 0.5 ml of an overnight culture were added to 1 ml of 33 % sterile glycerol solution and stored at –80 °C.

2.1.2.4 *E.coli* strains and culture conditions

    E. coli strain DHD5α from Stratagene (F´*glnV44 thiA*-1 Δ*(argF-lac)* U169 *deoR endA1 gyrA96 hsdR17 recA1 supE44* (Ø80lacZΔM15) Nal^r) was used.

Rich medium composed of 1 % tryptone, 0.5 % yeast extract, 0.5 % NaCl was utilized. The plates were made with the addition of 1.5 % agar. Cultivation was made at 37 °C. For preparation of selective media, ampicillin was added to a final concentration of 100 µg/ml when selecting for ampicillin resistance and kanamycin to 20 µg/ml when selecting for kanamycin resistance. For blue/white screens, 100 µl of an IPTG/X-Gal solution (2.4 mg/ml IPTG, 10 mg/ml X-Gal dissolved in Dimethylformamide) were spread before plating of the transformants.

2.1.3 Plasmids

2.1.3.1 Plasmid collection

E. coli			
Name	**Selection marker/ Replication origin**	**Description**	**Source**
pUK1921	*Kan^R* *ori*	*E. coli*-cloning vector	Heinisch, 1993
S. cerevisiae			
pJJH447	*Amp^R* *ori* *URA3* *2μ*	YEp352-derivative, carrying the *GAL1/10* promoter	Heinisch

2.1.3.2 Plasmid construction

Name	Vector restriction	Insert description	restriction
pUK1921-ynl∆Asp	*Bam*HI/*Sph*I	PCR product from YNL∆ASP DNA performed with primers 03.05 and 03.06	*Bam*HI/*Sph*I
pJJH447-YNL152w	*Bam*HI/*Sph*I	PCR product from genomic DNA performed with primers 03.05 and 03.06	*Bam*HI/*Sph*I

2.1.4 Oligonucleotides

Number	Name	Sequence
00.53	leu2- 3´out	5´-GCCGAAGAAGTTAAGAAAATCCTTGC-3´
03.05	YNL152end Sph	5´-GGGCGCATGCGAAGAGGCCGCCTTTTAGTTG-3´
03.06	YNL152start Bam	5´-GGCAGGATCCATGTCCGAAGAAGTATGGATGG-3´
03.07	YNL152del 5´(Xba)	5´-GGTCGCCCACCTTGTATTGCACGGG-3´
03.44	KanMX-3´ out	5´-GGTCGCCCACCTTGTATTGCACGGG-3´
03.45	KanMX-5´ out	5´-GGAATTTAATCGCGGCCTCG-3´
04.33	YNL152th vor	5´GGCGGGTACCATATGTCCGAAGAAGTATGGAAG-3´

Number	Name	Sequence
04.34	**YNL152th nach**	5´-GGCGCTGCAGGTTTAGATCGGCGGTGAGGG-3´
04.35	**YNL152th Bam**	5´-GGCGGGATCCATATGTCCGAAGAAGTATGGAAT GG -3´
04.57	**YNL152seq1**	5´-GGCACTATATTCATTGAGTTG-3´
04.58	**YNL152seq2**	5´ -CGAATACAAAATTCCATTTTGCC-3´
05.25	**KlLEU2raus3**	5´ -GGTATGCTTGAAATCTCAAGG-3´
05.26	**YNLdelD forward**	5´-CCGCAGATCTGAAAATGACGCATTTTATTCTTCC -3´
05.27	**YNLdelD reverse**	5´-CCGCAGATCTTTCGTCGTAAGACAACGAAGTTA CACC-3´

2.2 Methods

2.2.1 Transformation

2.2.1.1 Transformation of *E. coli*

Transformation of *E. coli* was performed with the Rubidium chloride method (Hanahan *et al.*, 1991).

2.2.1.2 Transformation of *S. cerevisiae*

Transformation of *S. cerevisiae* was performed with the lithium-acetate method (Gietz *et al.*, 1995).

2.2.2 Sporulation, tetrad analysis and determination of the mating type

For sporulation, the desired diploid strain was first grown overnight in 3-5 ml YEPD at 30 °C. Cells were centrifuged in a table-top centrifuge at 3,000 rpm for 5 min and after re-suspention in 0.5 ml sterile water, dropped on a 1% potassium acetate plate. After 2-3 days at 30 °C cells were examined under the microscope to detect the appearance of tetrads. The sporulating cells were then re-suspended in 500 µl distilled water and incubated 10-15 min in presence of 5µl β-glucuronidase/arylsulfatase (Roche, Mannheim). The spores were dissected on 1.5 % agar plates, using a Micromanipulator instrument (Singer MSM system series 300). After tetrad dissection, the different strain's markers were checked by replica-plating on the correspondent auxotrophic plate. The mating type was determined by crossing with two tester strains (LD3R-7B [*MATa leu1*] SMC-19A [*MATα leu1*]). After one day incubation at 30 °C, cells were replicated on to synthetic medium without amino acids. Under such conditions only diploids are able to grow, and the mating type could be inferred.

2.2.3 Serial dilution assays

The serial dilution assays were performed as follows. Cells were grown overnight in the corresponding liquid media at 30 °C. After determination of the OD_{600} (Beckman Coulter spectrophotometer DU 800), the overnight cultures were diluted to an OD of 0.2 and grown at 30 °C for another 6 h. Cultures were diluted again to an OD of 0.2, and progressive dilutions of 10^{-1}, 10^{-2}, 10^{-3}, 10^{-4} were made. 5 µl of each dilution together with the undiluted culture were dropped on to the different media. Plates were incubated for up to 6 days at 30 °C. To monitor the growth of the cells, pictures of the plates were obtained with a scanner after variable incubation times.

2.2.4 Growth curves

2.2.4.1 Growth curves in rich medium

5 ml YEPD pre-cultures were inoculated and grown overnight. The overnight cultures were then used to inoculate at an initial OD_{600} of 0.2, 20 ml of YEPD contained in 100 ml Erlenmeyer flasks. After determination of the initial OD_{600} (t_0), the cultures

were grown with shaking (150 rpm) at 30 °C and aliquots were taken at different intervals to determine the OD_{600} (Beckman Coulter spectrophotometer DU 800).

.

2.2.4.2 Growth curves in media with different carbon sources

Growth curves with *YNL152w* expressed under the control of the inducible *GAL1/10* promoter, were performed in YEP plus 2% glucose (YEPD), raffinose (YEPRaf) or galactose (YEPGal) as carbon sources. YEP and the sugar solutions were autoclaved independently, and mixed together shortly before inoculation. Pre-cultures of 5ml YEPRaf were inoculated and grown overnight. After determination of the OD_{600} the overnight cultures were centrifuged at 5,000 rpm for 3min (Heraeus Megafuge) and cells were washed 3 times in sterile water. They were re-suspended in 1ml of sterile water and then inoculated at an initial OD_{600} of 0.2 in 20 ml of YEPGlc, YEPRaf and YEPGal in 100 ml Erlenmeyer flasks. Cultures were grown in a shaker (150 rpm) at 30 °C and aliquots were taken at different intervals to determine the OD_{600} (Beckman Coulter spectrophotometer DU 800).

2.2.5 Analysis of DNA

2.2.5.1 Preparation of plasmid DNA from *E. coli*

Plasmid-DNA from *E. coli* was isolated using the "High Pure Plasmid Isolation Kit" (Roche, Mannheim), according to the manufacturer's instructions.

2.2.5.2 Preparation of plasmid DNA from *S. cerevisiae*

To prepare plasmid DNA from yeast, 5 ml overnight cultures were centrifuged at 3,000 rpm for 3 min in a table-top centrifuge; the pellet was re-suspended in 250 µl suspension-buffer from the "High Pure Plasmid Isolation Kit" (Roche, Mannheim). After adding 100 µg of glass beads, the cells were broken by shaking for 3min in a "IKA-Vibrax-VXR" at 4 °C. The following steps were performed according to the manufacturer's instructions for the isolation of plasmid-DNA from *E.coli*. The plasmid-DNA was eluted in 30 µl elution buffer and 10 µl were used to transform *E. coli*.

2.2.5.3 Preparation of chromosomal DNA from *S. cerevisiae*

Cells from a 3 ml overnight culture were centrifuged at 4,000 rpm for 3 min in a table-top centrifuge, and the pellet re-suspended in 300 µl spheroplast-buffer (50 mM NaPO$_4$ buffer, 0.9 M sorbitol and 0.1 M EDTA). The cell-wall was enzymatically digested by 1 h incubation at 37 °C with 10 µl zymolyase 100 T (2.5mg/ml). Then, a 30 min incubation at 65 °C was performed in the presence of 50 µl 0.5 M EDTA and 50 µl 10 % w/v SDS solution. After 5 min cooling at room temperature, 150 µl 5 M KAc (pH = 8.6) was added. The cell lysate was incubated for 1h on ice and centrifuged at 10,000 rpm for 10 min to remove the cell debri. To precipitate the DNA, 500 µl of the supernatant were mixed with 340 µl of isopropanol and incubated for 5 min at room temperature, before centrifugation at 13,000 rpm for 15 min. The sediment was re-suspended in 100 µl DNAse-free RNAse-solution (50 mM Tris-HCl, 10 mM EDTA, 0,2 mg/ml RNAse H and 150 mM sodium acetate) and incubated for 30 min at 37 °C. After adding, 10 µl of 3 M sodium acetate and 250 µl pure ethanol, the DNA was precipitated again (15 min 13,000 rpm centrifugation). A washing Step with 70 % ethanol was performed and the DNA was finally dissolved in 50 µl of sterile water and stored at –20 °C.

2.2.5.4 Isolation of DNA fragments from agarose gels

To isolate specific DNA fragments after a restriction, the desired fragment was first separated by electrophoresis on a 0.7 % agarose gel and then cut under a UV lamp (λ = 312 nm). Later on the DNA fragment was purified using the "QIAquick Gel Extraction" kit (Quiagen) or the "High Pure PCR Product Purification Kit" (Roche, Mannheim) following in each case the instructions provided by the manufacturer.

2.2.5.5 Purification of PCR products

The PCR products were purified using the "High Pure PCR Product Purification Kit" (Roche, Mannheim), following the instructions provided by the manufacturer.

2.2.5.6 Manipulation of DNA

2.2.5.6.1 Restriction, dephosphorylation and ligation of DNA

Restriction, dephosphorylation and ligation of DNA were all performed according to the instructions provided by the enzyme's manufacturers.

2.2.5.6.2 Separation of DNA fragments by gel electrophoresis

The analysis of DNA fragments was performed by agarose gel electrophoreses. DNA fragments were separated in 0.7 % agarose-gels (dissolved in $1 \times$ TAE or $1 \times$ TBE buffer). As running buffer 1×TAE (40 mM Tris pH = 8, 20mM acetic acid and 2 mM EDTA-sodium salt) or 1×TBE (89 mM Tris pH = 8.3, 89 mM boric acid and 2 mM EDTA Na_2-salt) was used. A mixture of λ-DNA digested with *Hind*III and with *Eco*RI/ *Hind*III was used as a size marker for the DNA bands. The DNA bands were visualized by incubation of the agarose gel in a 0.5 μg/ml ethidium bromide solution, and exposition to UV light (λ = 366 nm),

2.2.5.7 Sequencing of plasmid DNA

The sequencing service was provided by the ZMG-Center for Medical Genetics Osnabrück (www.*genetik-osnabrueck.de*). The plasmid DNA was prepared with the "High Pure Plasmid Isolation Kit" (Roche, Mannheim). The DNA sample was delivered together with the chosen primers, the latter with a concentration of 10 pmol/μl as requested.

2.2.5.8 Polymerase chain reaction (PCR)

The PCR reactions were performed using the "Expand[TM] High Fidelity PCR System" from the company Roche Applied Sciences, Penzberg. The reaction mix was composed of 250 μM from the dNTP mix, 0.25 pmol/μl of oligonucleotides and 2.75 mM of $MgCl_2$ in a final volume of 50 μl. 1 μl of the DNA polymerase (3.5 U/μl) was added before starting the PCR program. The latter consisted in an initial step of 3 min at 95 °C, followed by 35 cycles with a denaturing step of 50 sec at 94 °, an annealing step of

90 sec at 58 °C and an elongation step at 72 °C with the time adjusted to one minute per 1.2 Kb of template DNA. After the last cycle, a final elongation step of 20 min at 72 °C was added to complete the incomplete double strand synthesis.

2.2.6 β-galactosidase activities

2.2.6.1 Preparation of crude extracts

Initially, 5 ml of YEPD or YEPD/1 M sorbitol were inoculated and grown overnight. Afterwards the overnight cultures were used to inoculate 25 ml of YEPD or YEPD/1 M sorbitol, at an initial OD_{600} of 0.25. The YEPD cultures were grown for 6 h at 37 °C (Pkc1p-pathway inducing conditions) whereas the YEPD/1 M sorbitol cultures were grown at 30 °C (Pkc1p-pathway non-inducing conditions). After determination of the OD_{600} the cultures were centrifuged at 2,500 rpm for 2 min (Heraeus Megafuge), followed by two washing steps in 3 ml distilled water. The pellet was re-suspended in 0.5 ml 50 mM potassium phosphate buffer pH = 7 and 0.5 g of glass beads were added. Afterwards, cells were mechanically broken by shacking the tubes for 10 min in a "IKA-Vibrax-VXR" at 4 °C. Then, 0.5 ml of 50mM potassium phosphate buffer was added and the liquid content was transferred to a microfuge tube and centrifuged at 4 °C with 13,000 rpm for 10 min in a microfuge. Finally, the crude extracts (supernatant) were obtained and stored at 4 °C and the pellet was discarded.

2.2.6.2 Determination of the protein concentration

The protein concentration of the crude extracts was determined by the Biuret method. 50 µl of the crude extract were added to a 1.5 ml microfuge tube containing 950 µl distilled water and 500 µl of the Biuret reagent (10 N NaOH, 1 % copper sulfate). After 20 min incubation at room temperature, the absorbance was measured against a blank at 290 nm (Beckman Coulter spectrophotometer DU 800). Using a conversion factor (obtained with BSA as standard) the absorbance values were converted to protein concentration values in mg/ml.

2.2.6.3 Determination of specific β-galactosidase activities

To quantify the β-galactosidase activities in crude extracts, 950 µl of preheated (30 °C) *lacZ* buffer (60 mM Na_2HPO_4, 40 mM NaH_2PO_4, 10 mM KCl, 1 mM $MgSO_4$, 1 mg/ml ONPG [o-Nitro phenyl-β-D-Galactopyranoside], pH 7.0), were mixed with 50 µl of crude extract and incubated at 30 °C until yellow colour developed. The reaction was stopped by the addition of 500 µl 1 M Na_2CO_3, and the absorbance of the samples was measured against a blank at 420 nm (Beckman Coulter spectrophotometer DU 800).

2.2.6.4 Specific activities

The specific β-galactosidase activities were calculated with the following formula:

$$\text{Specific activity (mU/mg protein)} = \frac{1,000 \times A \times V_{total}}{min \times \varepsilon \times m_{protein} \times V_{ce} \times d}$$

A = Absorption at 420 nm

ε = Extinction coefficient (for o-Nitro phenol $\varepsilon = 4.5 \times 10^3$ M^{-1} cm^{-1})

V_{total} = total volume in the reaction mix (1500 µl)

V_{ce} = volume of the crude extract (µl)

d = Path length of the cuvette (1 cm)

$m_{protein}$ = protein concentration of the crude extract (mg/ml)

min = reaction time in minutes

2.2.6.5 Qualitative β-galactosidase plate assays

As a fast way to qualitatively assess β-galactosidase activity in cell patches, they were replicated on an test plate composed of synthetic media plus 20 mM potassium phosphate buffer pH = 7.0. Previous to the replication, 100 µl of an X-Gal solution (2 % w/v X-Gal dissolved in DMF) were spread on the test plate and incubated for around 15 min at room temperature. The replicated test plate was first incubated at 30 °C for one day, and then transferred to 37 °C for one to two days, until the blue colour developed.

2.2.7 Cell imaging and microscopy

2.2.7.1 Bright field microscopy

To visualize dividing yeast cells with bright field microscopy, cultures in YEPD or synthetic medium (the latter for fluorescence microscopy) were inoculated and grown overnight at 30 °C unless otherwise stated. The overnight cultures were used to re-inoculate at an initial OD_{600} of 0.2 and when the cultures reached an OD_{600} between 0.6-0.8 (early logarithmic phase), 3 µl of the sample were spread on a slide and observed under the microscope (Zeiss Axioplan2 Imaging). Samples were first visualized with the $10 \times$ objective to facilitate the focus and pictures were obtained with an installed camera ("COOL SNAP^{TM} HQ" Photometrics) using the $100 \times$ objective.

2.2.7.2 Fluorescence microscopy

2.2.7.2.1 Visualization of GFP labeled proteins

To visualize GFP labeled proteins, yeast cells were first grown overnight in synthetic medium at 30 °C. The overnight cultures were used to re-inoculate at an initial OD_{600} of 0.2. Once the cultures reached an OD_{600} between 0.6-0.8, 3 µl of the sample were spread on a slide and observed under the fluorescence microscope (Zeiss Axioplan2 Imaging) using the GFP filter and adjusting the exposition time to the signal. Pictures were obtained with an installed camera ("COOL SNAP^{TM} HQ" Photometrics) using the $100 \times$ objective.

2.2.7.2.2 Visualization of DAPI stained cells

Yeast cells were grown overnight in synthetic medium at 30 °C. 1 ml from the overnight cultures was centrifuged at 3,000 rpm for 5 min in a table-top centrifuge. After discarding the supernatant, the pellet was re-suspended in 500 µl 70 % ethanol and incubated for 5 min in the presence of 1 µl of the DAPI (5 mg/ml) fluorescent dye. Two washing steps were performed with 1 ml sterile water and the cells were finally re-suspended in 1 ml sterile water. 3 µl of the sample were spread on a slide and observed under the fluorescence microscope (Zeiss Axioplan2 Imaging) using the DAPI filter and

adjusting the exposition time to the signal. Pictures were obtained with an installed camera ("COOL SNAP^{TM} HQ" Photometrics) using the 100 × objective.

2.2.7.3 Time-lapse microscopy

To perform time-lapse microscopy cells were first prepared as described in **2.2.7.2.1**. Then, 3 µl of the early logarithmic growing cells were spread on an agarose matrix (25 % v/v YEP, 2 % w/v glucose and 0.05 % w/v agarose), contained on the concavity of a special time-lapse slide. The fluorescence microscope (Zeiss Axioplan2 Imaging) was focused on a dividing cell or a group of dividing cells, and set to make a bright field image followed by a GFP-fluorescence image at 5 min intervals for up to 10 h ("COOL SNAP^{TM} HQ" Photometrics). In this way the dynamics of the GFP signal could be monitored throughout the time.

2.2.7.4 D.I.C. microscopy

Cells were prepared as described in **2.2.7.1**, and were observed under the D.I.C. microscope (Leica). Samples were first visualized with the 10 × objective to facilitate the focus and pictures were obtained with an installed camera (Leica DFC 320) using the 100 × objective.

2.2.8 Flow cytometry

The flow cytometry analysis was performed with a BD FACSAria^{TM} cell-sorting system (Biosciences). Before processing the cells, they were fixed and stained with Sytox Green (Invitrogen Molecular Probes, Leiden) with the following protocol: Initially, cell were grown overnight at 30 and 37 °C in rich medium. These cultures were used to re-inoculate at an initial OD_{600} of 0.05 and were grown at 30 and 37 °C until they rich an OD_{600} between 0.6-0.8. Afterwards, 10^7 cells from the exponentially growing cultures were centrifuged at 2,000 rpm for 5 min and the supernatant discarded. After two washing steps in 1ml distilled water, 1 ml cold 70 % ethanol was added (at this point cells can be stored indefinitely at 4 °C). To process the cells, 0.3 ml were taken from the suspension (approximately 2-3 × 10^6 cells) and added to 3 ml 50 mM sodium citrate buffer in a 5 ml Falcon tube containing 0.1 mg/ml RNase A. The falcon

tube was incubated for 2 h at 37 °C. Finally, to stain the cells, 0.5 ml 50 mM sodium citrate buffer containing 2 μM Sytox Green was added to reach a final concentration in the sample of 1 μM. Measurements were performed with the three FACS parameters FSC (forward scatter), SSC (side scatter) and FITC (fluorescein isothiocyanate) set to 157 v, 378 v and 348 v, respectively. To estimate the average cell size, a calibration was made using microsphere of 1, 2, 4, 6, 10 and 15 μm. The obtained mean FSC values were plotted against the microsphere size and a linear regression was fitted to the plot (R^2 = 0.98). The resulting equation was used to calculate the cell size with the mean FSC values obtained for each strain.

2.2.9 Bonferroni test

After applying a one-way ANOVA, the Bonferroni test or Bonferroni correction was used for multi-comparison of means. This test is used to reduce the probability of committing a type one error (the error of incorrectly declaring significant a difference, effect or relationship that in fact resulted by chance), by adjusting downwards the significance alpha level of each individual test. Thus, it is ensured that the overall risk for a number of tests remains at the initial alpha level (for this work $\alpha = 0.05$).

3. Results

3.1 Phenotypic analysis of *ynl152w* mutants

YNL152w was originally identified as a mutant in a screen for putative negative regulators of the cell wall integrity signaling pathway (Schmitz, 2001). In this chapter, the phenotypic analyses of different *ynl152w* mutants will be described, as a first attempt to characterize the function of the encoded protein.

3.1.1 Serial dilution assay with the mutant strain Tn24 in the presence of caffeine

As explained in section **1.3.2**, the mutant strain Tn24 (carrying a transposon inserted within the C-terminus of Ynl152wp) was isolated in a genetic screen searching for putative negative regulators of the Pkc1p pathway (Schmitz, 2001). However, growth phenotypes related to Pkc1p-signalling had not been analyzed in detail yet. Although the mechanism by which caffeine acts on the yeast cell wall is still obscure, mutants defective in components of the Pkc1p pathway usually show altered sensitivities to this drug. This could also be shown here for the mutant strain Tn24, which displays an increased resistance to 15 mM caffeine in serial dilution assays as compared to the isogenic wild-type strain (**Fig 3.1**).

3.1.2 Viability analysis of the *ynl152w* deletion under conditions of osmotic stabilization

Whereas the transposon-insertion mutant analyzed above was still viable, the null mutant obtained in the systematic deletion has been reported to be lethal under standard growth conditions (Giaever *et al.*, 2002). Mutants defective in many of the components of the Pkc1p MAP kinase cascade show a tendency to lyse with small buds at high temperatures (37 °C; reviewed in Levin, 2005). These phenotypes can be rescued by the addition of 1 M sorbitol to the medium, which works as an osmotic stabilizer (reviewed

in Heinisch *et al.*, 1999). If Ynl152wp was directly involved in the regulation of the Pkc1p pathway, the lethality of *ynl152wΔ* could be caused by a deregulation of the
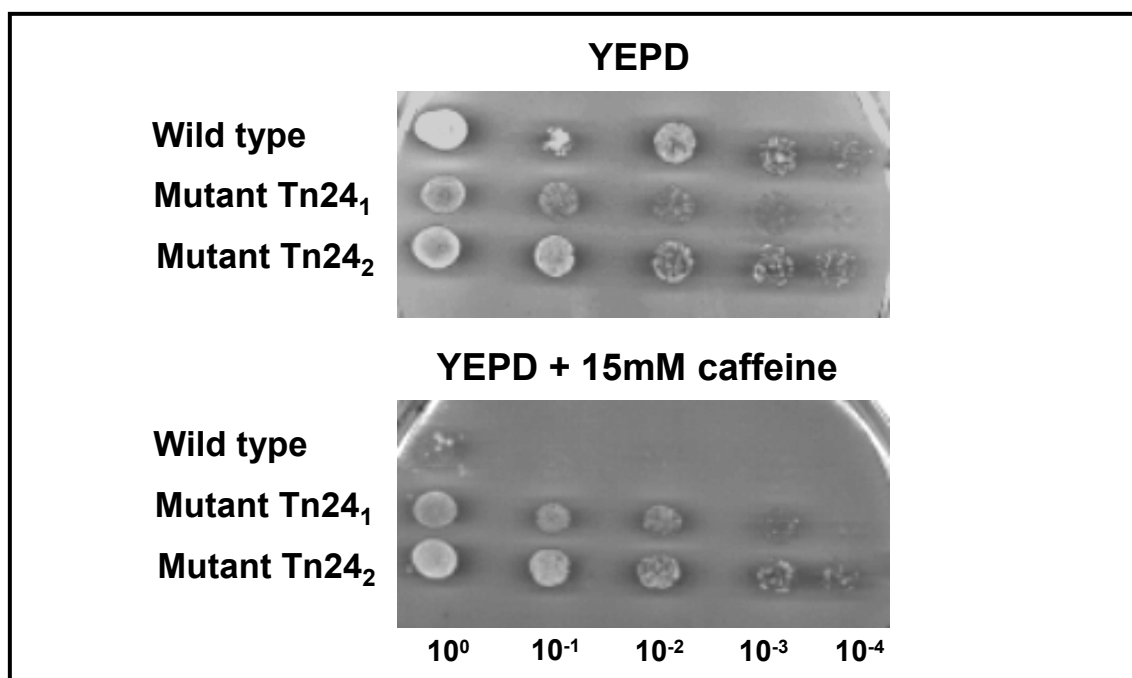
Fig. 3.1 Serial dilution test on YEPD and in the presence of 15 mM caffeine. Two independent cultures of Tn24 were assayed. Wild-type = MCH-7B.

pathway. Then, the presence of 1 M sorbitol would restore cell viability to the *ynl152wΔ* deletion. To test this, a heterozygous deletion (*YNL152w/ynl152w::KanMX*) was constructed in the diploid strain MCH-22D and subjected to tetrad analysis. Spores were allowed to germinate on rich medium supplemented with 1 M sorbitol and the resulting clones were phenotypically characterized. As shown in **Fig. 3.2**, a maximum of two viable spores were obtained from all tetrads analyzed (18 triads and 8 tetrads). Moreover, all the viable progeny carried a wild-type copy of *YNL152w*, as deduced from the sensitivity to G418. A single clone that was resistant to G418 was indeed still a diploid, since it was able to sporulate. Thus, the *ynl152w* deletion is not viable even under conditions of osmotic stabilization.

5 tetrads + 6 triads   **3 tetrads + 12 triads**
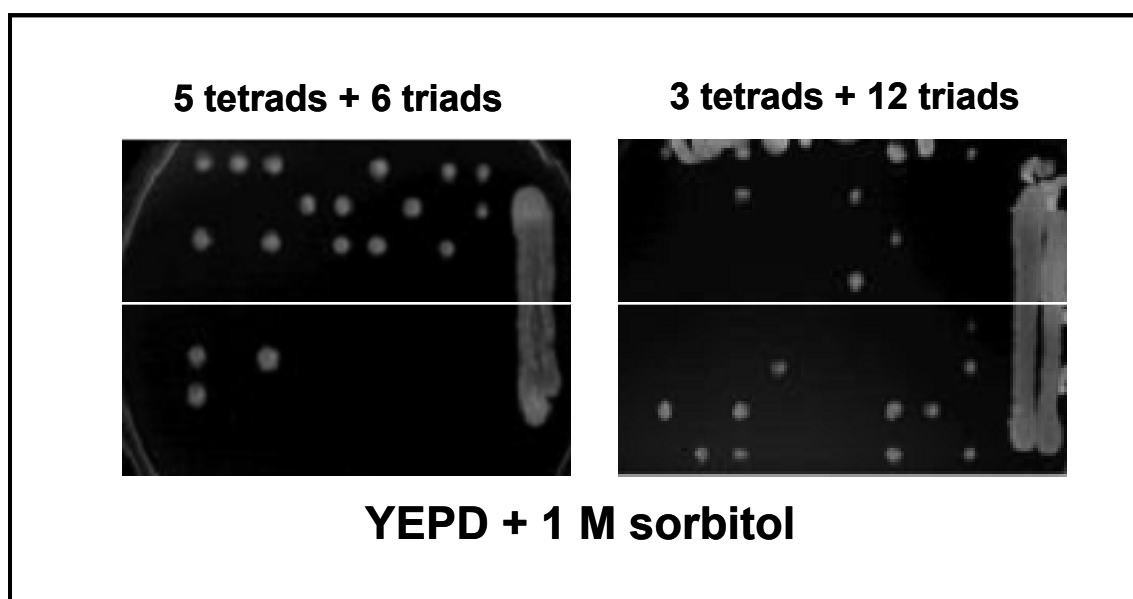
YEPD + 1 M sorbitol

**Fig. 3.2 Tetrad analysis of the heterozygous strain MCH-22D (*YNL152w/ynl152w::kanMX*) in the presence of 1 M sorbitol. After dissection, segregants were allowed to grow for 3 days at 30 °C, prior to documentation. No more than two viable spores were obtained per tetrad.**

3.1.3 Conditional expression of *YNL152w*

As described above, a complete deletion of the *YNL152w* open reading frame is lethal. Therefore, the coding sequence was placed under the control of the *GAL1/10*-promoter (*GAL1/10*p) to allow conditional expression. This promoter permits transcription when cells are grown on galactose, but is shut down in the presence of glucose. Two distinct versions of the *GAL1/10*p-*YNL152w* construct were used: i) A plasmid-borne which uses the multicopy plasmid pJJH447 and ii) a genomic version in which the *GAL1/10*p promoter is inserted in the genome 5′ to the translation initiation codon of *YNL152w*.

3.1.3.1 Conditional episomal *YNL152w* expression

As a first measure, the multicopy vector pJJH447 (2μm-*URA3-GAL1/10*p) was used to place the *YNL152w*-ORF under the control of the inducible promoter. The respective construct was first introduced into distinct strains and then subjected to several phenotypic analyses.

Fig. 3.3 shows a serial dilution test performed in 2 % galactose, and in the presence of 5 mM and 7.5 mM caffeine. Three independent transformants were assayed, each of them carrying the pJJH447 multicopy vector with the *YNL152w* gene under *GAL1/10*p control. They were obtained by transforming the wild-type strain HD56-5A, with three pJJH447-*YNL152w* clones derived from three independent PCRs. Clones (1) and (3) were completely sequenced, and no PCR error was detected (see attached CD for sequence files). In the presence of 7.5 mM caffeine all three overexpressing strains are slightly more sensitive to caffeine. Although this single phenotype is not sufficiently conclusive, it is consistent with a role of Ynl152wp in the down-regulation of the Pkc1p-pathway.
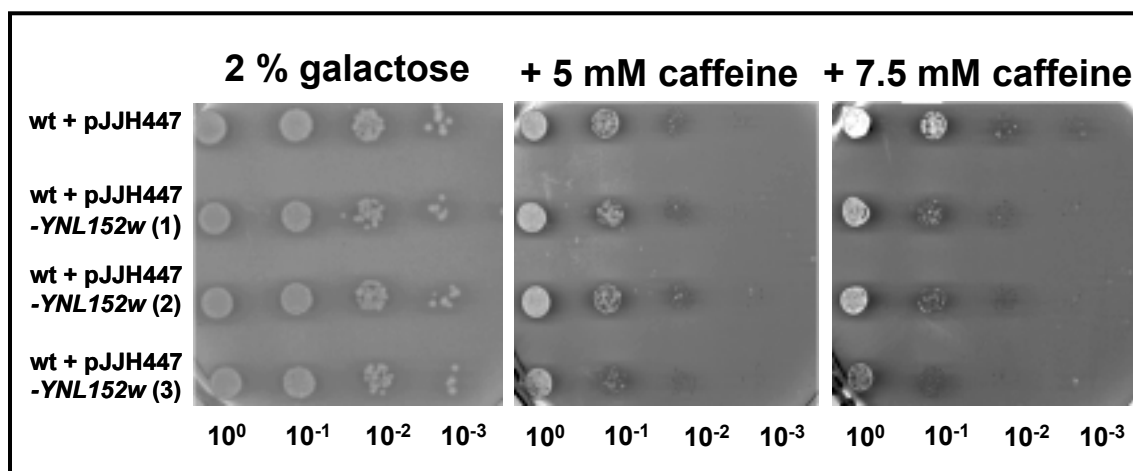
Fig. 3.3 Serial dilution assays of multicopy transformants overexpressing *YNL152w*. All media contained 2 % galactose and caffeine as indicated. Assays were performed on synthetic medium lacking uracil. Three *YNL152w* overexpressing transformants were assayed, each of them carrying the multicopy plasmid pJJH447 with the *YNL152w* gene cloned behind the inducible *GAL1/10* promoter. Each clone derives from an independent PCR reaction.

To study the effect of episomal complementation of the *ynl152w* deletion, the heterozygous diploid strain MCH-22D (*YNL152w/ynl152w::KanMX*) was transformed with the three pJJH447-*YNL152w* constructs used in the previous experiment. Transformants were sporulated and tetrads were dissected. The desired segregants carrying both the deletion cassette and the multicopy plasmid (G418[+] and Ura[+]) were

selected. They were incubated at 30 °C on synthetic plates containing 2 % galactose or 2 % glucose, and on YEPD plates containing 200mg/l G418 plates. **Fig. 3.4** shows a typical example for three out of the eight analyzed segregants. Strikingly, all segregants were able to grow in presence of 2 % glucose similar to the wild-type (*YNL152w*/pJJH447). This was an unexpected result considering that in the presence of 2 % glucose, the expression of *YNL152w* (which is an essential gene) should be strongly
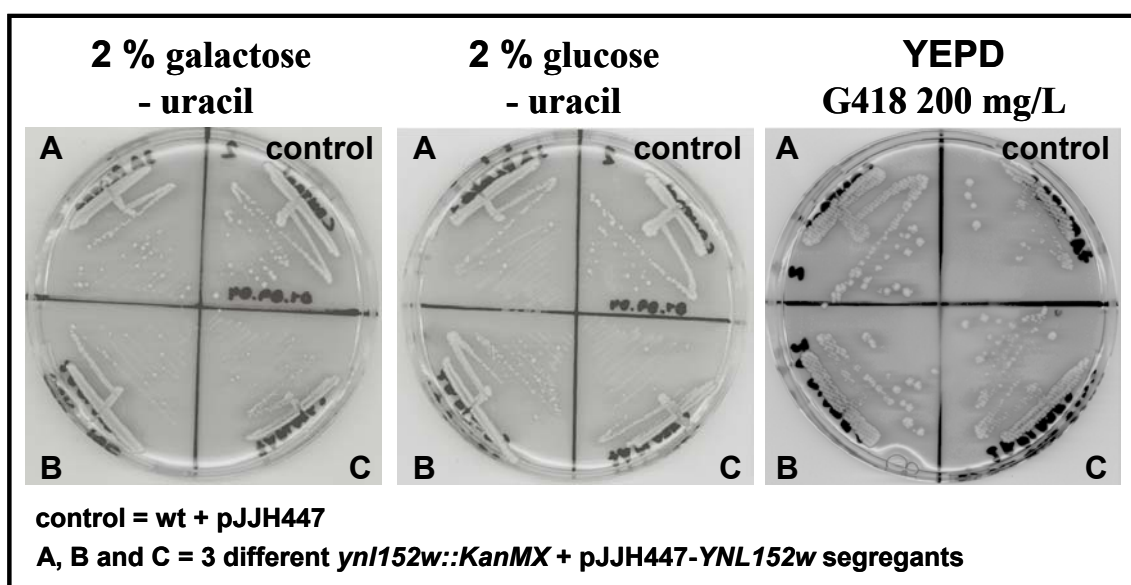
Fig. 3.4 Replication of three segregants carrying the *ynl152w::KanMX* complemented with pJJH447-*YNL152w*. The gene *YNL152* is cloned behind the inducible *GAL1/10*p promoter of the multicopy plasmid pJJH447, therefore its expression level is induced in 2% galactose and repressed in 2% glucose. The presence of the *KanMX* deletion cassette was confirmed by the resistance to 200mg/L of G418.

repressed and therefore only extreme low amounts of the Ynl152wp protein would be produced. Thus, in addition to the G418 resistance, it was necessary to corroborate the genotype of these strains. Therefore, a control PCR was performed to detect the presence of the *KanMX* deletion cassette in the genome (**Fig. 3.5**).
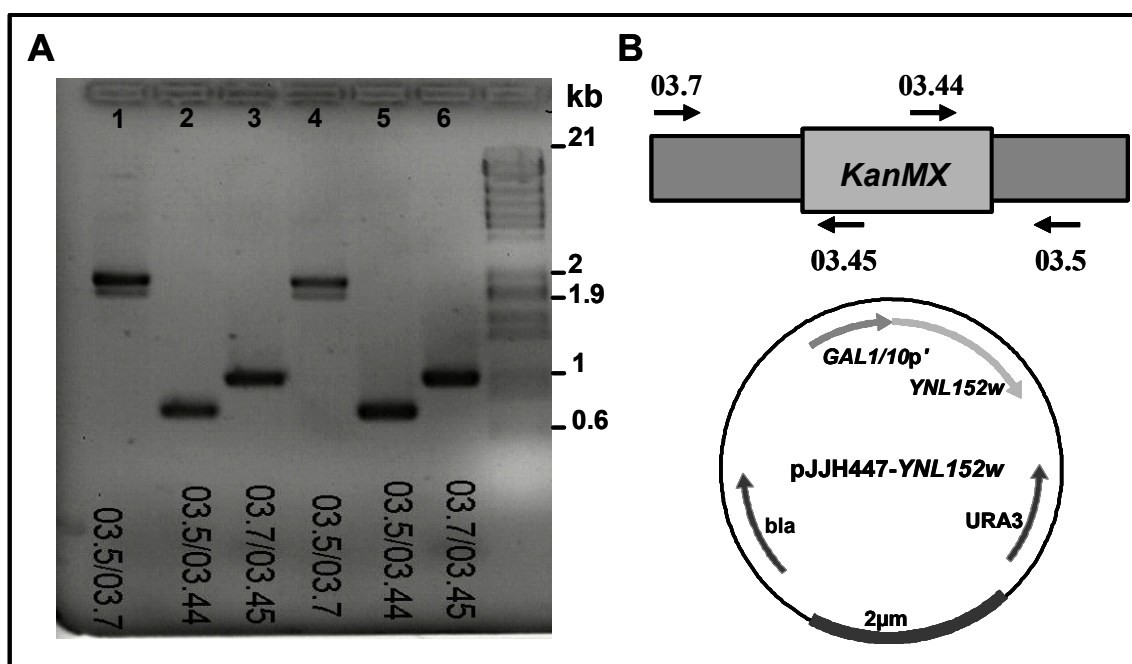
Fig. 3.5 Control PCRs with NaOH lysates of 2 segregants (*ynl152w::KanMX* + pJJH447-*YNL152w*) of the MCH-22D heterozygous strain. A PCR experiment was designed to confirm the presence of the *KanMX* deletion cassette. A) Agarose picture showing the PCR products, in all cases the right bands were obtained. Lanes 1-3 and 4-6 correspond to two analyzed segregants. B) Schematic representation of the different primer combinations used for the PCRs. The multicopy plasmid carrying the *YNL152w* wild-type copy does not contain any sequences corresponding to the oligonucleotides employed, except for 03.5. Numbers correspond to the oligonucleotides used in each reaction (See section 2.1.4).

Lanes 1-3 and 4-6 represent three different PCR reactions of two analyzed segregants. In every case the expected bands were observed, and the presence of the *KanMX* deletion cassette confirmed. In lanes 1 and 4 a second smaller band of less intensity is visible. This could either result from a unspecific product or from a contamination in the template DNA containing a wild-type copy of *YNL152w*.

The growth of the *ynl152w* deletion with the plasmid-borne conditional copy of the wild-type gene under repressing conditions, could have two reasons: (1) The Ynl152wp is only essential for germination but not for vegetative growth or (2) a very low level of *YNL152w* expression is sufficient to support growth. To distinguish between both propositions, a counter-selection experiment with 5-fluoro-orotic acid (5-FOA) was made. 5-FOA is converted to toxic 5-fluorouracil in yeast strains expressing a functional *URA3* gene, which encodes an orotidine-5'-monophosphate decarboxylase (Boeke *et al.*, 1984; Boeke *et al.*, 1987). Thus, *URA3*-based plasmids will be chased

from transformants growing on 5-FOA medium. However, if the plasmid carries an essential gene, the respective transformants will fail to grow on 5-FOA. As shown in **Fig. 3.6** both wild-type strains transformed with either pJJH447 or pJJH447-*YNL152w* are 5-FOA resistant, indicating that they were able to lose the plasmid. In contrast, in the deletion pJJH447-*YNL152w* is essential and transformants are 5-FOA sensitive. Hence, they can not lose the plasmid. This result shows that *YNL152w* is indeed essential for vegetative growth and indicates that a low *YNL152w* expression level (on glucose) generates sufficient protein for cell division.
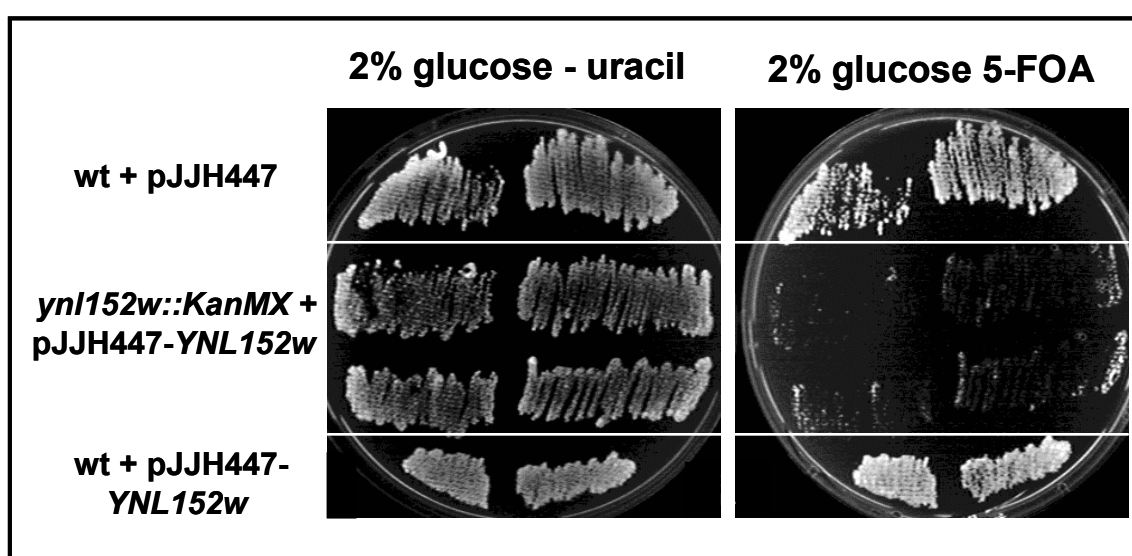
Fig. 3.6 Counter-selection with 5-fluoro-orotic acid of pJJH447-*YNL152w*. The control wild-type strains show 5-FOA resistance and therefore were able to lose the plasmid. In contrast the complementation in *ynl152w::KanMX* + pJJH447-*YNL152w* resulted in 5-FOA sensitivity.

It has been observed that a *trp1*-mutation has a significant influence on the phenotypes of cell integrity signaling mutants (Boeke *et al.*, 1984; Boeke *et al.*, 1987; Queralt and Igual, 2004). Therefore, a heterozygous deletion was constructed in the strain DHD5 (*YNL152w/ynl152w::KanMX*) as described above for MCH-22D, and used in the following experiments. Again, the heterozygous diploid was transformed with either pJJH447 (2μ-*URA3*) or pJJH447-*YNL152w*, sporulated and subjected to tetrad analyses. Segregants carrying the plasmids in conjunction with either a wild-type or a deletion at

Table 3.1 Calculation of kinetic parameters in glucose, raffinose and galactose. The generation time (t_g) and the specific growth rate (μ) were calculated within the exponential region from each of the growth curves presented in Fig. 3.7.

A

	Generation time t_g [min] and specifc growth rate μ [h^{-1}]					
strain	glucose		raffinose		galactose	
	t_g	μ	t_g	μ	t_g	μ
wt + pJJH447	115	0.36	144	0.29	143	0.29
wt + pJJH447 -*YNL152w*	209	0.20	271	0.15	240	0.17
deletion + pJJH447 -*YNL152w*	151	0.28	165	0.25	176	0.24

B

	Generation time t_g [min] and specifc growth rate μ [h^{-1}]					
strain	glucose		raffinose		galactose	
	t_g	μ	t_g	μ	t_g	μ
wt + pJJH447	125	0.33	179	0.23	282	0.15
wt + pJJH447 -*YNL152w*	205	0.20	298	0.14	326	0.13
deletion + pJJH447 -*YNL152w*	131	0.32	186	0.22	476	0.09

the *YNL152w* locus were further analyzed. To assess the dependence on *YNL152w* expression levels more accurately, growth curves of different transformants on various media were obtained. Three different carbon sources were used: 2 % glucose, 2 % raffinose and 2 % galactose; which should lead to low, intermediate, and high expression levels from the *GAL1/10* promoter, respectively. The haploid wild-type strain HD56-5A, carrying the empty plasmid or the pJJH447-*YNL152w* construct was used as control. The results of two independent experiments are summarized in **Fig. 3.7** and **Table 3.1**. Compared to the wild-type strain transformed with the control vector pJJH447, transformants carrying the *GAL1/10*p-*YNL152w* fusion showed a reduced growth rate on all media. Unexpectedly however, the *ynl152w*-deletion strain transformed with the latter construct showed a similar growth behavior on glucose
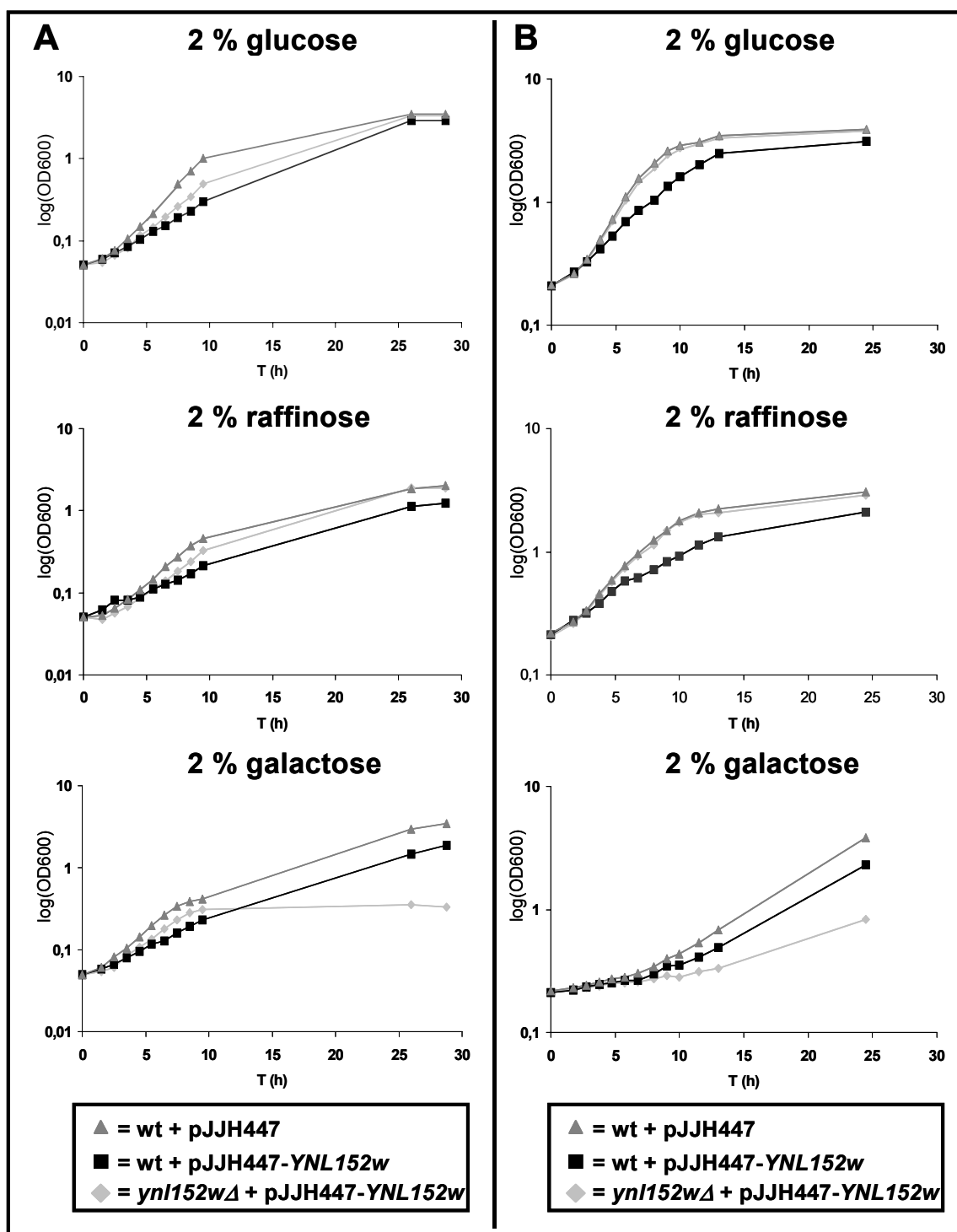
Fig. 3.7 Growth curves of the *ynl152wΔ* + pJJH447-*YNL152w* strain in different carbon sources. The curves were performed at 30 °C in synthetic media lacking uracil with glucose, raffinose or galactose; which correspond respectively to low, intermediate and high *YNL152*w expression levels. As controls the wild-type strain HD56-5A transformed with the empty pJJH447 plasmid or with pJJH447-*YNL152w* were used. A and B represent two independent experiments. Cultures were shaken at 150 rpm.

medium (i.e. under repressing conditions that should lead to a drastic decrease in Ynl152wp levels). Moreover, galactose seems to exert an inhibitory effect on growth of the deletion strain (*ynl152w::KanMX*/pJJH447-*YNL152w*) upon prolonged incubation. The morphology of the cells was monitored throughout growth by microscopic inspection. Upon prolonged incubation in glucose medium, swollen cells and formation of aggregates was observed (**Fig. 3.8**) in the deletion strain transformed with pJJH447-*YNL152w*. This indicates that the cells are indeed affected by the low *YNL152w* expression levels.

Neither on raffinose nor on galactose aberrant morphological phenotypes could be detected as compared to the control cultures.
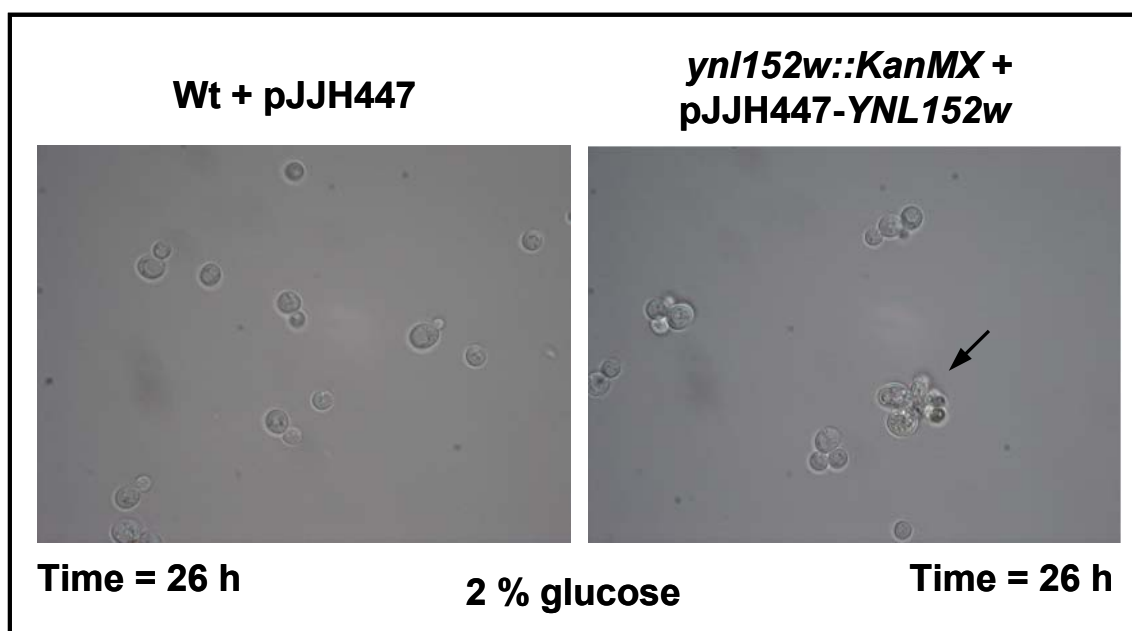
**Fig. 3.8 D.I.C images of the *ynl152w::KanMX* + pJJH447-*YNL152w* complementation strain.** In the previous growth curves, the morphology of the cells was monitored under the microscope at certain intervals. Under repressing conditions and at late time points, a morphologic phenotype with swollen cells and formation of aggregates was observed for the deletion strain (right picture).

3.1.3.2 Conditional expression of *YNL152w* from a genomic copy

To avoid the drawbacks derived from the use of a multicopy plasmid (such as variable plasmid-copy numbers) and to allow for a stable inheritance of the conditional expression allele, a strain carrying the genomic *YNL152w* allele under the control of the *GAL1/10* promoter was constructed. Again, the growth behavior of the resulting strain (HD56-5A/*GAL1/10*p-*YNL152w*) was determined on glucose, raffinose and galactose media (**Fig. 3.9**). As a control, the wild-type strain HD56-5A, which carries the *YNL152w* gene under the control of its own promoter was employed. **Table 3.2** shows
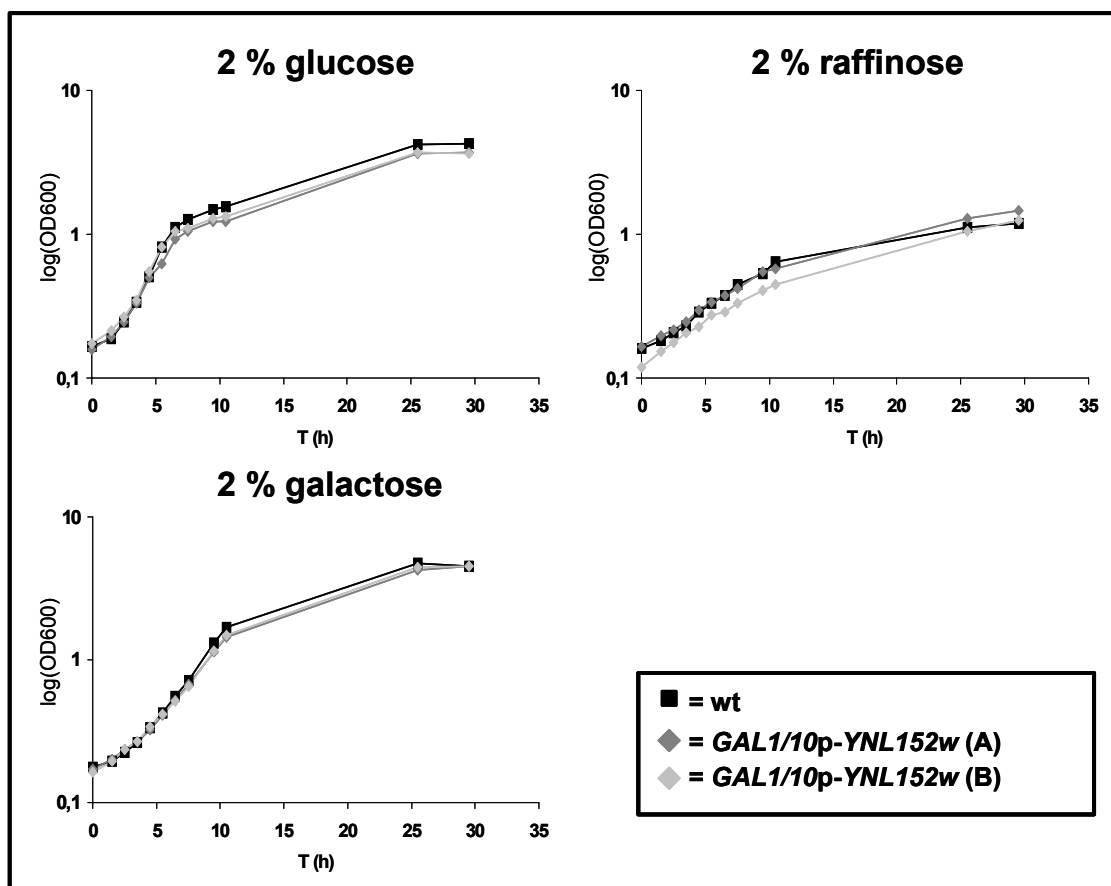
**Fig. 3.9 Growth curves of the genomic *GAL1/10*p-*YNL152w* strain in different carbon sources. The curves were performed in synthetic media with glucose, raffinose or galactose; which correspond respectively to low, intermediate and high *YNL152*w expression levels. As control the wild-type strain HD56-5A carrying *YNL152w* under control of its own promoter was used. Two replicas, A and B were made for *GAL1/10p-YNL152w*.**

the calculated generation times and the specific growth rates in the three different conditions. The wild-type strain displays the lowest generation times, but in all conditions the kinetic parameters were very similar to those of strains carrying the conditional expression allele. The generation times measured in the presence of 2 % glucose were only slightly lower for the latter strains compared to the wild-type control. These results suggest that a very low expression level of *YNL152w* is sufficient to support cell growth.

Table 3.2. Calculation of kinetic parameters in glucose, raffinose and galactose. The generation time (t_g) and the specific growth rate (μ) were calculated from the growth curves performed with the genomic *GAL1/10*p-*YNL152w* strain.

	Generation time t_g [min] and specifc growth rate μ [h^{-1}]					
strain	**glucose**		**raffinose**		**galactose**	
	t_g	μ	t_g	μ	t_g	μ
wt	107	0.39	298	0.14	156	0.27
***GAL1/10*p -*YNL152w* (A)**	127	0.33	320	0.13	170	0.24
***GAL1/10*p -*YNL152w* (B)**	116	0.36	339	0.12	161	0.26

Morphological phenotypes associated with growth on glucose are depicted in **Fig. 3.10**. 2.5 h after inoculation, the phenotype can hardly be distinguished in the genomic *GAL1/10*p-*YNL152w* strain from that of the wild-type control. However after 5 h, a clear phenotype can be observed with swollen cells and formation of aggregates. Finally, in samples taken 8 h after inoculation, large elongated cells and big aggregates with irregular shape are formed.

To confirm the aberrant morphologies observed above, cells were also grown on plates with different carbon sources: Synthetic media with 2 % glucose; YEP-glycerol-ethanol and YEP-Gal. As shown in **Fig. 3.11**, the reproducible phenotypes observed on glucose and glycerol plates confirmed the importance of Ynl152wp for morphogenesis.
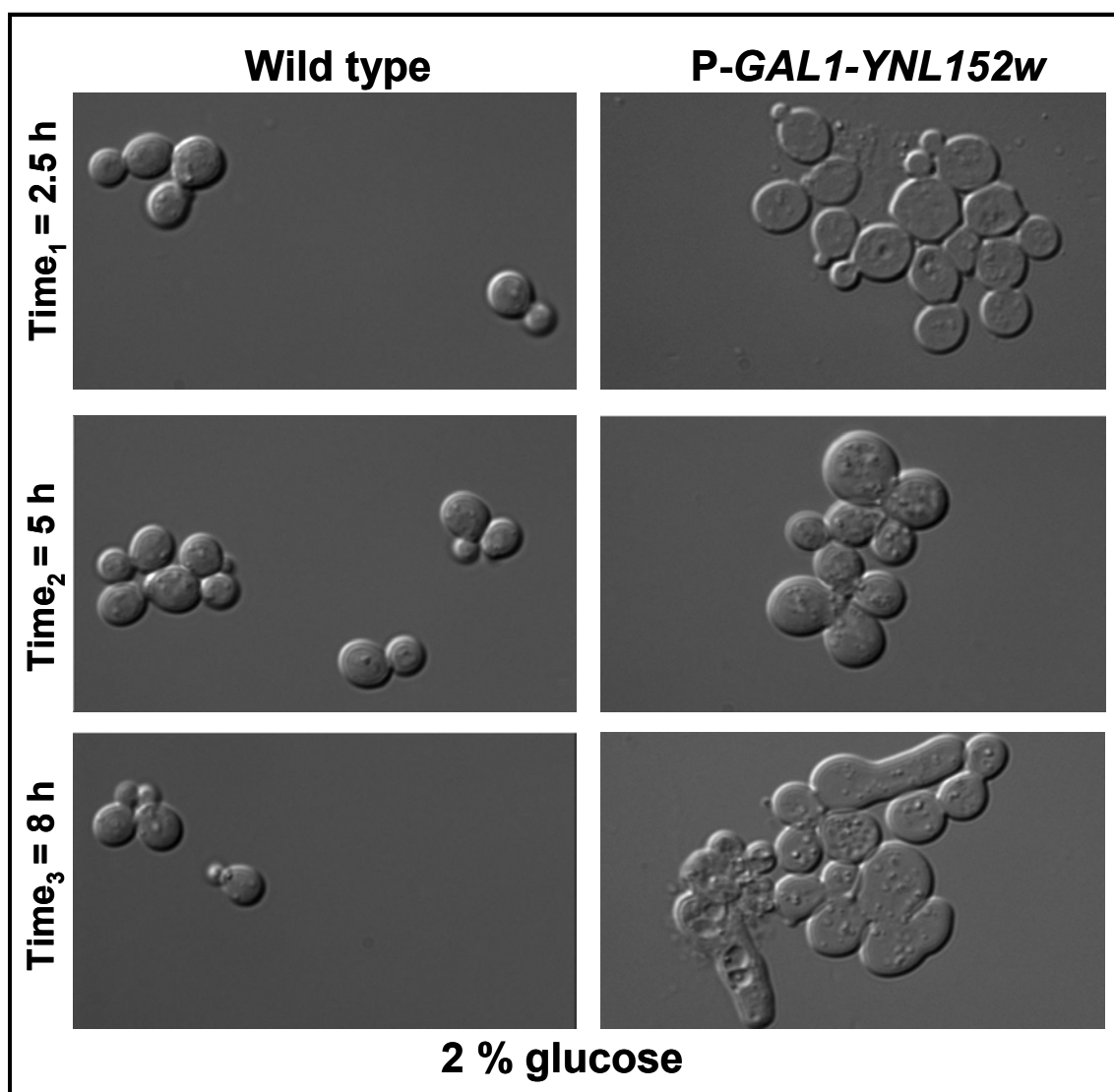
Fig. 3.10 Bright field images of the genomic *GAL1/10*p-*YNL152w* **strain growing in glucose. To follow the morphology of the cells throughout the time, samples were taken at different time intervals and observed under the microscope. The pictures were made with identical magnification.**

 In contrast, the cell's morphology looked quite normal on galactose plates. Only occasionally a phenotype probably associated with the over-expression could be observed on these plates. However, this phenotype was very weak and characterized by the presence of some swollen cells.
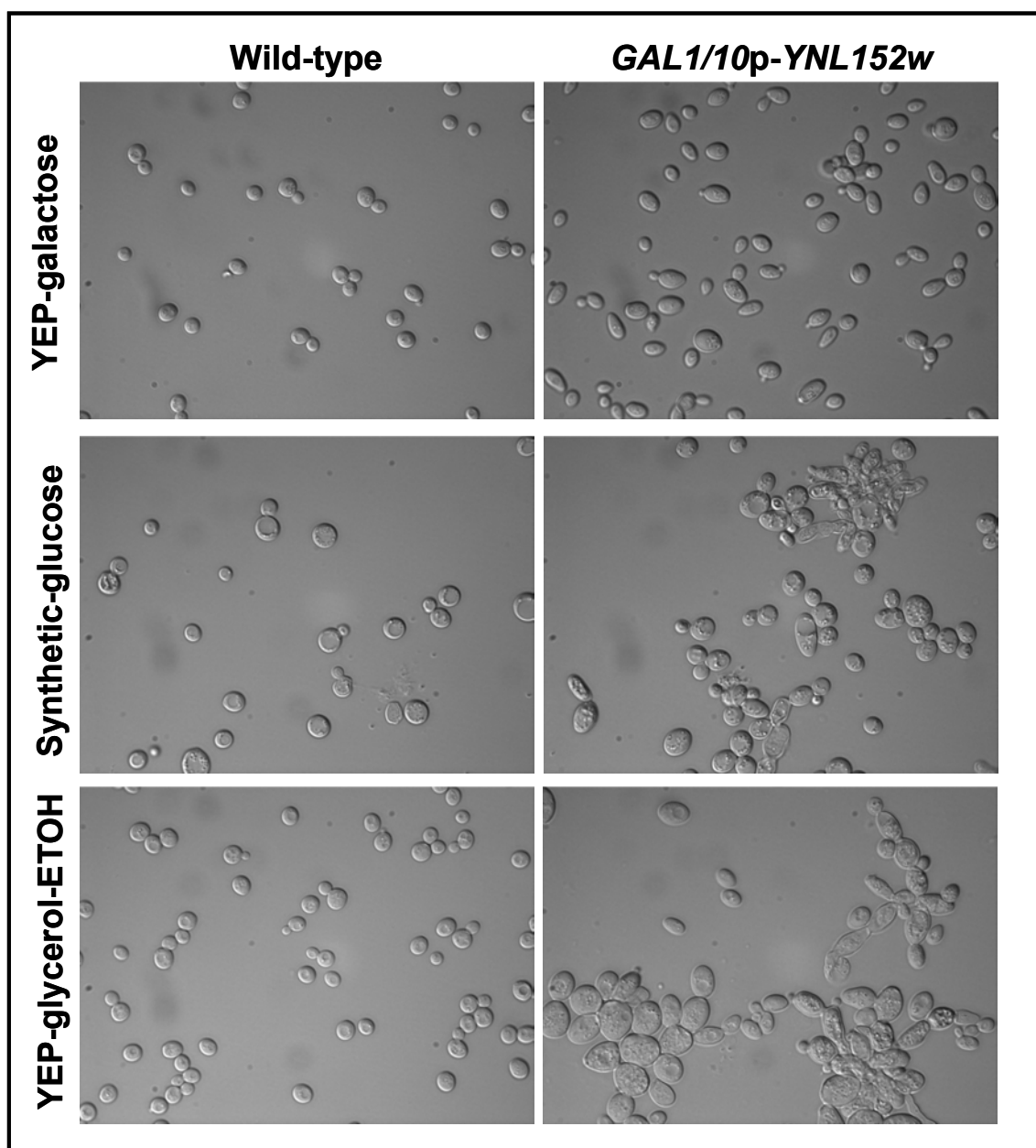
Fig. 3.11 D.I.C images of the genomic *GAL1/10p-YNL152w* strain grown in media with three different carbon sources. All strains were grown on plates overnight at 30 °C.

3.2 Analysis of successive Ynl152wp C-terminal truncations

The viability of the originally isolated transposon mutant in contrast to the complete deletion of *YNL152* (compare **3.1.2**) suggested that the C-terminal end of the encoded protein may be dispensable for function. In order to investigate to what extent the protein can be shortened and still confer viability, a series of deletions were constructed

from the 3'-end of the gene, with insertion of a dual stop-codon to terminate translation. Thus a series of isogenic strains was available (**Fig 3.12**) and the associated phenotypes were assessed as described in the following sections.
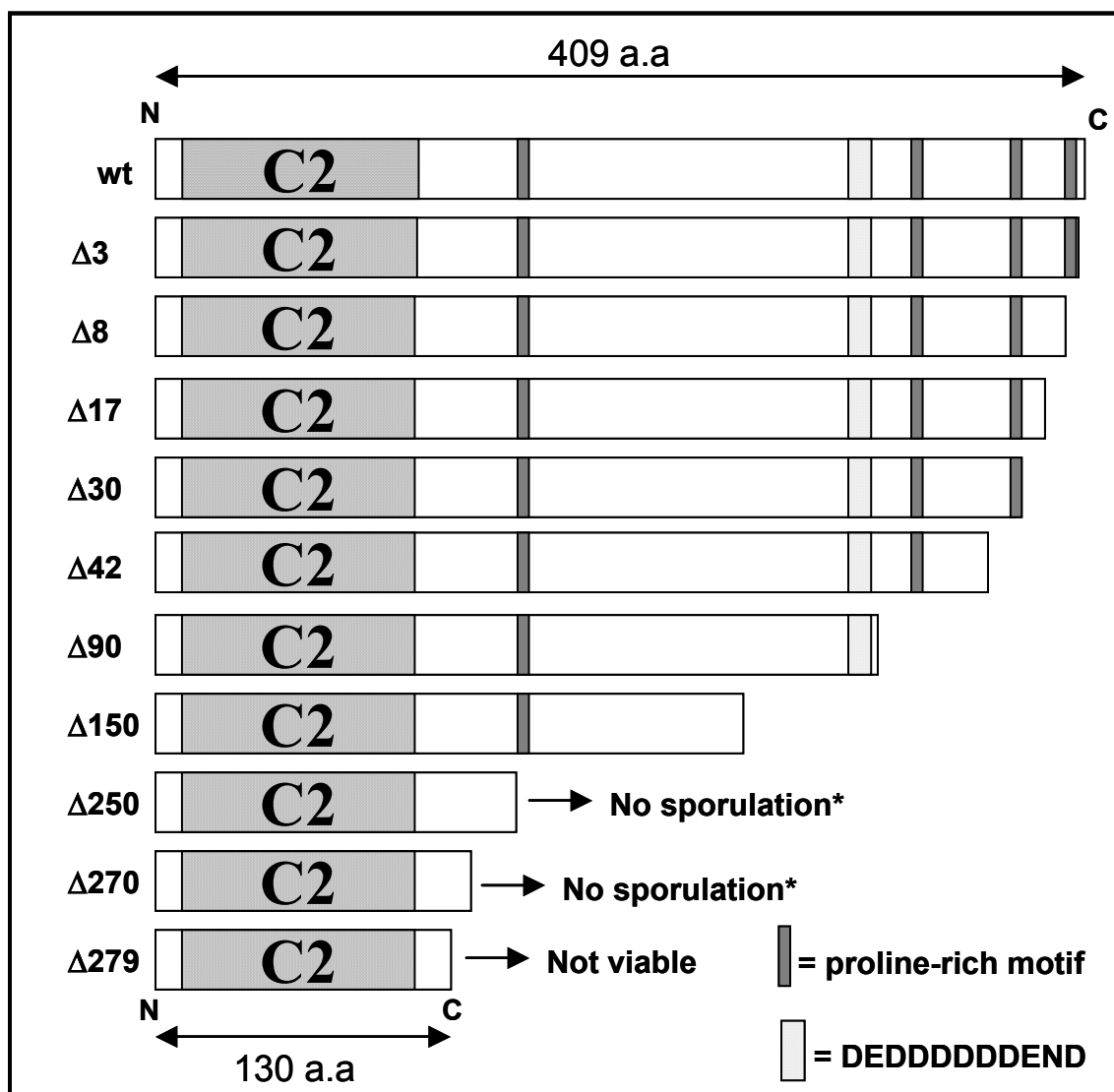
Fig. 3.12 Schematic representation of all the *ynl152w* C-terminal deletions employed for cell viability analyses. A total of ten *ynl152w* C-terminal truncations of different lengths as well as an internal deletion of the aspartate rich region (all kindly provided by R.Rodicio) were analyzed.

*= Sporulation was tested with the respective homozygous diploid strains.

3.2.1 Cell viability of different *ynl152w* truncation mutants

A series of 3'-deletions in the *YNL152w* coding sequence was obtained in a diploid strain. These were then sporulated and subjected to tetrad analyses (**Fig. 3.12**). Strikingly, only the truncation of the C-terminal 279 amino acids representing 68% of the total protein was lethal, as judged from a 2:0 segregation for spore viability. Viable segregants invariably lacked the selection marker used to introduce the truncation. Nevertheless, starting from *ynl152wΔ250* the cells were no longer able to sporulate and the viability was considerably reduced as well (e.g. 13 viable spores out of 40 in *ynl152wΔ270*). In the next section, many other phenotypes associated with the different deletion strains will be shown.

3.2.2 Morphological phenotypes

As described in the previous chapters, a strain carrying the *YNL152w* gene under the

strain	expected PCR product (kb)
1) ynl152wΔ3	3.76
2) ynl152wΔ8	3.28
3) ynl152wΔ17	3.72
4) ynl152wΔ30	3.68
5) ynl152wΔ42	3.65
6) ynl152wΔ90	3.50
7) ynl152wΔ150	3.32
8) ynl152wΔ250	3.02
9) ynl152wΔ270	2.96
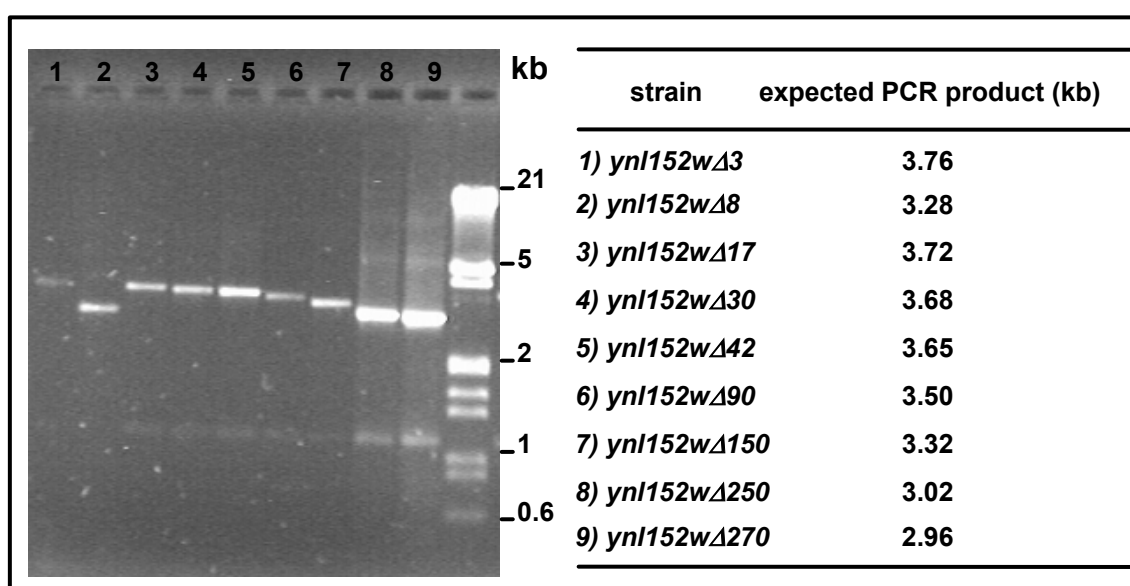
Fig. 3.13 Control PCR with primers 03.05 and 03.06 to confirm the genotype of the Ynl152wp C-terminal truncations. Lanes 1-9 correspond respectively to *ynl152wΔ3, Δ8, Δ17, Δ30, Δ42, Δ90, Δ150, Δ250* and *Δ270*. In all cases the right bands were obtained. The reason for the smaller band observed in lane 2 is that *ynl152wΔ8* was constructed with the KanMX deletion cassette, instead of *Kl LEU2* like in the rest of the deletion strains. Also diploid strains were constructed and controlled by PCR (data not shown).

control of the inducible *GAL1/10* promoter shows a morphological phenotype when grown under repressing conditions. Considering that the C-terminal truncation of the Ynl152wp protein could lead to a loss of the protein function, it would be logical to expect a similar morphology at least for some of the analyzed truncations. But before starting with the microscopic analysis of the C-terminal truncations, it was necessary to confirm the genotype of each *ynl152w* deletion strain. **Fig. 3.13** shows a control PCR performed with the Ynl152wp C-terminal truncations. As evident from **Fig 3.14**, the
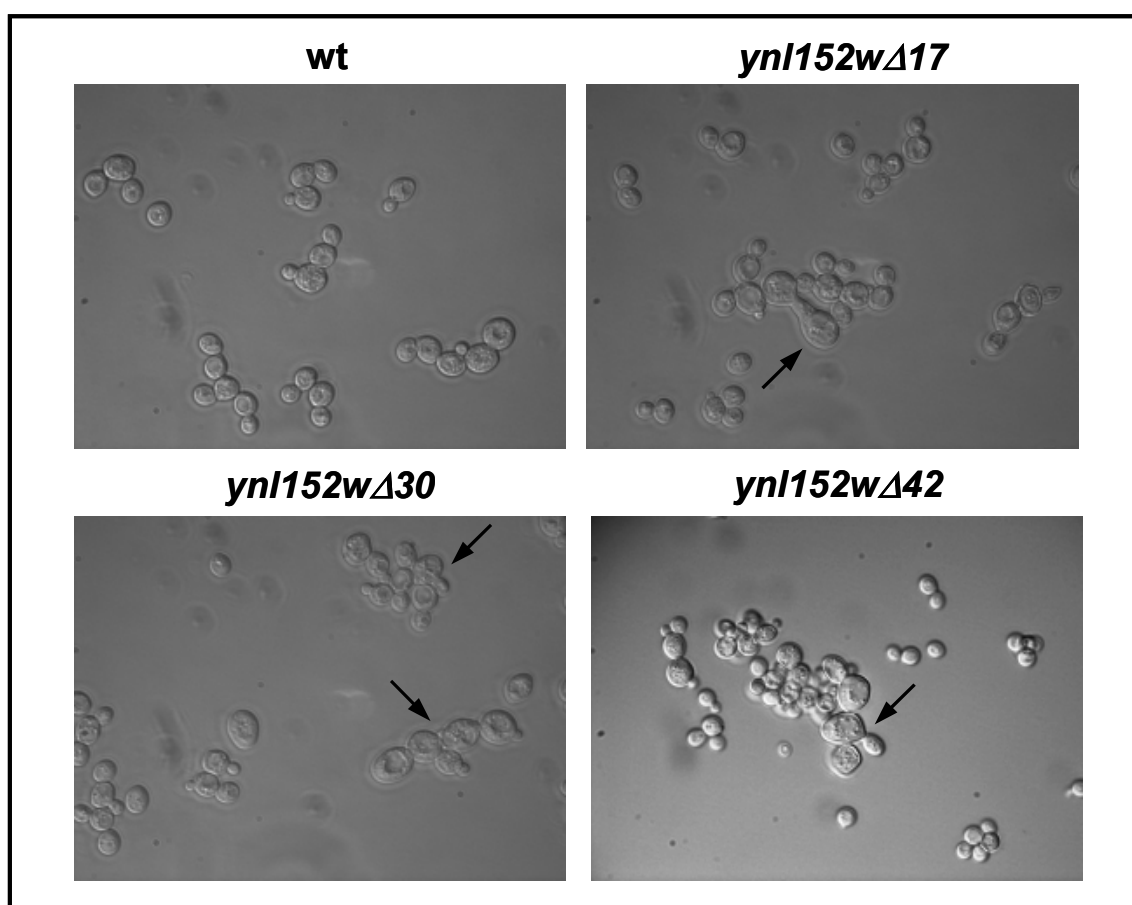
Fig. 3.14 D.I.C images showing a morphologic phenotype in the diploid strains homozygous for the indicated *YNL152w* allele. The phenotype was characterized by the presence of chained cells and swollen cells with irregular shapes. The cells were grown in YEPD at 37.

shorter truncations led to distinct morphological phenotypes (swollen cells; cluster formation) as compared to the wild-type, at least when grown at an elevated temperature

(37 °C). A much severer morphology was observed for the larger truncations *ynl152wΔ150-Δ270*, with formation of big aggregates and the appearance of very large cells with irregular shapes. Apparently also lysed cells could be observed in the large truncations (**Fig. 3.15**). This strong phenotype was seen under normal growth conditions, and is reminiscent of that from the genomic *GAL1/10*p-*YNL152w* strain when grown under repressing conditions.
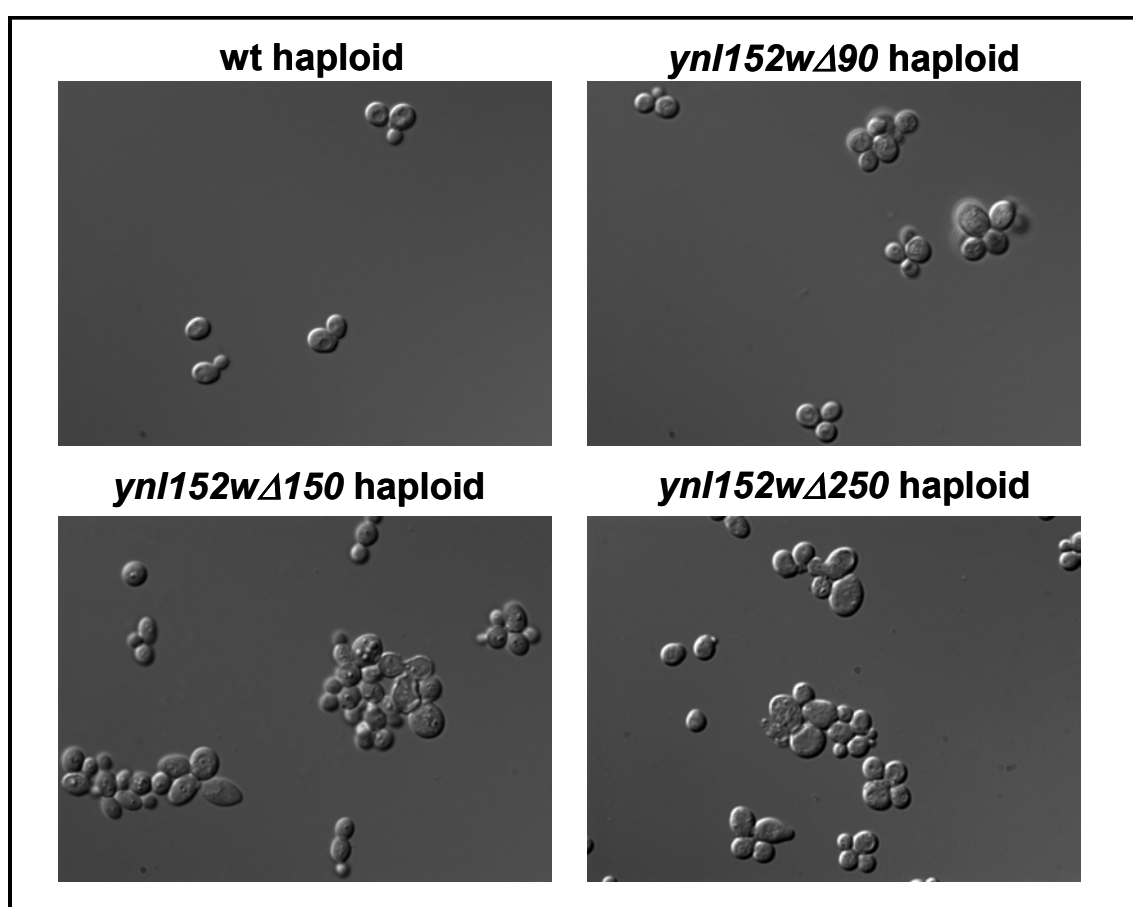
Fig. 3.15 Bright field images of the large C-terminal *ynl152w* truncations showing a morphologic phenotype. Starting from *ynl152wΔ150* a severe phenotype was observed, characterized by the formation of big irregular aggregates and the appearance of very large cells with irregular forms. The cells shown in the pictures were grown in synthetic glucose media at 30 °C.

The previous morphological phenotypes suggest a defect in cell division and probably also in the nuclear distribution. To investigate the latter possibility, DAPI stained cells from both *ynl152wΔ150* and *ynl152wΔAsp* (which also shows a strong

morphologic phenotype see **3.2.6**), were examined with the fluorescence microscope. As shown in the pictures from **Fig. 3.16**, the nuclear segregation is abnormal in both
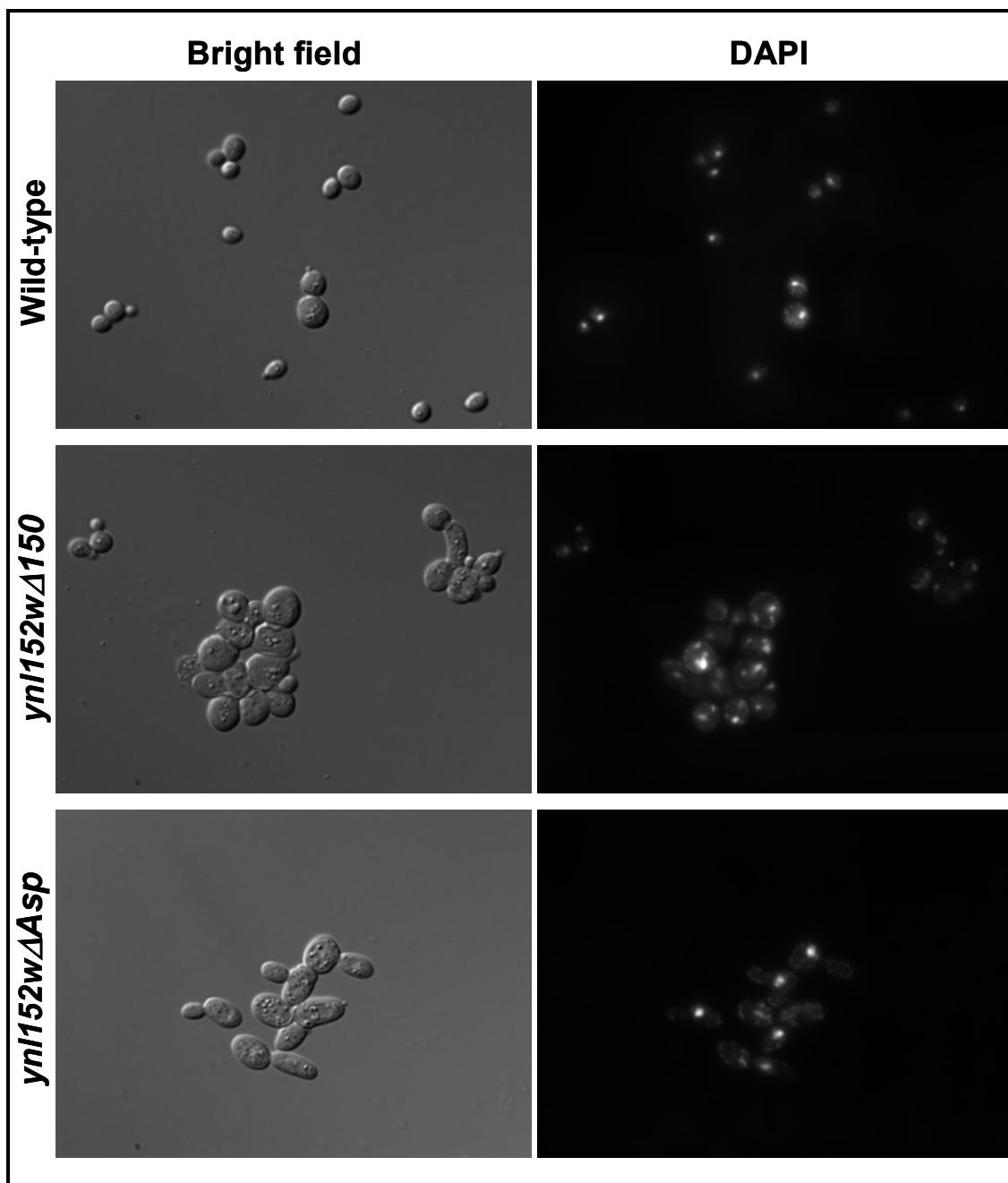
Fig. 3.16 Visualization by DAPI staining of the nuclear segregation in the mutants *ynl152wΔ150* **and** *ynl152wΔAsp***.**

deletion strains. Thus, the aggregate forming cells show in some cases more than one nucleus and in other cases no nucleus at all.

During the construction of the *ynl152wΔ150* homozygous diploid strain, a defect in the sporulation process was detected under the microscope. Thus, asci were frequently formed from budding cells, which is not the case in wild-type diploids. In addition some asci contained more than 4 spores (**Fig. 3.17**).
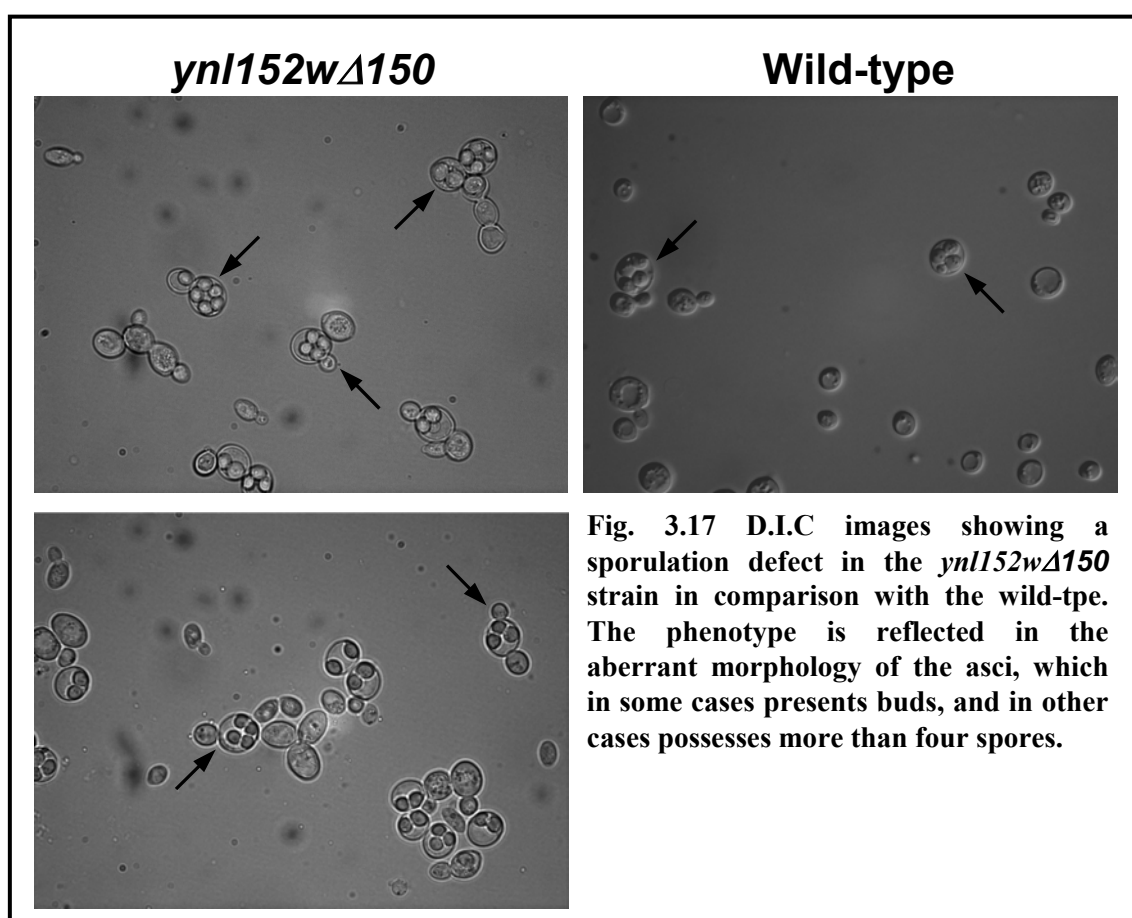
Fig. 3.17 D.I.C images showing a sporulation defect in the *ynl152wΔ150* strain in comparison with the wild-tpe. The phenotype is reflected in the aberrant morphology of the asci, which in some cases presents buds, and in other cases possesses more than four spores.

3.2.3 FACS analyses of truncations

In the previous section two distinct morphological phenotypes were described for short or large truncations. In both cases the phenotypes were difficult to quantify. Furthermore, it was shown that nuclear distribution is also affected. Therefore a flow cytometry experiment was performed to determine the DNA content of the cells as well as the average cell size. The DNA content was estimated for each truncation
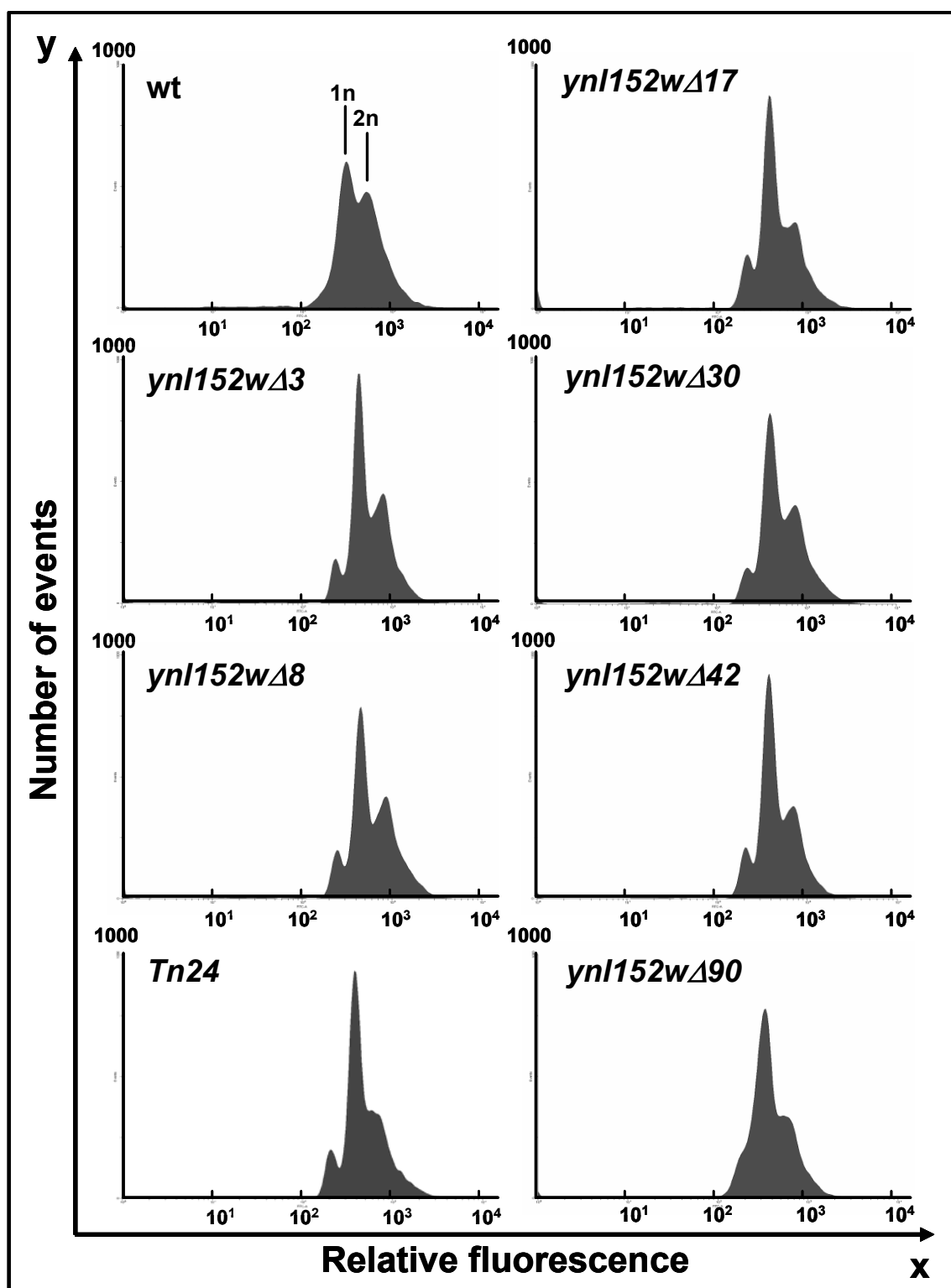
Fig. 3.18 Flow cytometry analysis of the Ynl152wp C-terminal truncations. The DNA content (1n, 2n) was determined for each deletion strain by measuring the fluorescence of sytox green stained cells. Cells were cultured at 30 °C and in each case 20,000 events were recorded.

by measuring the fluorescence of sytox green stained cells. Cells were cultured at 30 °C and in each case 20,000 events were recorded. **Fig. 3.18** and **Fig. 3.19** show the respective histograms. Again, different results were obtained for the truncations in the distribution of DNA content as well as in the cell size (**Table 3.3**). In the short truncations *ynl152wΔ3-Δ90*, in general a population of smaller cells could be observed

Table 3.3 Flow cytometry analysis of the Ynl152wp C-terminal truncations. The mean relative cell size was determined for each deletion strain. Cells were cultured at 30 °C and 37 °C, in each case 20,000 events were recorded.

|	Estimated mean cell size (μm)	
strain	**cultivation temperature**	
	30 °C	**37 °C**
Wild-type	9.5	-
ynl152wΔ3	8.8	9.9
ynl152wΔ8	9.5	10.7
Tn24	8.3	9.6
ynl152wΔ17	7.5	10.1
ynl152wΔ30	8.8	10.8
ynl152wΔ42	7.5	11.2
ynl152wΔ90	7.2	10.1
ynl152wΔ150	11.7	13.7
ynl152wΔ250	13.9	14.9
ynl152wΔ270	16.1	18.4

Fig. 3.19 Flow cytometry analysis of the large Ynl152wp C-terminal truncations. The DNA content (1n, 2n) was determined for each deletion strain by measuring the fluorescence of sytox green stained cells. Cells were cultured at 30 °C and in each case 20,000 events were recorded.

as well as the appearance of a third peak of low fluorescence, corresponding to a DNA content <1n (**Fig. 3.18**). Also the histogram obtained with the Tn24 strain shows the same pattern like the equivalent *ynl152wΔ8* truncation. Starting from *ynl152wΔ150* a dramatic change was observed with an increase in cell size (**Table 3.3**) and a shift of the histogram to the right with the appearance of a fluorescence peak corresponding to a DNA content of >2n (**Fig. 3.19**). The latter result would reflect the presence of the observed big aggregates which carry more than 2n DNA contents.

The same flow cytometry experiment was carried out for each truncation, but with cells grown at 37 °C. Compared to the one performed at 30 °C, the fluorescence

histograms showed very similar distribution patterns of the DNA content, however the average cell size was even higher (**Table 3.3**).

3.2.4 Vegetative growth and caffeine sensitivity

Continuing with the phenotypic analyses of the Ynl152p truncations, growth curves were obtained in liquid media with a selected group of short and large truncations, to assess the effect on cell growth. This study was complemented with serial dilution assays performed on YEPD plates and in the presence of 15mM caffeine to test for sensitivity. **Table 3.4** shows the specific growth rates obtained in liquid YEPD for *Ynl152wΔ8, Δ42, Δ250* and *Δ270*. As shown in the **Table 3.4** the growth rates were very similar between the truncations. Nevertheless, the two largest truncations (*Δ250* and *Δ270*) grew a little more slowly. It should be noticed that these strains showed the highest average cell size, which may obstruct the data obtained by absorption measurements (Koch, 1970). The lack of an obvious growth defect was confirmed by the drop test made with *ynl152wΔ8, Δ42* and *Δ250* in YEPD and in the presence of

Table 3.4 Kinetic parameters with different *ynl152w* C-terminal truncations. The values were calculated from different growth curves performed in liquid YEPD.

strain	Specific growth rate [h^{-1}]	Generation time [min]
wt	0.33	125
ynl152wΔ8	0.45	92
ynl152wΔ42	0.45	92
ynl152wΔ150	0.45	93
ynl152wΔ250	0.42	99
ynl152wΔ270	0.40	102

15 mM caffeine. As seen in **Fig. 3.20 A** *ynl152wΔ250* grows worse in YEPD as compared to the wild-type and the shorter deletion strains. It is also more sensitive to 15mM caffeine. In contrast, the shorter truncation strains (*ynl152wΔ3-Δ90* **Fig. 3.20 B**) behave like the wild-type. These results show that cell growth is negatively affected only by the largest truncations.
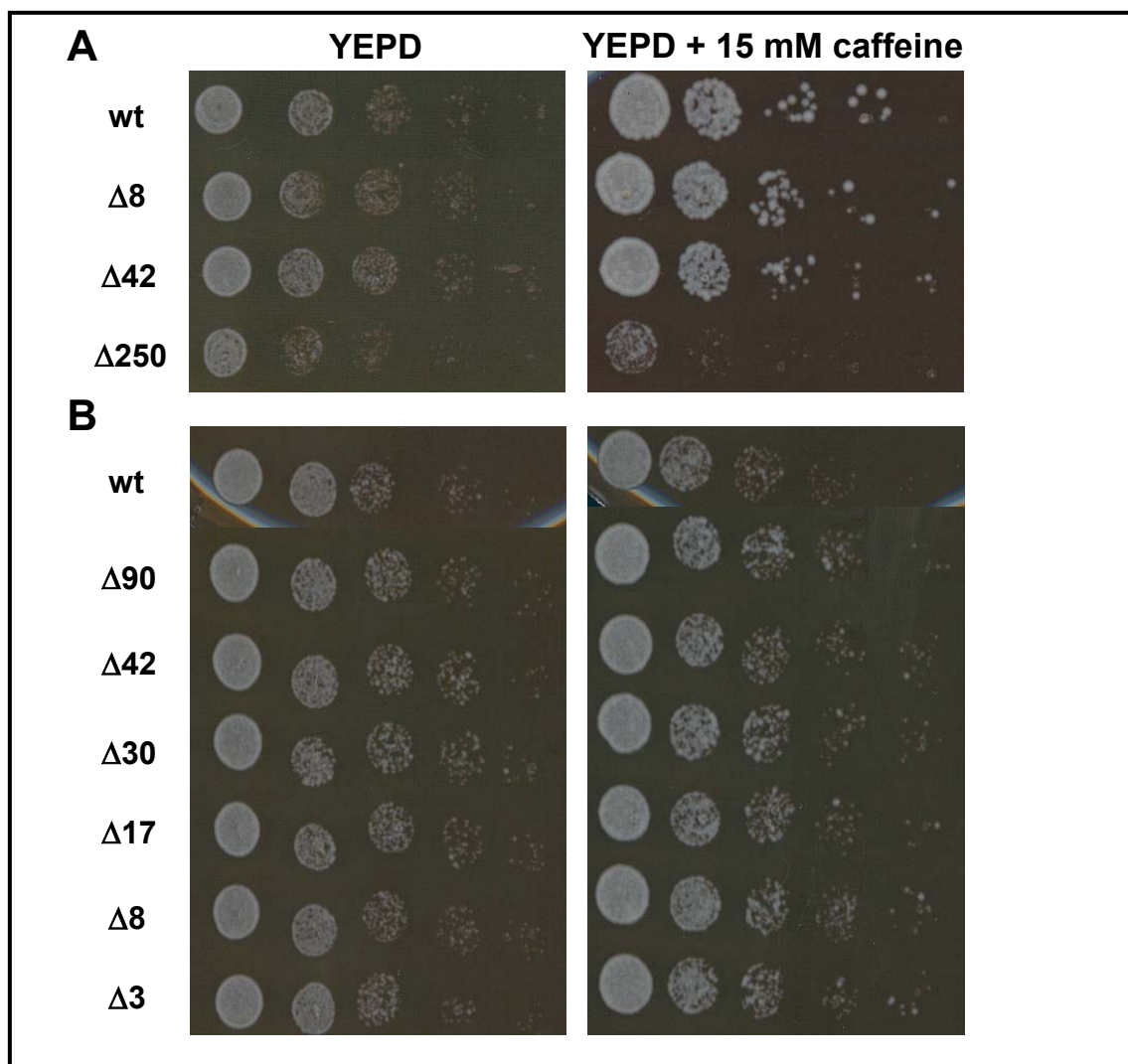

Fig. 3.20 Serial dilution assays in YEPD and in the presence of 15mM caffeine with distinct Ynl152wp C-terminal truncations. A) *ynl152wΔ8*, *Δ42* and *Δ250* were assayed against a wild-type control. **B)** *ynl152wΔ3*, *Δ8*, *Δ30*, *Δ42* and *Δ90* were assayed in this case.

3.2.5 Effect on Pkc1p cell integrity pathway

YNL152w originally appeared in a screen for negative regulators of the Pkc1p cell wall integrity pathway using transposon mutagenesis (Schmitz, 2001). Therefore the activity of the latter was further assessed, **Table 3.5** summarizes the effect of the different truncations on the pathway activity, which was indirectly determined using an integrated *lexA-RLM1-lacZ* reporter construct. For the investigated truncations, the strains described in section **3.2.2** were crossed to the *lexA*-integrant, sporulated and subjected to tetrad analyses. Segregants carrying either wild-type or truncation alleles of *YNL152w* were again checked by PCR except for the mutant Tn24, which was selected by the segregation pattern of selection marker.

Table 3.5 summarizes the result of two independent experiments for each strain (**A** and **B**), in which β-galactosidase activities were measured under inducing conditions (cultures grown for 6 h in YEPD at 37 °C) for three different Tn24 segregants. For each of them, a wild-type segregant from the same tetrad was used as a control. The absolute values of β-galactosidase activity show a high variation between the different experiments, and among the three tetrads. However, when comparing the activity of Tn24 with that of the wild-type by calculating the activity ratio **Q** (**mut/wt**), the obtained values were fairly reproducible. In segregant$_1$ and segregant$_3$ the β-galactosidase activity of Tn24 was very similar to the wild-type, with **Q** values around one, in both replicas. Conversely, in segregant$_2$ the activity of Tn24 was much lower than the wild-type. But, considering that in two tetrads out of three the Tn24 and wild-type activities were very similar, it could be assumed this is the right tendency. Together, these results suggest that under inducing conditions there is no significant difference in the Pkc1p-pathway activity between the wild-type and the Tn24 mutant strain. It is noteworthy to mention that the control experiments performed under stabilized conditions (cultures grown in YEPD + 1M sorbitol at 30 °C), gave expected very low β-galactosidase activities (between 0.2-20 mU/mg protein) in contrast to the high values observed under inducing conditions.

Since no significant differences were found between the Pkc1p-pathway activity of the mutant Tn24 and the wild-type, larger truncations were tested for the activity of the pathway. Therefore, the activity of the pathway was first measured in the *ynl152wΔ42* strain.

Table 3.5 Specific β-galactosidase activities (mU/mg of protein) with the *lexA-RLM1-lacZ* integrated report construct. The measurements were made under inducing conditions of the Pkc1p-pathway (YEPD at 37 °C). Three different mutant segregants were assayed together with the correspondent wild-type segregant. A and B represent two independent experiments with the same segregants. The activities are expressed as the average of two independent measurements from each crude extract. All segregants were checked by PCR except for the Tn24 ones, selected by the segregation pattern of the selection marker.

ynl152w construct	wt-segregant	*ynl152w* mutant	Q (mut/wt)
A			
$Tn24_1$	417 ± 28	545 ± 5	1.3
$Tn24_2$	424 ± 24	78 ± 1	0.2
$Tn24_3$	72 ± 11	71 ± 34	1.0
B			
$Tn24_1$	200 ± 1	342 ± 15	1.7
$Tn24_2$	332 ± 18	13 ± 6	(<0.1)
$Tn24_3$	75 ± 20	84 ± 18	1.1
A			
$\Delta42_1$	714 ± 21	95 ± 12	0.1
$\Delta42_2$	714 ± 71	89 ± 5	0.1
$\Delta42_3$	87 ± 4	84 ± 11	1.0
B			
$\Delta42_1$	283 ± 21	66 ± 27	0.2
$\Delta42_2$	231 ± 97	58 ± 38	0.3
$\Delta42_3$	53 ± 6	49 ± 23	0.9
A			
$\Delta150_1$	493 ± 126	329 ± 4	0.7
$\Delta150_2$	387 ± 39	202 ± 36	0.5
$\Delta150_3$	160 ± 8	132 ± 35	0.8
B			
$\Delta150_1$	767 ± 75	636 ± 243	0.8
$\Delta150_2$	549 ± 141	566 ± 135	1.0
$\Delta150_3$	544 ± 125	320 ± 4	0.6

It should be recalled, that *ynl152wΔ42* shows a morphological phenotype (see **Fig. 3.14**). Table 3.4 shows the β-galactosidase activities obtained under inducing condition, of two independent experiments (A and B), for three different *ynl152wΔ42* and wild-type segregants. Like in the Tn24 construct, the variation in the β-galactosidase activities was high between both replica experiments. However, in this case the values of β-galactosidase activity are very similar among the segregants excluding wt$_3$, in which the activity is very reduced compared to wt$_1$ and wt$_2$. Calculating the β-galactosidase activity ratio Q, it is clear that in segregant$_1$ and segrgant$_2$ the activities are consistently lower in the mutants Δ42$_1$ and Δ42$_2$. Thus, in two of the three analyzed segregants, the activities of *ynl152wΔ42* were significantly lower than in the wild type. The control experiments performed under stabilizing conditions gave expected low β-galactosidase activities (between 0.9-5.0 mU/mg protein).

Continuing with the analysis of the Pkc1p-pathway activity in *ynl152w* truncated mutants, it was necessary to investigate whether the tendency displayed by *ynl152wΔ42* is kept in a mutant with an even larger truncation of the C-terminus. Consequently, a similar experiment was performed, but using the mutant strain *ynl152wΔ150*. Like *ynl152wΔ42*, the strain *ynl152wΔ150* exhibits a morphological phenotype, but much severer (see **Fig. 3.15**). As shown in **Table 3.5**, there was again a considerable variation in the β-galactosidase activities, when referring to the absolute value. Nevertheless, the examination of the activity ratio **Q** reveals very similar and fairly reproducible β-galactosidase activities for the three segregants in both replica experiments. In all cases **Q** was close to one (varying from 0.8-0.5) looking at the associated standard error a significant difference between the β-galactosidase activities of *ynl152wΔ150* and the wild-type can not be inferred. Again, the control experiments carried out under stabilizing conditions, resulted in low activity values (between 7.0-22.0 mU/mg protein).

3.2.6 Phenotypic analysis of an internal deletion

Apart from the proline-rich motifs depicted in **Fig. 3.12**, another potentially important region of the Ynl152w protein is an aspartate-rich domain. This domain is located between amino acids 303-313 and consists of the sequence DEDDDDDDEND. In the last two sections an abrupt change in the phenotype was described for the larger

C-terminal truncations, starting from *ynl152wΔ150*. The single evident difference between the *ynl152wΔ150* strain and the immediately preceding *ynl152wΔ90*, is the lack of the aspartate-rich domain in the former. Therefore, a mutant strain (*ynl152wΔAsp*) with a deletion of the sequence encoding the aspartate domain, was investigated. Notably, the *ynl152wΔAsp* strain exhibits morphological phenotypes very similar to those described for the large C-terminal truncations, i.e. the appearance of big aggregates and very large elongated cells (**Fig. 3.21**).
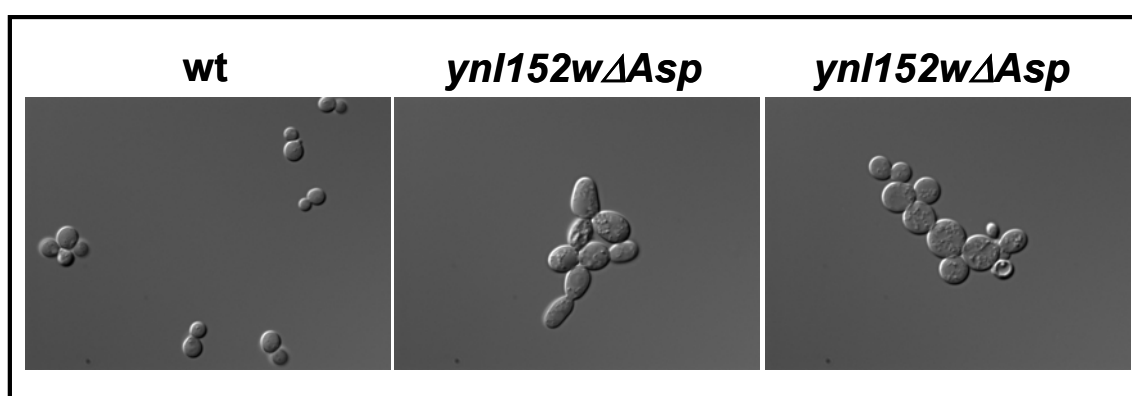
Fig. 3.21 Bright field images showing a morphologic phenotype of the *ynl152wΔAsp* strain. The *ynl152wΔAsp* strain exhibits a morphologic phenotype with the appearance of big aggregates and very large elongated cells. Cells were grown in rich liquid medium at 30 °C. All pictures were made with identical magnification.

Also coincident with the large *ynl152w* C-terminal truncations, the flow cytometry analysis of *ynl152wΔAsp* revealed a high average cell size (**Fig. 3.22 B**). Nevertheless, as shown in **Fig. 3.22 A** the distribution of the DNA content does not exactly fit with the histograms observed for the large *ynl152w* C-terminal truncations, although it does differ from the wt. Indeed, the *ynl152wΔAsp* histogram is shifted to the right indicating a higher proportion of the population containing 2n or more DNA content. The phenotype observed in the *ynl152wΔAsp* strain, suggests that the aspartate-rich domain may play an important role in the function of the Ynl152w protein.
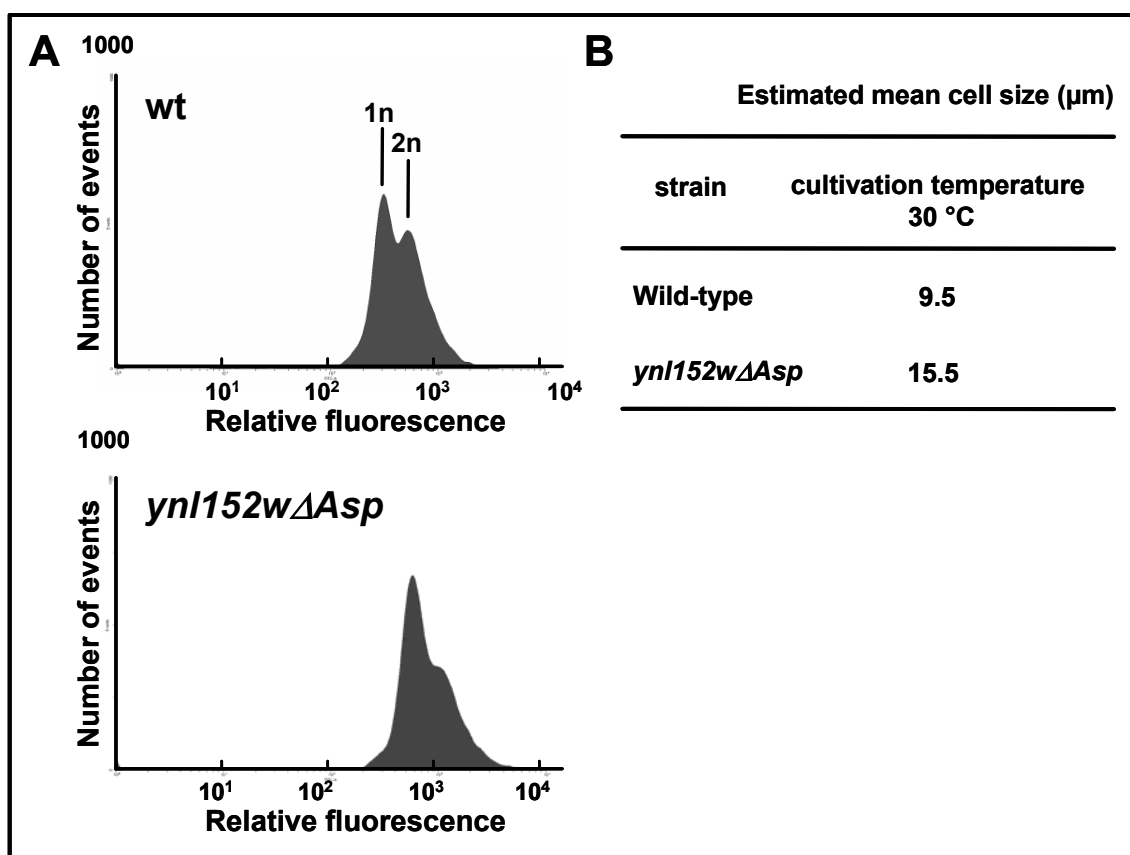
Fig. 3.22 Flow cytometry analysis of the *ynl152wΔAsp* strain. A) The DNA content was determined by the fluorescence of sytox green stained cells. Cells were cultured at 30 °C and 20,000 events were recorded. B) The mean relative cell size was determined.

3.3 Analysis of cytokinesis defects in *ynl152w* mutants: Stability of the Hof1 protein

The phenotypes of *ynl152w* mutants described above clearly indicate a function of the encoded protein in cytokinesis. In addition, two independent studies have shown a two-hybrid interaction between Ynl152wp and the Hof1 protein which participates in cytokinesis (Vallen *et al.*, 2000). Furthermore, it has been reported that degradation of Hof1p during cytokinesis is necessary for a proper cell separation, and mutants lacking this degradation show morphologies similar to the ones described above for the *ynl152w* mutants. Therefore, the stability of the Hof1 protein was determined in different *ynl152w* mutant backgrounds.
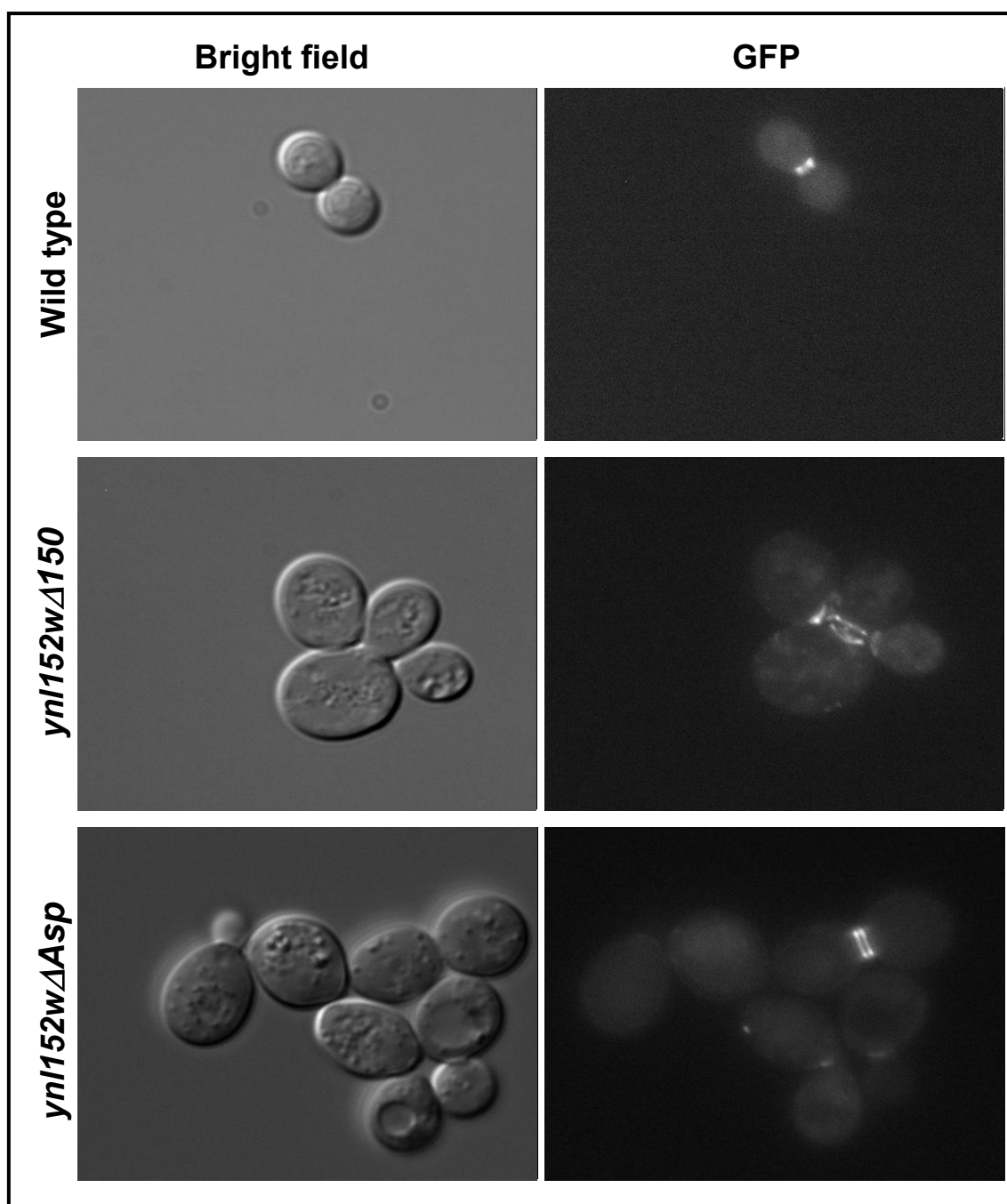
Fig. 3.23 Hof1p-GFP localization in the wild-type and the mutant strains *ynl152wΔ150* and *ynl152wΔsp*. In a typical counting-experiment of Hof1p-GFP signals, a bright field image of the cell was made followed by a fluorescence image to count the Hof1p-GFP rings. The pictures were made with identical magnification.

### 3.3.1 Quantification of Hof1p-GFP signals in different *ynl152w* mutant backgrounds

As a first approach to study the stability of the Hof1p protein, the number of Hof1p-GFP signals per cell or cell cluster was counted in different *ynl152w* mutant backgrounds. Exponentially growing cultures were observed under the fluorescence microscope and budding-cells as well as Hof1p-GFP fluorescent rings, were quantified (**Fig. 3.23**). Four *ynl152w* mutant strains were selected for the experiment: The aspartate-rich domain deletion strain *ynl152wΔAsp*, and the deletion strains *ynl152wΔ42, Δ90* and *Δ150*. If Ynl152wp was involved in the degradation of Hof1p, the Hof1p protein should be stabilized and result in a higher proportion of Hof1p-GFP signals. Consistent with this prediction, the mean value of Hof1p-GFP signals per cell population (See **Table 3.6**) was significantly higher in the mutant strains *ynl152wΔAsp* and *ynl152wΔ150* as compared to the wild-type (Bonferroni t-test at $p<0.05$). Interestingly the number of Hof1p-GFP double rings was significantly higher in *ynl152wΔAsp*, as compared to the other strains (Bonferroni t-test at $p<0.05$).

Table 3.6 Stability of Hof1p. Counting of Hof1p-GFP signals in the wild-type and in different *ynl152w* mutant backgrounds. The values of the Hof1p-GFP signals, were determined from at least 3 independent experiments summed up in the table (5 in case of wt, *ynl152wΔ150* and *ynl152wΔAsp*).

Counting of Hof1p-GFP signals			
Strain	signals	double rings	budding cells
wt	33 (14 %)	2 (0.9 %)	229
ynl152wΔ42	48 (26 %)	2 (1.0 %)	182
ynl152wΔ90	55 (28 %)	2 (1.0 %)	196
ynl152wΔ150	102 (43 %)	14 (5.6 %)	235
ynl152wΔAsp	135 (56 %)	71 (30 %)	240

3.3.2 Determination of the retention time of Hof1p-GFP at the bud neck

The stabilization of Hof1p-GFP was further investigated by time-lapse experiments of single dividing cells in the *ynl152w* mutants which showed the highest number of Hof1p-GFP signals per cell population (*ynl152wΔ150* and *ynl152wΔAsp* **Table 3.6**). For this purpose, growing cells in the early exponential phase were put on a slide carrying an agarose slice supplemented with YEP and glucose. A group of dividing cells was selected, and the time-lapse was started with a series of bright field and fluorescence images at intervals of 5 min. In the ideal situation the signal would appear and fade within the observation time. However, in many occasions the signals were already present at the start and therefore the initial time point was unknown. The mean values obtained for the Hof1p retention time in both situations (T_0 = determined by appearance of the GFP-signal and T_0 = undetermined due to the presence of the signal at the start) are summarized in **Table 3.7**.

Table 3.7 Estimation by time lapse of the Hof1p retention time in the wild-type and in the mutants *ynl152wΔ150* and *ynl152wΔAsp*. The Hof1p-GFP retention time was estimated in two different circumstances, with the initial T_0 = determined or undetermined.

Estimation of the Hof1p retention time				
Strain	Avergage retention time (min) T_0= determined	Analyzed cells	Avergage retention time (min) T_0= undetermined	Analyzed cells
wt	70 ± 18	3	43 ± 18	4
ynl152wΔ150	183 ± 29	12	141 ± 51	4
ynl152wΔAsp	238 ± 12	3	162 ± 64	7

Naturally the average values obtained for Hof1p retention time were lower and with a bigger error when the initial time point T_0 was undetermined (**Table 3.7**, third row). Thus, in each analyzed strain, the real value of the Hof1p retention time should be close to the ones obtained in the situation when T_0 was determined (**Table 3.7**, first row).

Indeed, the estimated value of the Hof1p retention time in the wild-type coincides with published values (Hof1p-GFP retention time $\cong$ 55 min; Blondel *et al.*, 2005). Invariably the retention time of Hof1p was dramatically increased in the mutant strains as compared to the wild-type.

3.3.3 Cellular localization of Ynl152wp

Ynl152wp has been shown to be evenly distributed within the cytoplasm, by a C-terminal GFP-fusion obtained in a genome-wide approach (Huh *et al.*, 2003). Since the results described above indicate an important function of the C-terminal sequences, an N-terminal GFP-fusion was analyzed in the following (**Fig. 3.24**). For this purpose, an
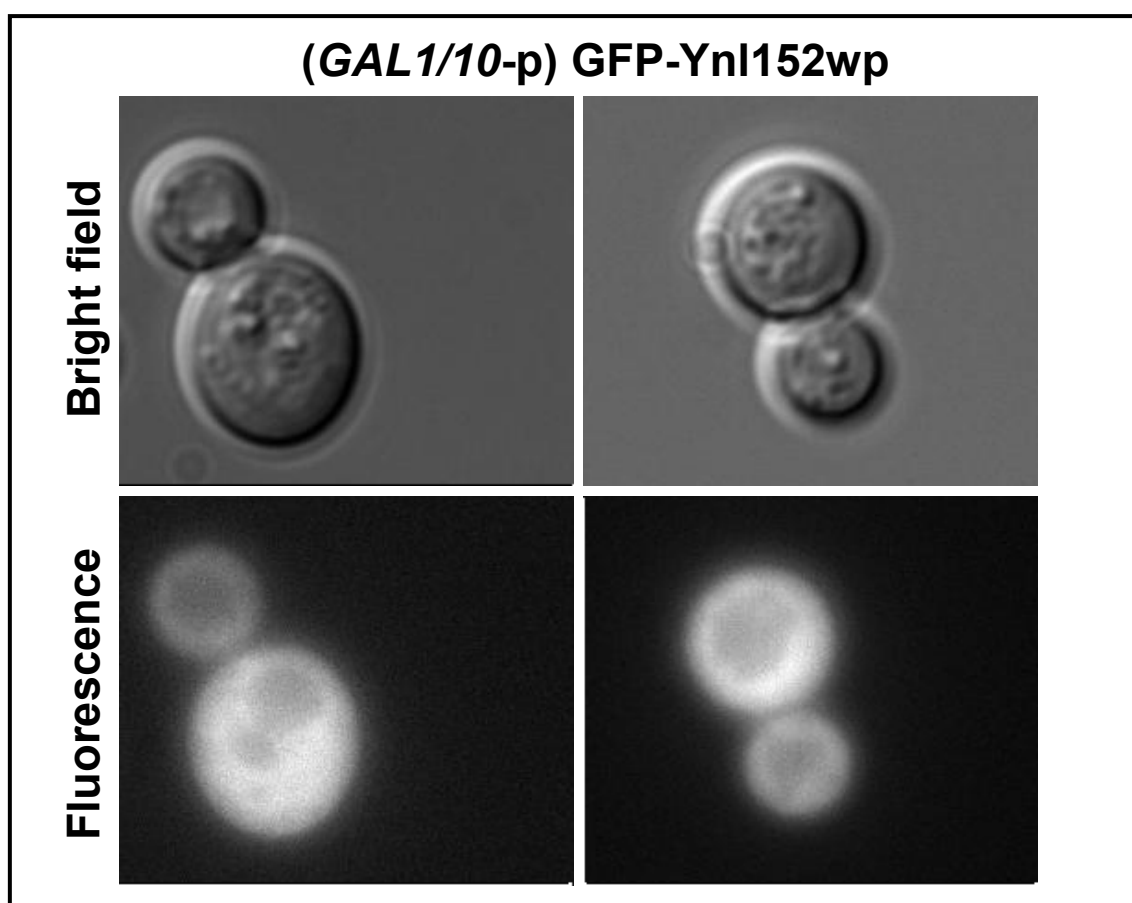
Fig. 3.24 Cellular localization of an amino terminal GFP-Ynl152wp fusion under control of the inducible *GAL1/10* promoter. The upper panels show the bright field images of the cell, whereas the lower show the correspondent fluorescence images with the cellular localization of the GFP-Ynl152wp fusion.

amino terminal GFP-Ynl152wp fusion was constructed and expressed under the control of the inducible *GAL1/10* promoter. This construct was also found evenly distributed within the cytoplasm. Only a bright signal surrounding the vacuole was observed, but this could result from the over-expression from the *GAL1/10* promoter.

4. Discussion

4.1 Influence of *YNL152w* on the Pkc1p cell integrity pathway

The original Tn24 transposon mutant was first isolated during a screen searching for putative negative regulators of the pathway (Schmitz, 2001). Hence the initial hypothesis was that *YNL152w* would be involved in the down-regulation of the Pkc1p pathway, although given the characteristics of the screen the interaction could be of a more indirect nature (see introduction). In the following the phenotypic analysis performed in relation to this signaling will be discussed.

4.1.1 Caffeine resistance of the Tn24 transposon mutant strain

As a first approach a serial dilution assay was performed in presence of caffeine. The mutant Tn24 showed a caffeine resistance phenotype (**Fig. 3.1**), which is consistent with a role for *YNL152w* as a down-regulator. Thus, mutants defective in components of the Pkc1p pathway usually display increased sensitivities to this drug. Nevertheless, the effect caused by caffeine on the cell wall still remains obscure (Levin, 2005; Lum *et al.*, 2004), and therefore this result could only be taken as a first hint for the connection between *YNL152w* and the Pkc1p pathway.

4.1.2 Viability of the *ynl152w* deletion mutant under osmotic stabilization

In contrast to the Tn24 strain, the null mutant obtained in the systematic deletion has been reported to be lethal under standard growth conditions (Giaever *et al.*, 2002). If Ynl152wp was directly involved in the regulation of the Pkc1p pathway, the lethality of *ynl152wΔ* could be caused by a deregulation of the pathway. Then, the presence of 1 M sorbitol would restore cell viability to the *ynl152wΔ* deletion. In a tetrad analysis, the deletion could not be rescued by osmotic stabilization (**Fig. 3.2**). In principle, this rules out a direct effect of *YNL152w* on the Pkc1p-pathway regulation. This expected result, suggests that Ynl152wp is not a component of the Pkc1p pathway.

4.1.3 Caffeine sensitivity of the pJJH447-*YNL152w* overexpressing strain

Another experiment that could give more clues on the subject was the analysis of the *YNL152w* overexpression, again in the presence of caffeine. A strain carrying the multicopy plasmid pJJH447 with *YNL152w* under control of the inducible *GAL1/10* promoter, showed slightly more sensitivity towards caffeine (7.5 mM) when assayed under inducing conditions (2% galactose, **Fig. 3.3**). Like **4.1.1** this result is consistent with a role for *YNL152w* as a down-regulator of the Pkc1p pathway. However, for the reasons explained above (**4.1.1**) regarding the caffeine effect on the cell wall, this result can not be taken as conclusive evidence to support a role for *YNL152w* as a negative regulator.

4.1.4 Determination of the Pkc1p pathway activity using an integrated *lexA-RLM1-lacZ* reporter construct

To determine more specifically the influence of *YNL152w* on the activity of the Pkc1p pathway, a series of activity assays were performed using the integrative *lexA-RLM1-lacZ* reporter in different *ynl152w* mutant backgrounds. A defect in a negative regulator would result in an elevated activity of the β-galactosidase reporter. However, either no alteration (Tn24 and *ynl152wΔ150*) or even decreased activities (*ynl152wΔ42*) were observed in the transposon and truncation mutants (**Table 3.5**). This stands in contrast to the original genetic screen in which *YNL152w* was identified (Schmitz, 2001), using a very similar reporter system.

Due to the considerable degree of variations observed for the assays in this work, which has also been reported (Straede *et al.*, 2007; in press), the question of pathway activation awaits a more reliable test system. An immunological detection of Mpk1 phosphorylation, as previously reported (de Nobel *et al.*, 2000), could not be performed within the scope of this work. Finally, besides the mentioned intrinsic variation of the reporter system, another factor that could have contributed to the observed total variation is the presence of a DNA segregation defect in the truncated mutants (**Fig. 3.16**). Mutants with associated chromosomal segregation defects, usually display high variations in this kind of reporter assays (H.P. Schmitz, personal communication).

4.2 Conditional expression of *Ynl152w*: Consequences of different expression levels

To shed some light on the function of Ynl152wp, galactose depletion assays were performed, using conditional expression of the encoding gene from the *GAL1/10* promoter. It turned out that both episomal and genomic conditional alleles conferred growth to a *ynl152w* deletion strain even on glucose media, i.e. under repressing conditions. This result was unexpected and indicates that very low levels of Ynl152wp are sufficient for *in vivo* function. It is possible that the expression of *YNL152w* is up-regulated at the post-transcriptional level thus; this would allow for a higher translation rate even in the presence of low mRNA copy numbers. Apparently this is the case for yeast proteins involved in regulatory processes (Beyer *et al.*, 2004). Alternatively, growth defects may be observed in the episomal allele only after very prolonged incubations under repressing conditions. One hint in this direction is provided by the aberrant morphologies of cells observed after 26 h on glucose. On the other hand, the strain carrying the genomic *GAL1/10*p-*YNL152w* allele showed a pronounced aberrant morphology already after 5 h under repressing conditions. Again, this indicates that very low levels of the encoded protein are sufficient to sustain several cell divisions. It should also be noted that the determination of growth parameters by the optical density of cell suspensions may have its pitfalls. Thus, the aggregation and the swelling of cells frequently observed in these experiments may obscure the spectrometric determinations (Koch, 1970).

4.3 Effects of truncations within the Ynl152wp C-terminal tail and the deletion of an internal aspartate-domain

The distinct phenotypes found during the analysis of successive Ynl152wp C-terminal truncations as well as from an internal *ynl152w* deletion, will be discussed in this section.

4.3.1 Importance of the proline-rich motifs for the function of Ynl152wp

The investigation of a series of Ynl152wp C-terminal truncations strikingly revealed that around 2/3 of the C-terminal tail of the protein are dispensable to confer viability (**Fig 3.12**). On the other hand, the deletion of the C2 phospholipid-binding like domain is lethal, and therefore its function is essential for cell viability (R. Rodicio, personal communication). Thus, the lethality of the *ynl152wΔ279* mutant may result from the extreme reduction of the protein length, which could interfere with the correct folding of the C2 domain. Regarding the phenotypes of the viable constructs, already in the short deletions *ynl152wΔ3-42* abnormal morphologies could be observed with the appearance of big swollen and chained cells (**Fig. 3.14**). Starting with *ynl152wΔ150* a much severer phenotype is observed with very large and swollen cells as well as the formation of big aggregates (**Fig. 3.15**). In addition to the aberrant morphologies, many other phenotypes were detected in the large deletions *ynl152wΔ150-Δ270*. Thus, the nuclear division was affected in the *ynl152wΔ150* mutant and it also had a sporulation defect, with formation of aberrant asci (**Fig. 3.16** and **Fig. 3.17**). The homozygous *ynl152wΔ250* diploid strain was no longer able to sporulate, whereas the haploid strain showed growth problems under normal cultivation conditions as well as caffeine sensitivity. This sharp contrast between the short and the large truncations was also reflected in the FACS analyses. In the *ynl152wΔ3-90* truncations the distribution of the DNA content was altered with the emergence of a low fluorescence peak, together with a subpopulation of smaller cells (**Fig. 3.18** and **Table 3.3**). Conversely in the *ynl152wΔ150-270* truncations the DNA distribution histogram is shifted to the right with the appearance of a high fluorescence peak and a constant increase in the average cell size (**Fig. 3.19** and **Table 3.3**). This somehow "quantitative" phenotype observed through the different truncations from *ynl152wΔ3-270*, could be related to the presence activity of proline-rich motifs (PRM). Thus the sequential deletion of the four motifs present in the amino acid sequence of Ynl152wp (**Fig. 3.12**), would explain the early appearance of a phenotype already in the *ynl152wΔ8* mutant (indeed there is already a phenotype in *ynl152wΔ3*, but this would be caused by the deletion of a pair of conserved amino acids immediately adjacent to the first PRM [**Fig. 4.1**]) and the increasing severity of the phenotype in the larger deletions. It has been previously reported, that such proline-rich motifs interact with SH3 protein domains (Tong *et al.*, 2002). Interestingly, two potential binding partners

Sla1p and Hof1p have been identified so far for Ynl152wp, both of them carrying SH3 domains (Ito *et al*., 2001; Tong *et al*., 2002). Therefore, it is possible that the observed phenotypes are caused, at least partially, by the gradual disruption of such interactions. The observed phenotypes also suggest that the four motifs would be required for a proper function of the Ynl152w protein. This is supported by a recent publication, where it has been shown that the three PRMs of the cytokinesis related Vrp1p are indispensable for its interaction with the Hof1 protein (Ren *et al*., 2005). It should be noticed that the amino acids sequence of the four PRMs in Ynl152wp are not identical. The motifs were originally found during a BLAST homology search, and besides the prolines also other conserved amino acids could be detected (**Fig 4.1**). Starting from the Ynl152wp C-terminus the first PRM has the most distinct amino acid sequence PTRKRPPP, whereas the rest are almost identical with the sequence PPLP, except for the third one in which L is replaced by I. Thus, three of the PRMs closely match the consensus motif for SH3 binding, PXXP, where P is proline and X any amino acid (Tong *et al*. 2002). In the work on the interaction of Vrp1p with Hof1p (Ren *et al*., 2005), the authors suggest that Vrp1p is the principal regulator interacting with the SH3 domain of Hof1p. The three PRMs of Vrp1p indispensable for this interaction consist of the sequence PXPXXPSS, with a N-terminal PX extension and a pair of serines immediately following at the C-terminal side. Strikingly, in Ynl152wp the two PRMs most proximal to the N-terminus also present such PX extensions while the third carries instead a similar PXX (**Fig 4.1**). Moreover, all these motifs are closely flanked at both sides by a single or by pairs of conserved serines. The sequence similarities with Vrp1p suggest that Ynl152wp would interact with Hof1p in a similar fashion, with the serines acting as stabilizers through the formation of hydrogen bonds with Hof1p residues (Ren *et al.*, 2005). Thus Ynl152wp may also play an important role in the regulation of the Hof1p SH3 domain, especially considering the stabilization observed in *ynl152w* mutant backgrounds (see below).

Several of the observations discussed above indicate a role of *YNL152w* in cytokinesis. It has been reported that degradation of Hof1p during cytokinesis is necessary for a proper cell separation, and mutants lacking the degradation pathway show morphological defects (Blondel *et al*., 2005), which are similar to the ones found in the *ynl152w* mutants described here. In fact, a higher number of Hof1p-GFP signals at the bud neck were detected in the four selected *ynl152w* mutant strains (i.e. the aspartate-rich domain deletion strain *ynl152wΔ4sp*, and the deletion strains
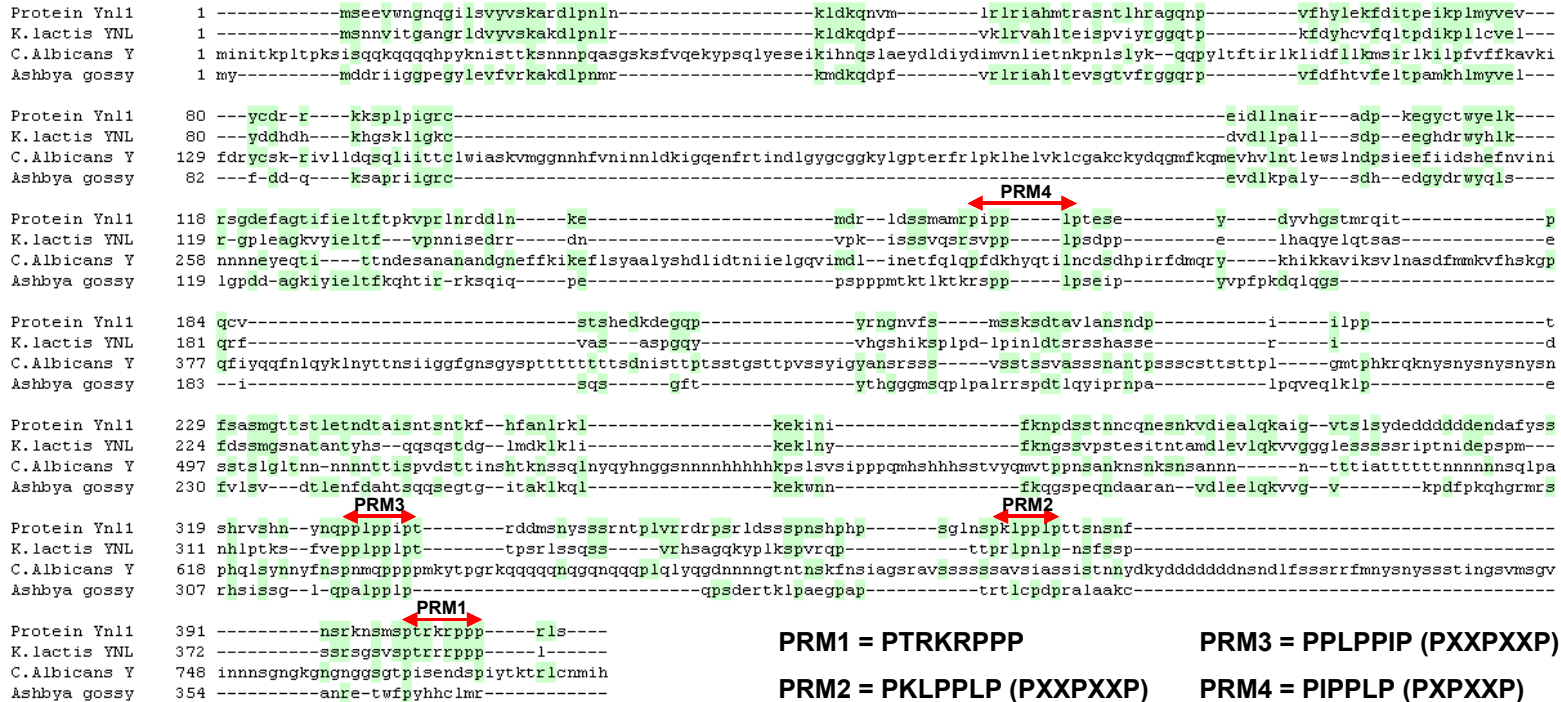
Fig. 4.1 Ynl152wp fungal BLAST homology alignment. The 3 best scores correspond to unnamed proteins of _K. lactis_ (NRRL Y-1140) and _A. gossypii_ (ATCC 10895), and to an hypothetical protein of _C. albicans_ (SC5314), repectively. Interestingly, within the conserved regions of Ynl152wp 4 proline-rich motifs (PRM) were identified. PRMs 2-4 present the first described and most common consensus sequence PXXP, which binds to SH3 domains. Strinkingly, these motifs carry N-terminal PXX extensions (or the similar PX in PRM4) just like the 3 PRMs of Vrp1p, which is a reported binding partner of Hof1p (Ren _et al._, 2005). Also coincident with Vrp1p, all 4 PRMs of Ynl152wp carry flanking conserved serine residues.

ynl152wΔ42, Δ90 and *Δ150*, **Table 3.6**). The statistical analysis indicates that indeed the number of rings per budding cell population is significantly higher in *ynl152wΔ150* and *ynl152wΔAsp* as compared to the wild-type (Bonferroni t-test at p<0.05). Perhaps, Hof1p-GFP is also at least slightly stabilized in the *ynl152wΔ42* and *Δ90* mutant backgrounds, but the method employed is not sensitive enough to detect it. Notably, the number of counted double rings was significantly higher in the *ynl152wΔAsp*. However the significance of this result at the moment is unclear. Structures like the one shown in **Fig. 3.23** for *ynl152wΔ150* could be frequently observed during the study. The coexistence of four Hof1p-GFP rings in that cluster of four cells is not only a sign of protein stabilization, but also of a defective cytokinesis. As seen in the introduction this process is spatially and temporally tightly regulated (Balasubramanian *et al.*, 2004) and the division of a cell should not start until the previous cell cycle is completed, like in this case.

Time-lapse experiments revealed that the retention time of the Hof1p-GFP signal was increased approximately by a factor of 3 in the above mentioned *ynl152w* mutants (**Table 3.7**). This indicates that Ynl152wp interferes with the process of Hof1p degradation. However, how exactly this is mediated remains to be determined.

Considering the phenotypes of *ynl152wΔ250* and *Δ270* (which were more severe than the one reported for a *hof1* deletion mutant [Vallen *et al.*, 2000]), and the essential function of the C2 phospholipid-binding like domain, certainly Ynl152wp exerts other functions apart from its interaction with Hof1p. One could speculate that Ynl152wp interacts with other binding partners mediating the degradation of other important proteins via the proteasome pathway.

4.3.2 The role of the aspartate rich domain

A strain with a short internal deletion of the aspartate rich sequence displayed the same phenotypes as the larger *ynl152wΔ150* truncation. This indicates that the concentration of negatively charged amino acids in the DEDDDDDDEND motif would mediate an important function of Ynl152wp. Several possible explanations are feasable: (1) It is possible that the domain is only required for a proper folding of the protein, which in turn would be needed for the correct functioning of the PRMs. (2) The domain could directly interact with a positively charged region of a binding partner, thus

facilitating the interaction with the PRMs. For example the domain could modulate the interaction between the cytokinesis related Hof1 protein and Ynl152wp. Recently the data from two independent genome-wide two-hybrid studies (Ito *et al.*, 2001; Tong *et al.*, 2002) was confirmed in our lab with a two hybrid experiment in which the SH3 domain of Hof1p was tested against Ynl152wp (A. Jendretzki, personal communication). Hence, to test the former proposition it would be necessary to repeat the study with the *ynl152wΔAsp* mutant, to check whether this interaction is disrupted. Interestingly, in *Mycobacterium tuberculosis* an interaction between a stretch of four aspartates from the FtsZ protein and a negatively charged region of FtsW has been reported. FtsZ is a bacterial homologue of tubulin an its function is crucial to bacterial cell division (Datta *et al.*, 2002). (3) Finally, it can not be excluded that the aspartate rich domain could interact with a third binding partner, which could be acting as a mediator of the PRMs activity. Although the absence of the aspartate rich domain would explain the abrupt change in the phenotype of the large truncations (commencing with *ynl152wΔ150*), apparently the fourth PRM proximal to the N-terminus is also required. This is supported by the fact that the two largest viable truncations (*ynl152wΔ250* and *Δ270*) lacking this motif, showed an even stronger phenotype compared to *ynl152wΔ150* (i.e. a complete lack of sporulation, a reduced growth, and an increased average cell size).

As a final point, some key issues should still be addressed to further characterize the function of the essential *YNL152w* gene: (1) A complementation with a biochemical approach of the genetic studies regarding the Ynl152wp-Hof1p interaction as well as the regulation of the *YNL152w* expression. (2) The confirmation and analysis of its interaction with the Sla1 protein, which is involved in endocytosis and actin dynamics (Warren *et al.*, 2002) and therefore could represent a link between protein degradation and cell division. (3) The investigation of the N-terminal C2 phospholipid-binding like domain, whose deletion is lethal and for which a phospholipid binding activity has been proposed (Hazbun *et al.*, 2003) based on homology alingments. (4) The identification of new Ynl152wp binding partners which could contribute to solve the complex molecular puzzle behind such dynamic processes like cell division and protein degradation.

5. Summary

The essential gene *YNL152w* was previously found in a screen designed to isolate putative negative regulators of the *S. cerevisiae* Pkc1p pathway. Lethality of the *ynl152w* deletion could not be rescued by osmotic stabilization. On the other hand, serial dilution assays performed on caffeine with the Tn24 transposon mutant and a *YNL152w* overexpressing strain showed phenotypes consistent with a role for this gene as a down-regulator of the Pkc1p signaling pathway. Activity assays were performed with a *lexA-RLM1-lacZ* integrated reporter in different *ynl152w* truncated mutants. In contrast to the original screen, there were no differences or the activities were even lower in the mutants as compared to the control.

In order to analyze the consequences of different expression levels, *YNL152w* was expressed under the control of the *GAL1/10* promoter. Growth curves were performed under high (galactose), intermediate (raffinose) and low (glucose) expression levels. Strikingly, both strains carrying the conditional allele were able to grow under repressing conditions. However, an aberrant morphology was detected suggesting that the cells are indeed affected by low amounts of Ynl152w protein.

A series of successive Ynl152wp C-terminal truncations (*ynl152wΔ3- ynl152wΔ270*) was analyzed to determine cell viability and to investigate the function of the protein. Remarkably, about 2/3 of the protein were dispensable to confer viability. Microscopic analyses of the viable constructs revealed an aberrant morphology characteristic of a cytokinesis defective mutant, with the appearance of swollen cells and formation of big aggregates. Interestingly, the phenotype was more pronounced in the larger truncations (*ynl152wΔ150-ynl152wΔ270*). This was also reflected in the FACS analysis. Although all mutants showed an altered DNA histogram distribution, the larger ones displayed apparently higher DNA contents accompanied by an increment in the average cell size. Coherent with these results time-lapse experiments with a large truncated mutant (*ynl152wΔ150*) showed a stabilization of the SH3 protein Hof1p at the bud neck. This protein is involved in septum formation and has been reported as a binding partner of *YNL152w* in two independent works. The phenotypes observed in the truncated mutants could be attributed to the presence of 4 proline rich motifs (PRM). Such motifs have been reported to interact with SH3 domains like Vrp1p, in which its 3 PRMs are required to mediate an interaction with Hof1p. Finally, an internal deletion of an aspartate rich domain present in the Ynl152wp sequence also displayed a phenotype very similar to that of the largest truncations. Therefore, this domain must play an important role in the function of the Ynl152wp protein.

6. Bibliography

Adamo, J.E., Rossi, G., and Brennwald, P. (1999) The Rho GTPase Rho3 has a direct role in exocytosis that is distinct from its role in actin polarity. *Mol Biol Cell* **10**: 4121-4133.

Adamo, J.E., Moskow, J.J., Gladfelter, A.S., Viterbo, D., Lew, D.J., and Brennwald, P.J. (2001) Yeast Cdc42 functions at a late step in exocytosis, specifically during polarized growth of the emerging bud. *J Cell Biol* **155**: 581-592.

Adams, A.E., and Pringle, J.R. (1984) Relationship of actin and tubulin distribution to bud growth in wild-type and morphogenetic-mutant *Saccharomyces cerevisiae*. *J Cell Biol* **98**: 934-945.

Antonin, W., Holroyd, C., Tikkanen, R., Honing, S., and Jahn, R. (2000) The R-SNARE endobrevin/*VAMP-8* mediates homotypic fusion of early endosomes and late endosomes. *Mol Biol Cell* **11**: 3289-3298.

Arvanitidis, A., and Heinisch, J.J. (1994) Studies on the function of yeast phosphofructokinase subunits by in vitro mutagenesis. *J Biol Chem* **269**: 8911-8918.

Aspenstrom, P. (1997) A Cdc42 target protein with homology to the non-kinase domain of FER has a potential role in regulating the actin cytoskeleton. *Curr Biol* **7**: 479-487.

Ayscough, K.R., Eby, J.J., Lila, T., Dewar, H., Kozminski, K.G., and Drubin, D.G. (1999) Sla1p is a functionally modular component of the yeast cortical actin cytoskeleton required for correct localization of both Rho1p-GTPase and Sla2p, a protein with talin homology. *Mol Biol Cell* **10**: 1061-1075.

Ayscough, K.R. (2005) Coupling actin dynamics to the endocytic process in *Saccharomyces cerevisiae*. *Protoplasma* **226**: 81-88.

Balasubramanian, M.K., McCollum, D., Chang, L., Wong, K.C., Naqvi, N.I., He, X., Sazer, S., and Gould, K.L. (1998) Isolation and characterization of new fission yeast cytokinesis mutants. *Genetics* **149**: 1265-1275.

Balasubramanian, M.K., Bi, E., and Glotzer, M. (2004) Comparative analysis of cytokinesis in budding yeast, fission yeast and animal cells. *Curr Biol* **14**: R806-818.

Barral, Y., Mermall, V., Mooseker, M.S., and Snyder, M. (2000) Compartmentalization of the cell cortex by septins is required for maintenance of cell polarity in yeast. *Mol Cell* **5**: 841-851.

Bender, A., and Pringle, J.R. (1989) Multicopy suppression of the cdc24 budding defect in yeast by *CDC42* and three newly identified genes including the ras-related gene *RSR1*. *Proc Natl Acad Sci U S A* **86**: 9976-9980.

Benedetti, H., Raths, S., Crausaz, F., and Riezman, H. (1994) The *END3* gene encodes a protein that is required for the internalization step of endocytosis and for actin cytoskeleton organization in yeast. *Mol Biol Cell* **5**: 1023-1037.

Bi, E., Maddox, P., Lew, D.J., Salmon, E.D., McMillan, J.N., Yeh, E., and Pringle, J.R. (1998) Involvement of an actomyosin contractile ring in Saccharomyces cerevisiae cytokinesis. *J Cell Biol* **142**: 1301-1312.

Bi, E. (2001) Cytokinesis in budding yeast: the relationship between actomyosin ring function and septum formation. *Cell Struct Funct* **26**: 529-537.

Blondel, M., Bach, S., Bamps, S., Dobbelaere, J., Wiget, P., Longaretti, C., Barral, Y., Meijer, L., and Peter, M. (2005) Degradation of Hof1 by SCF(Grr1) is important for actomyosin contraction during cytokinesis in yeast. *Embo J* **24**: 1440-1452.

Boeke, J.D., LaCroute, F., and Fink, G.R. (1984) A positive selection for mutants lacking orotidine-5'-phosphate decarboxylase activity in yeast: 5-fluoro-orotic acid resistance. *Mol Gen Genet* **197**: 345-346.

Boeke, J.D., Trueheart, J., Natsoulis, G., and Fink, G.R. (1987) 5-Fluoroorotic acid as a selective agent in yeast molecular genetics. *Methods Enzymol* **154**: 164-175.

Casamayor, A., and Snyder, M. (2002) Bud-site selection and cell polarity in budding yeast. *Curr Opin Microbiol* **5**: 179-186.

Caviston, J.P., Longtine, M., Pringle, J.R., and Bi, E. (2003) The role of Cdc42p GTPase-activating proteins in assembly of the septin ring in yeast. *Mol Biol Cell* **14**: 4051-4066.

Chant, J., and Pringle, J.R. (1991) Budding and cell polarity in *Saccharomyces cerevisiae*. *Curr Opin Genet Dev* **1**: 342-350.

Chant, J. (1999) Cell polarity in yeast. *Annu Rev Cell Dev Biol* **15**: 365-391.

Chuang, J.S., and Schekman, R.W. (1996) Differential trafficking and timed localization of two chitin synthase proteins, Chs2p and Chs3p. *J Cell Biol* **135**: 597-610.

Cope, M.J., Yang, S., Shang, C., and Drubin, D.G. (1999) Novel protein kinases Ark1p and Prk1p associate with and regulate the cortical actin cytoskeleton in budding yeast. *J Cell Biol* **144**: 1203-1218.

Datta, P., Dasgupta, A., Bhakta, S., and Basu, J. (2002) Interaction between FtsZ and FtsW of *Mycobacterium tuberculosis*. *J Biol Chem* **277**: 24983-24987.

de Nobel, H., Ruiz, C., Martin, H., Morris, W., Brul, S., Molina, M., and Klis, F.M. (2000) Cell wall perturbation in yeast results in dual phosphorylation of the Slt2/Mpk1 MAP kinase and in an Slt2-mediated increase in *FKS2-lacZ* expression, glucanase resistance and thermotolerance. *Microbiology* **146 (Pt 9)**: 2121-2132.

DeMarini, D.J., Adams, A.E., Fares, H., De Virgilio, C., Valle, G., Chuang, J.S., and Pringle, J.R. (1997) A septin-based hierarchy of proteins required for localized deposition of chitin in the *Saccharomyces cerevisiae* cell wall. *J Cell Biol* **139**: 75-93.

Dewar, H., Warren, D.T., Gardiner, F.C., Gourlay, C.G., Satish, N., Richardson, M.R., Andrews, P.D., and Ayscough, K.R. (2002) Novel proteins linking the actin cytoskeleton to the endocytic machinery in *Saccharomyces cerevisiae*. *Mol Biol Cell* **13**: 3646-3661.

Errington, J., Daniel, R.A., and Scheffers, D.J. (2003) Cytokinesis in bacteria. *Microbiol Mol Biol Rev* **67**: 52-65, table of contents.

Evangelista, M., Blundell, K., Longtine, M.S., Chow, C.J., Adames, N., Pringle, J.R., Peter, M., and Boone, C. (1997) Bni1p, a yeast formin linking Cdc42p and the actin cytoskeleton during polarized morphogenesis. *Science* **276**: 118-122.

Fankhauser, C., Reymond, A., Cerutti, L., Utzig, S., Hofmann, K., and Simanis, V. (1995) The S. pombe cdc15 gene is a key element in the reorganization of F-actin at mitosis. *Cell* **82**: 435-444.

Faty, M., Fink, M., and Barral, Y. (2002) Septins: a ring to part mother and daughter. *Curr Genet* **41**: 123-131.

Giaever, G., Chu, A.M., Ni, L., Connelly, C., Riles, L., Veronneau, S., Dow, S., Lucau-Danila, A., Anderson, K., Andre, B., Arkin, A.P., Astromoff, A., El-Bakkoury, M., Bangham, R., Benito, R., Brachat, S., Campanaro, S., Curtiss, M., Davis, K., Deutschbauer, A., Entian, K.D., Flaherty, P., Foury, F., Garfinkel, D.J., Gerstein, M., Gotte, D., Guldener, U., Hegemann, J.H., Hempel, S., Herman, Z., Jaramillo, D.F., Kelly, D.E., Kelly, S.L., Kotter, P., LaBonte, D., Lamb, D.C., Lan, N., Liang, H., Liao, H., Liu, L., Luo, C., Lussier, M., Mao, R., Menard, P.,

Ooi, S.L., Revuelta, J.L., Roberts, C.J., Rose, M., Ross-Macdonald, P., Scherens, B., Schimmack, G., Shafer, B., Shoemaker, D.D., Sookhai-Mahadeo, S., Storms, R.K., Strathern, J.N., Valle, G., Voet, M., Volckaert, G., Wang, C.Y., Ward, T.R., Wilhelmy, J., Winzeler, E.A., Yang, Y., Yen, G., Youngman, E., Yu, K., Bussey, H., Boeke, J.D., Snyder, M., Philippsen, P., Davis, R.W., and Johnston, M. (2002) Functional profiling of the *Saccharomyces cerevisiae* genome. *Nature* **418**: 387-391.

Gietz, R.D., Schiestl, R.H., Willems, A.R., and Woods, R.A. (1995) Studies on the transformation of intact yeast cells by the LiAc/SS-DNA/PEG procedure. *Yeast* **11**: 355-360.

Gladfelter, A.S., Pringle, J.R., and Lew, D.J. (2001) The septin cortex at the yeast mother-bud neck. *Curr Opin Microbiol* **4**: 681-689.

Gladfelter, A.S., Bose, I., Zyla, T.R., Bardes, E.S., and Lew, D.J. (2002) Septin ring assembly involves cycles of GTP loading and hydrolysis by Cdc42p. *J Cell Biol* **156**: 315-326.

Goffeau, A., Barrell, B.G., Bussey, H., Davis, R.W., Dujon, B., Feldmann, H., Galibert, F., Hoheisel, J.D., Jacq, C., Johnston, M., Louis, E.J., Mewes, H.W., Murakami, Y., Philippsen, P., Tettelin, H., and Oliver, S.G. (1996) Life with 6000 genes. *Science* **274**: 546, 563-547.

Goode, B.L., and Rodal, A.A. (2001) Modular complexes that regulate actin assembly in budding yeast. *Curr Opin Microbiol* **4**: 703-712.

Gourlay, C.W., Dewar, H., Warren, D.T., Costa, R., Satish, N., and Ayscough, K.R. (2003) An interaction between Sla1p and Sla2p plays a role in regulating actin dynamics and endocytosis in budding yeast. *J Cell Sci* **116**: 2551-2564.

Gray, C.H., Good, V.M., Tonks, N.K., and Barford, D. (2003) The structure of the cell cycle protein Cdc14 reveals a proline-directed protein phosphatase. *EMBO J* **22**: 3524-3535.

Guertin, D.A., Trautmann, S., and McCollum, D. (2002) Cytokinesis in eukaryotes. *Microbiol Mol Biol Rev* **66**: 155-178.

Guo, W., Tamanoi, F., and Novick, P. (2001) Spatial regulation of the exocyst complex by Rho1 GTPase. *Nat Cell Biol* **3**: 353-360.

Hanahan, D., Jessee, J., and Bloom, F.R. (1991) Plasmid transformation of *Escherichia coli* and other bacteria. *Methods Enzymol* **204**: 63-113.

Harkins, H.A., Page, N., Schenkman, L.R., De Virgilio, C., Shaw, S., Bussey, H., and Pringle, J.R. (2001) Bud8p and Bud9p, proteins that may mark the sites for bipolar budding in yeast. *Mol Biol Cell* **12**: 2497-2518.

Hazbun, T.R., Malmstrom, L., Anderson, S., Graczyk, B.J., Fox, B., Riffle, M., Sundin, B.A., Aranda, J.D., McDonald, W.H., Chiu, C.H., Snydsman, B.E., Bradley, P., Muller, E.G., Fields, S., Baker, D., Yates, J.R., 3rd, and Davis, T.N. (2003) Assigning function to yeast proteins by integration of technologies. *Mol Cell* **12**: 1353-1365.

Heinisch, J.J. (1993) *PFK2*, *ISP42*, *ERG2* and *RAD14* are located on the right arm of chromosome XIII. *Yeast* **9**: 1103-1105.

Heinisch, J.J., Lorberg, A., Schmitz, H.P., and Jacoby, J.J. (1999) The protein kinase C-mediated MAP kinase pathway involved in the maintenance of cellular integrity in *Saccharomyces cerevisiae*. *Mol Microbiol* **32**: 671-680.

Heinisch, J.J. (2005) Baker's yeast as a tool for the development of antifungal kinase inhibitors--targeting protein kinase C and the cell integrity pathway. *Biochim Biophys Acta* **1754**: 171-182.

Hicke, L., Zanolari, B., Pypaert, M., Rohrer, J., and Riezman, H. (1997) Transport through the yeast endocytic pathway occurs through morphologically distinct

compartments and requires an active secretory pathway and Sec18p/N-ethylmaleimide-sensitive fusion protein. *Mol Biol Cell* **8**: 13-31.

Hsu, S.C., Ting, A.E., Hazuka, C.D., Davanger, S., Kenny, J.W., Kee, Y., and Scheller, R.H. (1996) The mammalian brain rsec6/8 complex. *Neuron* **17**: 1209-1219.

Hu, F., Wang, Y., Liu, D., Li, Y., Qin, J., and Elledge, S.J. (2001) Regulation of the Bub2/Bfa1 GAP complex by Cdc5 and cell cycle checkpoints. *Cell* **107**: 655-665.

Huh, W.K., Falvo, J.V., Gerke, L.C., Carroll, A.S., Howson, R.W., Weissman, J.S., and O'Shea, E.K. (2003) Global analysis of protein localization in budding yeast. *Nature* **425**: 686-691.

Hwa Lim, H., Yeong, F.M., and Surana, U. (2003) Inactivation of mitotic kinase triggers translocation of MEN components to mother-daughter neck in yeast. *Mol Biol Cell* **14**: 4734-4743.

Ito, T., Chiba, T., Ozawa, R., Yoshida, M., Hattori, M., and Sakaki, Y. (2001) A comprehensive two-hybrid analysis to explore the yeast protein interactome. *Proc Natl Acad Sci U S A* **98**: 4569-4574.

Jacoby, J.J., Kirchrath, L., Gengenbacher, U., and Heinisch, J.J. (1999) Characterization of *KLBCK1*, encoding a MAP kinase kinase kinase of *Kluyveromyces lactis*. *J Mol Biol* **288**: 337-352.

Johnson, D.I. (1999) Cdc42: An essential Rho-type GTPase controlling eukaryotic cell polarity. *Microbiol Mol Biol Rev* **63**: 54-105.

Jonsdottir, G.A., and Li, R. (2004) Dynamics of yeast Myosin I: evidence for a possible role in scission of endocytic vesicles. *Curr Biol* **14**: 1604-1609.

Kaksonen, M., Sun, Y., and Drubin, D.G. (2003) A pathway for association of receptors, adaptors, and actin during endocytic internalization. *Cell* **115**: 475-487.

Kamei, T., Tanaka, K., Hihara, T., Umikawa, M., Imamura, H., Kikyo, M., Ozaki, K., and Takai, Y. (1998) Interaction of Bnr1p with a novel Src homology 3 domain-containing Hof1p. Implication in cytokinesis in *Saccharomyces cerevisiae*. *J Biol Chem* **273**: 28341-28345.

Klis, F.M., Mol, P., Hellingwerf, K., and Brul, S. (2002) Dynamics of cell wall structure in *Saccharomyces cerevisiae*. *FEMS Microbiol Rev* **26**: 239-256.

Koch, A.L. (1970) Turbidity measurements of bacterial cultures in some available commercial instruments. *Anal Biochem* **38**: 252-259.

Korinek, W.S., Bi, E., Epp, J.A., Wang, L., Ho, J., and Chant, J. (2000) Cyk3, a novel SH3-domain protein, affects cytokinesis in yeast. *Curr Biol* **10**: 947-950.

Kubler, E., and Riezman, H. (1993) Actin and fimbrin are required for the internalization step of endocytosis in yeast. *EMBO J* **12**: 2855-2862.

Kusch, J., Meyer, A., Snyder, M.P., and Barral, Y. (2002) Microtubule capture by the cleavage apparatus is required for proper spindle positioning in yeast. *Genes Dev* **16**: 1627-1639.

Lee, S.E., Frenz, L.M., Wells, N.J., Johnson, A.L., and Johnston, L.H. (2001) Order of function of the budding-yeast mitotic exit-network proteins Tem1, Cdc15, Mob1, Dbf2, and Cdc5. *Curr Biol* **11**: 784-788.

Levin, D.E. (2005) Cell wall integrity signaling in *Saccharomyces cerevisiae*. *Microbiol Mol Biol Rev* **69**: 262-291.

Lippincott, J., and Li, R. (1998) Dual function of Cyk2, a cdc15/PSTPIP family protein, in regulating actomyosin ring dynamics and septin distribution. *J Cell Biol* **143**: 1947-1960.

Lippincott, J., and Li, R. (2000) Involvement of PCH family proteins in cytokinesis and actin distribution. *Microsc Res Tech* **49**: 168-172.

Lippincott, J., Shannon, K.B., Shou, W., Deshaies, R.J., and Li, R. (2001) The Tem1 small GTPase controls actomyosin and septin dynamics during cytokinesis. *J Cell Sci* **114**: 1379-1386.

Lipschutz, J.H., and Mostov, K.E. (2002) Exocytosis: the many masters of the exocyst. *Curr Biol* **12**: R212-214.

Lord, M., Inose, F., Hiroko, T., Hata, T., Fujita, A., and Chant, J. (2002) Subcellular localization of Axl1, the cell type-specific regulator of polarity. *Curr Biol* **12**: 1347-1352.

Lum, P.Y., Armour, C.D., Stepaniants, S.B., Cavet, G., Wolf, M.K., Butler, J.S., Hinshaw, J.C., Garnier, P., Prestwich, G.D., Leonardson, A., Garrett-Engele, P., Rush, C.M., Bard, M., Schimmack, G., Phillips, J.W., Roberts, C.J., and Shoemaker, D.D. (2004) Discovering modes of action for therapeutic compounds using a genome-wide screen of yeast heterozygotes. *Cell* **116**: 121-137.

Luzio, J.P., Rous, B.A., Bright, N.A., Pryor, P.R., Mullock, B.M., and Piper, R.C. (2000) Lysosome-endosome fusion and lysosome biogenesis. *J Cell Sci* **113 (Pt 9)**: 1515-1524.

Moseley, J.B., and Goode, B.L. (2006) The yeast actin cytoskeleton: from cellular function to biochemical mechanism. *Microbiol Mol Biol Rev* **70**: 605-645.

Mulholland, J., Preuss, D., Moon, A., Wong, A., Drubin, D., and Botstein, D. (1994) Ultrastructure of the yeast actin cytoskeleton and its association with the plasma membrane. *J Cell Biol* **125**: 381-391.

Munn, A.L., Stevenson, B.J., Geli, M.I., and Riezman, H. (1995) *end5*, *end6*, and *end7*: mutations that cause actin delocalization and block the internalization step of endocytosis in Saccharomyces cerevisiae. *Mol Biol Cell* **6**: 1721-1742.

Nanninga, N. (2001) Cytokinesis in prokaryotes and eukaryotes: common principles and different solutions. *Microbiol Mol Biol Rev* **65**: 319-333 ; third page, table of contents.

Norden, C., Liakopoulos, D., and Barral, Y. (2004) Dissection of septin actin interactions using actin overexpression in *Saccharomyces cerevisiae*. *Mol Microbiol* **53**: 469-483.

Novick, P., and Schekman, R. (1979) Secretion and cell-surface growth are blocked in a temperature-sensitive mutant of *Saccharomyces cerevisiae*. *Proc Natl Acad Sci U S A* **76**: 1858-1862.

Novick, P., Field, C., and Schekman, R. (1980) Identification of 23 complementation groups required for post-translational events in the yeast secretory pathway. *Cell* **21**: 205-215.

Osman, M.A., Konopka, J.B., and Cerione, R.A. (2002) Iqg1p links spatial and secretion landmarks to polarity and cytokinesis. *J Cell Biol* **159**: 601-611.

Park, H.O., Chant, J., and Herskowitz, I. (1993) *BUD2* encodes a GTPase-activating protein for Bud1/Rsr1 necessary for proper bud-site selection in yeast. *Nature* **365**: 269-274.

Park, H.O., Sanson, A., and Herskowitz, I. (1999) Localization of bud2p, a GTPase-activating protein necessary for programming cell polarity in yeast to the presumptive bud site. *Genes Dev* **13**: 1912-1917.

Perez-Ortin, J.E., Garcia-Martinez, J., and Alberola, T.M. (2002) DNA chips for yeast biotechnology. The case of wine yeasts. *J Biotechnol* **98**: 227-241.

Piper, R.C., and Luzio, J.P. (2001) Late endosomes: sorting and partitioning in multivesicular bodies. *Traffic* **2**: 612-621.

Pruyne, D., and Bretscher, A. (2000) Polarization of cell growth in yeast. I. Establishment and maintenance of polarity states. *J Cell Sci* **113 (Pt 3)**: 365-375.

Queralt, E., and Igual, J.C. (2004) Functional distinction between Cln1p and Cln2p cyclins in the control of the *Saccharomyces cerevisiae* mitotic cycle. *Genetics* **168**: 129-140.

Raths, S., Rohrer, J., Crausaz, F., and Riezman, H. (1993) end3 and end4: two mutants defective in receptor-mediated and fluid-phase endocytosis in *Saccharomyces cerevisiae*. *J Cell Biol* **120**: 55-65.

Ren, G., Wang, J., Brinkworth, R., Winsor, B., Kobe, B., and Munn, A.L. (2005) Verprolin cytokinesis function mediated by the Hof one trap domain. *Traffic* **6**: 575-593.

Robinson, N.G., Guo, L., Imai, J., Toh, E.A., Matsui, Y., and Tamanoi, F. (1999) Rho3 of *Saccharomyces cerevisiae*, which regulates the actin cytoskeleton and exocytosis, is a GTPase which interacts with Myo2 and Exo70. *Mol Cell Biol* **19**: 3580-3587.

Rodal, A.A., Kozubowski, L., Goode, B.L., Drubin, D.G., and Hartwig, J.H. (2005) Actin and septin ultrastructures at the budding yeast cell cortex. *Mol Biol Cell* **16**: 372-384.

Roh, D.H., Bowers, B., Riezman, H., and Cabib, E. (2002a) Rho1p mutations specific for regulation of beta(1-->3)glucan synthesis and the order of assembly of the yeast cell wall. *Mol Microbiol* **44**: 1167-1183.

Roh, D.H., Bowers, B., Schmidt, M., and Cabib, E. (2002b) The septation apparatus, an autonomous system in budding yeast. *Mol Biol Cell* **13**: 2747-2759.

Sagot, I., Klee, S.K., and Pellman, D. (2002) Yeast formins regulate cell polarity by controlling the assembly of actin cables. *Nat Cell Biol* **4**: 42-50.

Sanders, S.L., and Field, C.M. (1994) Cell division. Septins in common? *Curr Biol* **4**: 907-910.

Schmidt, M., Bowers, B., Varma, A., Roh, D.H., and Cabib, E. (2002) In budding yeast, contraction of the actomyosin ring and formation of the primary septum at cytokinesis depend on each other. *J Cell Sci* **115**: 293-302.

Schmitz, H.P., (2001) Physiologische und genetische Untersuchungen zur Funktionregulatorischer Proteindomänen in der Signaltransduktion am Beispiel der Proteinkinase C von *Saccharomyces cerevisiae*. *PhD Thesis Duesseldorf University*.

Schott, D., Huffaker, T., and Bretscher, A. (2002) Microfilaments and microtubules: the news from yeast. *Curr Opin Microbiol* **5**: 564-574.

Shannon, K.B., and Li, R. (1999) The multiple roles of Cyk1p in the assembly and function of the actomyosin ring in budding yeast. *Mol Biol Cell* **10**: 283-296.

Shaw, J.A., Mol, P.C., Bowers, B., Silverman, S.J., Valdivieso, M.H., Duran, A., and Cabib, E. (1991) The function of chitin synthases 2 and 3 in the *Saccharomyces cerevisiae* cell cycle. *J Cell Biol* **114**: 111-123.

Shaw, J.D., Cummings, K.B., Huyer, G., Michaelis, S., and Wendland, B. (2001) Yeast as a model system for studying endocytosis. *Exp Cell Res* **271**: 1-9.

Simanis, V. (2003) Events at the end of mitosis in the budding and fission yeasts. *J Cell Sci* **116**: 4263-4275.

Smith, G.R., Givan, S.A., Cullen, P., and Sprague, G.F., Jr. (2002) GTPase-activating proteins for Cdc42. *Eukaryot Cell* **1**: 469-480.

Smythe, E., and Ayscough, K.R. (2003) The Ark1/Prk1 family of protein kinases. Regulators of endocytosis and the actin skeleton. *EMBO Rep* **4**: 246-251.

Spencer, S., Dowbenko, D., Cheng, J., Li, W., Brush, J., Utzig, S., Simanis, V., and Lasky, L.A. (1997) PSTPIP: a tyrosine phosphorylated cleavage furrow-associated protein that is a substrate for a PEST tyrosine phosphatase. *J Cell Biol* **138**: 845-860.

Stevens, R.C., and Davis, T.N. (1998) Mlc1p is a light chain for the unconventional myosin Myo2p in Saccharomyces cerevisiae. *J Cell Biol* **142**: 711-722.

Taheri, N., Kohler, T., Braus, G.H., and Mosch, H.U. (2000) Asymmetrically localized Bud8p and Bud9p proteins control yeast cell polarity and development. *EMBO J* **19**: 6686-6696.

Takizawa, P.A., DeRisi, J.L., Wilhelm, J.E., and Vale, R.D. (2000) Plasma membrane compartmentalization in yeast by messenger RNA transport and a septin diffusion barrier. *Science* **290**: 341-344.

TerBush, D.R., Maurice, T., Roth, D., and Novick, P. (1996) The Exocyst is a multiprotein complex required for exocytosis in *Saccharomyces cerevisiae*. *Embo J* **15**: 6483-6494.

Tolliday, N., VerPlank, L., and Li, R. (2002) Rho1 directs formin-mediated actin ring assembly during budding yeast cytokinesis. *Curr Biol* **12**: 1864-1870.

Tong, A.H., Drees, B., Nardelli, G., Bader, G.D., Brannetti, B., Castagnoli, L., Evangelista, M., Ferracuti, S., Nelson, B., Paoluzi, S., Quondam, M., Zucconi, A., Hogue, C.W., Fields, S., Boone, C., and Cesareni, G. (2002) A combined experimental and computational strategy to define protein interaction networks for peptide recognition modules. *Science* **295**: 321-324.

Uetz, P., Giot, L., Cagney, G., Mansfield, T.A., Judson, R.S., Knight, J.R., Lockshon, D., Narayan, V., Srinivasan, M., Pochart, P., Qureshi-Emili, A., Li, Y., Godwin, B., Conover, D., Kalbfleisch, T., Vijayadamodar, G., Yang, M., Johnston, M., Fields, S., and Rothberg, J.M. (2000) A comprehensive analysis of protein-protein interactions in *Saccharomyces cerevisiae*. *Nature* **403**: 623-627.

Vallen, E.A., Caviston, J., and Bi, E. (2000) Roles of Hof1p, Bni1p, Bnr1p, and myo1p in cytokinesis in *Saccharomyces cerevisiae*. *Mol Biol Cell* **11**: 593-611.

VerPlank, L., and Li, R. (2005) Cell cycle-regulated trafficking of Chs2 controls actomyosin ring stability during cytokinesis. *Mol Biol Cell* **16**: 2529-2543.

Visintin, R., Craig, K., Hwang, E.S., Prinz, S., Tyers, M., and Amon, A. (1998) The phosphatase Cdc14 triggers mitotic exit by reversal of Cdk-dependent phosphorylation. *Mol Cell* **2**: 709-718.

Walther, A., and Wendland, J. (2003) Septation and cytokinesis in fungi. *Fungal Genet Biol* **40**: 187-196.

Warren, D.T., Andrews, P.D., Gourlay, C.W., and Ayscough, K.R. (2002) Sla1p couples the yeast endocytic machinery to proteins regulating actin dynamics. *J Cell Sci* **115**: 1703-1715.

Wu, Y., Dowbenko, D., and Lasky, L.A. (1998) PSTPIP 2, a second tyrosine phosphorylated, cytoskeletal-associated protein that binds a PEST-type protein-tyrosine phosphatase. *J Biol Chem* **273**: 30487-30496.

Yoshida, S., and Toh-e, A. (2002) Budding yeast Cdc5 phosphorylates Net1 and assists Cdc14 release from the nucleolus. *Biochem Biophys Res Commun* **294**: 687-691.

Zahner, J.E., Harkins, H.A., and Pringle, J.R. (1996) Genetic analysis of the bipolar pattern of bud site selection in the yeast *Saccharomyces cerevisiae*. *Mol Cell Biol* **16**: 1857-1870.

Zeng, G., and Cai, M. (1999) Regulation of the actin cytoskeleton organization in yeast by a novel serine/threonine kinase Prk1p. *J Cell Biol* **144**: 71-82.

Zeng, G., Yu, X., and Cai, M. (2001) Regulation of yeast actin cytoskeleton-regulatory complex Pan1p/Sla1p/End3p by serine/threonine kinase Prk1p. *Mol Biol Cell* **12**: 3759-3772.

Zhang, X., Bi, E., Novick, P., Du, L., Kozminski, K.G., Lipschutz, J.H., and Guo, W. (2001) Cdc42 interacts with the exocyst and regulates polarized secretion. *J Biol Chem* **276**: 46745-46750.

Zhu, H., Bilgin, M., Bangham, R., Hall, D., Casamayor, A., Bertone, P., Lan, N., Jansen, R., Bidlingmaier, S., Houfek, T., Mitchell, T., Miller, P., Dean, R.A., Gerstein, M., and Snyder, M. (2001) Global analysis of protein activities using proteome chips. *Science* **293**: 2101-2105.

7. Abbreviations

ARD Aspartate rich domain
bp Base pair
BLAST Basic Local Alignment Search Tool
BSA Bovine serum albumin
°C Celsius degree
DAPI 4',6-diamidino-2-phenylindole
D.I.C. Differential interference contrast (microscopy)
DMF Dimethylformamide
DNA Deoxyribonucleic acid
dNTP Deoxyribonucleotide triphosphate
E. coli Escherichia coli
EDTA Ethylene diamine tetra-acetic acid
e.g. For example (from latin *exempli gratia*)
FACS Fluorescence-activated cell sorting
g, mg, μg Gram, milligram, microgram
G1 Gap one phase (cell cycle)
G2 Gap two phase (cell cycle)
Gal Galactose
GAP GTPase activating protein
GEF Guanine nucleotide exchange factor
GFP Green fluorescent protein
Glc Glucose
GTP Guanosine-5'-triphosphate
h Hour
i.e. That is (from latin *id est*)
KAc Potassium acetate
kb Kilobasepair
kDa Kilodalton
M Mitosis phase (cell cycle)
M, mM, μM Molar, millimolar, micromolar
min Minute
ml, l, μl Milliliter, liter, microliter
NaCl Sodium chloride
NaOH Sodium hydroxide
nm Nanometer
OD_{600} Optical density at a 600 nm wavelength
PCR Polymerase chain reaction
PEG Polyethylenglycol
pH negative logarithm ($\log_{10}$) of the hydroxonium concentration
PRM Proline rich motif
Raf Raffinose
RNA Ribonucleic acid
rpm Revolutions per minute
s Second
S Synthesis phase (cell cycle)
S. cerevisiae, Sc Saccharomyces cerevisiae
SDS Sodium Dodecyl Sulfate
S. pombe Schizosaccharomyces pombe

SPB Spindle Pole Body
TAE Tris Acetic acid EDTA-Na_2-salt
TBE Tris Boric acid EDTA-Na_2-salt
TBS Tris-buffered saline
Tris Tris Hydroxymethylaminoethane
U, mU Unit, Milliunit (Enzyme activity)
UV Ultraviolet radiation
wt Wild-type
X-Gal 5-bromo-4-chloro-3-indolyl-beta-D-galactopyranoside
YEPD Yeast Extract Peptone Dextrose (rich medium)
YNB Yeast Nitrogen Base

Nucleotides and Amino acids are represented with the single letter code (IUPAC-IUB Commission on Biochemical Nomenclature).

Acknowledgements

Coming to this point I realize that there is so many people that I have to thank that the writing of this section is a challenge itself.

I would like to start where this trip began, my family in Argentina. I am very thankful to my fathers Graciela and Damián, who were always a source of love and inspiration and a model of generosity and dedication. They have given me their unconditional support in all my important decisions. To my brother Tomás and my sisters Julieta and Gretel who helped me to become the person I am, it is nice to know I can always count on you. To all my big family, my Grand mothers Agui and Lila, to my uncles and aunts, and to my cousins. It would be an endless list to name you all, but every single of you have contributed with a positive thing. To my former supervisor in Cordoba Dr. Maria Angelica Perillo for her encouragement.

At this side of the ocean where I found myself in this moment, in Germany and other European countries there are also many persons to whom I am very thankful. To Prof. Dr. Jürgen Heinisch who gave me the opportunity to work in such an interesting field and because of his great dedication as a supervisor. To the members of the Committee, Prof. Dr. Karlheinz Altendorf who kindly took part on the evaluation process, to Prof. Dr. Joachim Ernst who accepted the invitation to Osnabrück and Dr. Hans Peter Schmitz who directly collaborated too, during the realization of this work. To the members of the Genetics laboratory, especially to Knut Jahreis, Kurt Schmid and Lucille Schmieding, Who were always willing to help me and for providing a relaxed working atmosphere. To Rosaura Rodicio for her contribution and valuable advice.

During my stay in Osnabrück I made wonderful friends with whom I shared unforgettable moments and constituted my adoptive family in Germany, Cesar and Carina I would not have survived all these years without your support. Also Dario, who helped me from the very first moment. I do not want to forget Rafa, "Pana", Maggie and Sandra with whom I shared many beautiful moments. Especial thanks to my dear Virginia who was the brightest light in the hardest part of such a long way, and gave me the strength to carry on. To my big friend and brother of life Gerardo, who accompanied me in the good and difficult moments throughout so many years and knows very well every single step that had to be climbed to reach this goal. I can not forget my friend Diego in Madrid, with whom I spent so many nice experiences. Finally, I could never

Erklärun über die Eigenständigkeit der erbrachten wissenschaftlichen Leistung und etwaige frühere Promotionsverfahren

Ich erkläre hiermit, dass ich die vorligende Arbeit ohne unzulässige Hilfe Dritter und ohne Benutzung anderer als der angegebenen Hilfsmittel angefertigt habe. Die aus Quellen direkt oder indirekt übernommenen Dateien und Konzepte sind unter Angabe der Quellen gekennzeichnet.

Für den inhaltlichen materiellen Erstellung der vorliegenden Arbeit waren keine anderen Personen beteiligt. Insbesondere habe ich hierfür nicht die entgeltliche Hilfe von Vermittlungs- zw. Beratungsdiensten in Anspruch genommen. Niemand hat von mir unmittelbar oder mittelbar geldwerte Leistungen für Arbeiten erhalten, die im Zusammenhang mit dem Inhalt der vorgelegten Dissertation stehen.

Ich habe bisher an keiner in- oder ausländischen Fakultät weder ein Gesuch um Zulassung zur Promotions eingereicht noch die vorliegende oder eine Andere Arbeit als Dissertation vorgelegt.

....
(Ort, Datum)   (Unterschrift)